

THE X-RAY STRUCTURAL STUDY OF  
SOME ORGANIC CRYSTALS.

THESIS  
PRESENTED FOR THE DEGREE OF  
DOCTOR OF PHILOSOPHY  
IN THE  
UNIVERSITY OF GLASGOW  
BY

JAMES SPENCE CLUNIE, B. Sc.

Chemistry Department.

October, 1960.

ProQuest Number: 13850716

All rights reserved

INFORMATION TO ALL USERS

The quality of this reproduction is dependent upon the quality of the copy submitted.

In the unlikely event that the author did not send a complete manuscript and there are missing pages, these will be noted. Also, if material had to be removed, a note will indicate the deletion.



ProQuest 13850716

Published by ProQuest LLC (2019). Copyright of the Dissertation is held by the Author.

All rights reserved.

This work is protected against unauthorized copying under Title 17, United States Code  
Microform Edition © ProQuest LLC.

ProQuest LLC.  
789 East Eisenhower Parkway  
P.O. Box 1346  
Ann Arbor, MI 48106 – 1346

## P R E F A C E.

This thesis describes researches conducted under the supervision of Professor J.M. Robertson in the Chemistry Department of the University of Glasgow from October, 1957 until October, 1960.

Some of the techniques of X-ray structural determination relevant to the present studies are enumerated in an introductory chapter. The following three chapters are devoted to a description of the known chemistry of isoclovene and of the X-ray diffraction studies conducted on the isomorphous hydrobromide and hydrochloride derivatives of isoclovene which have led to the elucidation of the latter structure. Some preliminary but as yet unsuccessful attempts to solve the crystal structure of photo-irradiated acridizinium bromide are described in the final chapter.

I wish to acknowledge my thanks to my supervisor, Professor J.M. Robertson for his encouragement, criticism and advice. I am also indebted to Dr. G.A. Sim and Dr. T.A. Hamor for many rewarding discussions throughout the course of this work. For computing facilities I am grateful to Dr. D.C. Gilles and the staff of the Computing

Laboratory at Glasgow University. To Mr. J.B. Findlay  
my thanks are due for the preparation of the photographs  
included in this thesis.

I am indebted to the Carnegie Trust for the  
Universities of Scotland for a research scholarship  
which enabled me to undertake this work.

-----

## S U M M A R Y.

Isoclovene,  $C_{15}H_{24}$ , is a liquid sesquiterpene of hitherto virtually unknown constitution. It forms two isomorphous hydrohalide derivatives, isoclovene hydrochloride and isoclovene hydrobromide, which crystallise in the monoclinic space group,  $P_2$ , with two molecules per unit cell.

An attempt was made initially to carry through a structural analysis of the hydrobromide derivative using the heavy atom technique and two dimensional Fourier methods. Only the (010) electron-density projection, when calculated on the basis of the heavy atom phases, gave an unambiguous representation of the molecule, but the prohibitive length of projection ( $13.8 \text{ \AA}$ ) prevented any significant resolution being achieved. The (001) electron-density projection provided a representation of the molecule and its superimposed mirror image due to the existence of the well known false symmetry centre which exists between two phase-determining atoms in the non-centric projections of space group  $P_2$ . Further spurious symmetry was present in the (100) electron-density projection because the heavy atom phases could only be coupled with about one half of the observed terms, those satisfying the condition  $k + l = 2n$ . Attempts to

correlate these three projections of the molecule on the basis of tentative trial structures were not successful.

The solution of the structure resulted from the application of superposition methods to a three dimensional sharpened Patterson function computed with data derived from the hydrochloride derivative. A three dimensional representation of the molecule and its superimposed mirror image was thereby obtained. This map was compared with the essentially analogous distribution given by a triple Fourier synthesis phased solely on the chlorine atom phases. The corresponding prominent peaks on both maps were assumed to indicate the most likely atomic sites. Thereafter, there existed the interpretational problem of selecting "true peaks" from their "mirror image" counterparts. Seven carbon atoms were located and included with chlorine in the initial phasing calculations. Four successive triple Fourier syntheses sufficed to reveal the structure. Two further  $F_0$  syntheses and twelve successive least squares cycles reduced the discrepancy over 976 observed terms to 12.5%.

This analysis has led to a determination of the molecular structure and relative configuration of isoclovene hydrochloride. From these results the structure of the parent compound, isoclovene, has been deduced.

Photo-irradiated acridizinium bromide,  $C_{26}N_2H_{20}Br_2$ , has been obtained in a crystalline form belonging to the monoclinic space group  $P2_1/m$  with two molecules per unit cell. The projections of the Patterson function on the three main zones have been examined but it has not yet proved possible to derive an entirely satisfactory trial structure for the most favourable (100), projection.

TABLE OF CONTENTS.

CHAPTER I: Some Methods of Crystal Structure Analysis.

	Page
1.1. Introduction . . . . .	1
1.2. The Structure Factor . . . . .	2
1.3. The Fourier Series Representation of the Electron Density . . . . .	3
1.4. Solution of the Phase Problem . . . . .	4
1.4.1. Trial-and-error Method . . . . .	4
1.4.2. The Patterson Function . . . . .	5
1.4.3. The Heavy-atom Method . . . . .	8
1.4.4. The Isomorphous Replacement Method . . . . .	10
1.4.5. Direct Methods . . . . .	12
1.5. Refinement of Crystal Structures . . . . .	13
1.5.1. The Fo Synthesis. . . . .	14
1.5.2. The Method of Least Squares . . . . .	16

CHAPTER II: The Chemistry of Isoclovene and Related Compounds

2.1. Introduction . . . . .	18
2.2. Isoclovene and the Caryophyllene Series of Sesquiterpenes . . . . .	19
2.3. The X-ray Crystallographic Approach to Structure Determination . . . . .	22

CHAPTER III: The Structure of Isoclovene:  
the Two-dimensional Analysis.

3.1. The Preliminary X-ray Crystallographic Survey . . . . .	24
3.2. Choice of Derivative for Structure Determination . . . . .	26

	Page
3.3. Collection of Intensity Data . . . . .	27
3.4. Two-dimensional Structure Analysis of Isoclovene Hydrobromide . . . . .	31
3.5. The (100) Projection . . . . .	31
3.6. The (001) Projection . . . . .	35
3.7. The (010) Projection . . . . .	37
3.8. Attempted Correlation of the (001) and (010) Projections . . . . .	38
3.9. Pseudo Three-dimensional Approach . . . . .	40
3.10. Appraisal of the Results of the Two-dimensional Analysis . . . . .	41

CHAPTER IV: The Three-dimensional Analysis  
of Isoclovene Hydrochloride.

4.1. Introduction . . . . .	43
4.2. Collection and Processing of the Experimental Data . . . . .	44
4.3. Correction and Correlation of Intensities.	46
4.4. The Three-dimensional Patterson Synthesis.	48
4.5. The Buerger Minimum Function . . . . .	49
4.6. Interpretation of the Minimum Function . .	51
4.7. Objective Approach to Structure Elucidation.	54
4.8. Refinement of the Structure . . . . .	60
4.8.1. $F_0$ Synthesis . . . . .	60
4.8.2. Least Squares Refinement . . . . .	61
4.9. Co-ordinates and Molecular Dimensions . .	67
4.10. Discussion . . . . .	77

CHAPTER V: Attempts to Solve the Crystal Structure  
of Photo-irradiated Acridizinium Bromide.

	Page
5.1. Introduction . . . . .	82
5.2. Preparation of Crystals . . . . .	83
5.3. Unit Cell Dimensions . . . . .	85
5.4. Measurement of Intensities . . . . .	85
5.5. N(Z) Distribution . . . . .	87
5.6. Attempted Structure Determination using Two-dimensional Methods . . . . .	89
5.6.1. The (100) Patterson Projection . . . . .	89
5.6.2. The (001) Patterson Projection . . . . .	91
5.6.3. The (010) Patterson Projection . . . . .	92
5.6.4. Analysis of the (100) Projection . . . . .	93

References:

97 - 101

Appendix I.

Appendix 2.

Appendix 3.

Appendix 4.

-----

CHAPTER I.

Some Methods of Crystal Structure Analysis.

# I. SOME METHODS OF CRYSTAL STRUCTURE ANALYSIS.

## 1.1. Introduction:

A crystal is a regular three dimensional array of atoms and, as von Laue and his collaborators first demonstrated in 1912, can therefore act as a three dimensional diffraction grating for X-radiation. The size and shape of the unit cell as well as information concerning the possible symmetry elements present can be deduced from the geometrical distribution of the diffracted rays ('reflections'). However, the scattered X-rays differ not only in direction but also in intensity and phase. The actual intensity of a given diffracted beam depends principally on the structure factor, which, besides being dependent on the direction of scattering, is also a function of the nature and arrangement of scattering material in the unit cell.

The structure factor can be represented by a complex number,  $F(hkl)$ , giving both the amplitude,  $|F(hkl)|$ , and phase,  $\alpha(hkl)$ , of the diffracted beam relative to that of an isolated electron at the origin of co-ordinates under the same experimental conditions. From the observed intensities can be derived values of  $|F(hkl)|^2$ , but the associated phase information is necessarily lost during the registration of the intensities either

photographically or by some other means. As a general consequence, no direct pathway exists between the X-ray intensities and the atomic distribution, and it is the essentially indirect deduction of the phases which constitutes the phase problem - the central difficulty of X-ray structural analysis.

1.2. The Structure Factor:

The structure factor,  $F(hk\ell)$ , of a crystal plane with diffraction indices,  $(hk\ell)$ , may be expressed in the form:

$$F(hk\ell) = \sum_{j=1}^N f_j \exp 2\pi i \{hx_j + ky_j + lz_j\} \dots\dots(1.1.)$$

where  $N$  is the total number of atoms in the unit cell,  $(x_j, y_j, z_j)$  are the atomic co-ordinates expressed as fractions of the cell edges and  $f_j$  is the scattering factor (atomic form factor) for the  $j^{\text{th}}$  atom. The term,  $f_j$ , can be resolved into two components thus

$$f_j = f_j^0 \exp \left( -B \frac{\sin^2 \theta}{\lambda^2} \right) \dots\dots\dots(1.2.)$$

$f_j^0$  being the atomic form factor calculated theoretically for the electron distribution of the particular atom at rest. The exponential term is included to allow for the fact that thermal vibrations, here assumed to be isotropic, tend to make the electron distribution more diffuse thereby decreasing the scattering power of the atom. In equation (1.2)

$$B = 8\pi^2 \overline{U^2} \dots\dots\dots(1.3.)$$

where  $\overline{U^2}$  is related to the mean square displacement of the

atom in question from its mean position in the crystal lattice.

1.3. The Fourier Series Representation of the Electron Density.

Since crystals can be considered as periodic distributions of scattering material (electrons), W.H.Bragg (1915) first suggested that the electron density,  $\rho(xyz)$ , could be conveniently expressed in the form of a triple Fourier Series. It can be shown that the coefficients of such a series are, in fact, the various structure factors.

$$\rho(xyz) = \sum_{-\infty}^{\infty} h \sum_{-\infty}^{\infty} k \sum_{-\infty}^{\infty} \ell \frac{F(hk\ell)}{V} \exp -2\pi i(hx + ky + \ell z) \dots (1.4.)$$

V is the volume of the unit cell.

Because the  $F(hk\ell)$  values are complex quantities representing both amplitude and phase it is sometimes more convenient to write equation (1.4) in the following form:

$$\rho(xyz) = \sum_{-\infty}^{\infty} h \sum_{-\infty}^{\infty} k \sum_{-\infty}^{\infty} \ell \frac{|F(hk\ell)|}{V} \cos \{2\pi(hx + ky + \ell z) - \alpha(hk\ell)\} \dots (1.5)$$

$\alpha(hk\ell)$ , the phase angle, is given by:

$$\alpha(hk\ell) = \tan^{-1} \frac{B}{A} \dots \dots \dots (1.6)$$

where  $A = \sum_j f_j \cos 2\pi(hx_j + ky_j + \ell z_j)$ , and

$$B = \sum_j f_j \sin 2\pi(hx_j + ky_j + \ell z_j)$$

are respectively the real and imaginary parts of the complex number,  $F(hk\ell)$ .

The problem of phase determination is simplified if the structure is centrosymmetric, since the phase angles are then restricted to either  $0^\circ$  or  $180^\circ$ , values which can be signified by ascribing respectively either a positive or a negative sign to the Fourier coefficients.

$$\rho(xyz) = \sum_{-\infty}^{\infty} h \sum_{-\infty}^{\infty} k \sum_{-\infty}^{\infty} l \frac{\pm |F(hkl)|}{V} \cos 2\pi(hx + ky + lz) \dots (1.7)$$

W.L.Bragg (1929) demonstrated how the computational labour can be eased by examining a projection of the electron-density onto an axial plane:

$$\rho(xy) = \sum_{-\infty}^{\infty} h \sum_{-\infty}^{\infty} k \frac{|F(hk0)|}{A} \cos \left\{ 2\pi(hx + ky) \pm \alpha(hk0) \right\} \dots (1.8)$$

A being the area of the (x,y) plane.

#### 1.4. Solution of the Phase Problem.

From a knowledge of the amplitudes and phases of the diffracted beams it should therefore be possible to determine the distribution of electron-density within the unit cell. Some of the indirect methods whereby approximations to the unknown phase angles may be obtained, and which have particular relevance to the present studies, will now be outlined.

##### 1.4.1. Trial-and-error Method.

This method can be employed when the chemical structure is simple and not in doubt. Since the solution of any

particular crystal structure depends on finding a set of atomic parameters, which, according to calculation, gives values for the intensities similar to those observed experimentally, a molecular model based on the structural formula can be tested positionally in the unit cell till there is sufficiently good agreement between calculated and observed structure amplitudes. Supplementary physical and geometrical data often help in the derivation of a satisfactory trial structure. Direct calculation of a Fourier Series using  $|F_0| = |F_{\text{obs}}(hkl)|$  values, i.e. the observed structure amplitudes as coefficients and the corresponding calculated phases will then give an approximation to the true electron-density, and the usual refinement processes may then be followed. Unfortunately, where there is no rigid trial model because of the possibility of free rotation of side chains about single bonds or where ring conformations are largely unknown, this method is of strictly limited utility.

#### 1.4.2. The Patterson Function.

A Fourier synthesis may be performed using not structure factors but rather  $|F(hkl)|^2$  values as coefficients whence the following function can be defined:

$$P(uvw) = \frac{1}{V} \sum_{-\infty}^{\infty} \sum_{-\infty}^{\infty} \sum_{-\infty}^{\infty} |F(hkl)|^2 \cos 2\pi(hu + kv + lw) \dots(1.9)$$

As was shown by A.L.Patterson (1934) the map of this function represents, in principle, a superposition of all possible interatomic vectors in the crystal. The Patterson method requires that only observed quantities be used and, consequently, the function can always be computed. Difficulties arise when attempts are made to interpret the resulting map for the method is subject to the inherent limitation that all the vectors arise from the origin point. Interpretation, therefore, becomes more difficult the more complex the structure. If there are  $N$  peaks in the real unit cell then  $N^2$  peaks will exist in the cell of the vector distribution -  $N$  of them superposed at the origin and  $\frac{N(N-1)}{2}$  related to the remaining  $\frac{N(N-1)}{2}$  by a centre of symmetry.

When only a projection of the Patterson function is considered, extensive overlap of vectors is usually experienced. Patterson (1935) and Yü (1942) have discussed how the resolution of peaks in the Patterson function may be improved by using a modification function.

It can be appreciated, therefore, that maximum information will usually be culled from the three dimensional synthesis, but Harker (1936) demonstrated that with space groups possessing certain symmetry operators, e.g. a two-fold screw axis, certain sections of the three dimensional

distribution - in this case  $v = \frac{1}{2}$  - contain useful information concerning the vectors between equivalent atoms of the structure.

If there is a small number of "heavy atoms" present in the unit cell then it is generally possible to locate them from the vector distribution since their vectors will be enhanced. The further unravelling of the Patterson function to reveal the position of the "light atoms" can often be accomplished by the use of "superposition methods".

Clastre and Gay (1950), Garrido (1950), Beevers and Robertson (1950) and McLachlan (1951) independently showed that vector maps could be solved by a device commonly called the vector shift method. If one of a pair of duplicate Patterson maps is translated appropriately with respect to the other, e.g. if a "heavy atom" vector peak of one is superposed on the origin peak of the other, then there is a high probability that the atoms in the crystal structure are represented by the coincidences on both maps. These methods depend on the fact that the Patterson function can be considered to represent a superposition of  $N$  displaced, weighted images of the crystal structure. Simultaneously, Buerger (1950, 1951) presented his image-seeking method based on vector set theory, which covered similar ground but from a more

general viewpoint. He showed that by using some type of image-seeking function, preferably a minimum function, an approximation to the electron density can be derived which is superior to that obtained by using merely vector shift methods..

1.4.3. In the heavy atom method of phase determination the positions of the few atoms having dominant scattering factors can usually be determined by Patterson methods, and hence their contributions to the various structure factors can readily be calculated. The phase angles so deduced, when coupled with the appropriate  $|F_o|$  values and incorporated into a Fourier synthesis, yield an approximation to the electron-density which will generally indicate further atomic sites. Better approximations to the phase angles can then be evaluated and the whole process recycled until the complete structure is revealed.

The classical example of this technique is the analysis of platinum phthalocyanine by Robertson and Woodward (1937). With one heavy atom in the asymmetric unit situated at a centre of symmetry and with this position taken as origin, the signs of the structure factors are all positive. One two-dimensional Fourier synthesis then revealed the entire structure.

Depending on the type of crystal structure several circumstances may arise which can limit the general applicability of this method of assigning phases.

(a) If the "heavy atom" is located at a special position in the asymmetric unit then it may not contribute to systematic classes of reflections. The best method of solution is to effect a Fourier synthesis based on the phase determined reflections alone. The resulting electron-density map will then give an imperfect impression of the true structure in that additional spurious symmetry will exist. The analysis of copper tropolone by Robertson (1951) was complicated by such difficulties in the initial stages.

(b) With non-centrosymmetrical crystals the phase angles may vary continuously between  $0^{\circ}$  and  $360^{\circ}$ . Additional complications can arise when the position of the "heavy atom" in the asymmetric unit simulates higher symmetry than that possessed by the space group itself. Such a situation was encountered by Carlisle and Crowfoot (1945) in their analysis of cholesteryl iodide. The two iodine atoms in the unit cell are related by a pseudo centre of symmetry. Consequently, a Fourier synthesis calculated solely on the basis of the iodine phases will represent a centrosymmetrical electron density distribution,

namely that of the true structure and its superimposed mirror image. The whole problem is thereby reduced to a difficult interpretational one.

It is worthwhile having some index for assessing the prospects of success using this method of phase determination. As a rough guide, Lipson and Cochran (1953) suggest that the square of the atomic number of the "heavy atom" should be approximately equal to the sum of the squares of the atomic numbers of the "light atoms", i.e.  $Z_{h.a.}^2 = \sum z_j^2$ . Although the majority of successful analyses have been performed when the ratio,  $Z_{h.a.}^2 / \sum z_j^2$ , has exceeded unity, several notable successes have been reported when the value of this ratio has been less than unity, e.g. the analysis of vitamin B<sub>12</sub> by Hodgkin et al. (1957).

1.4.4. The isomorphous replacement method offers a still more powerful approach to direct phase determination in that the phase of any structure factor is determined by considering the difference between the contributions made to a particular reflection by two isomorphous heavy atom derivatives. Two main cases can be recognised.

(a) Centrosymmetrical space groups. With a pair of isomorphous crystals of compounds RX<sub>1</sub> and RX<sub>2</sub>, where R represents the organic part of the molecule and X<sub>i</sub> the

replaceable "heavy atom", intensity data from these two crystals when placed on the same basis can enable most of the signs to be determined thus:

$$F(RX_1) - F(RX_2) = \Delta F = (f_{X_1} - f_{X_2}) \cos 2\pi(hx + ky + \ell z) \dots (1.10)$$

The location of the "heavy atom" can be determined from a Patterson synthesis. Calculation of a Fourier synthesis phased in this manner should reveal the general outline of the rest of the molecule. The classical example of this process is the two dimensional structure analysis of the phthalocyanines by Robertson (1935, 1936) and Robertson and Woodward (1937).

(b) Non-centrosymmetrical space groups. In this case changes in the general structure amplitude are more difficult to interpret when variable phase angles are involved. Moreover, with only a pair of isomorphous crystals available the isomorphous replacement method does not produce unique values for the phase angles, there being two possibilities. Such a complication was encountered by Bokhoven, Schoone and Bijvoet (1951) in their analysis of strychnine sulphate and strychnine selenate. A Fourier synthesis computed using both values for the phase angles results in a centre of symmetry being introduced at the origin. As in the

investigation of the structure of cholesteryl iodide (Carlisle and Crowfoot (1945)) this corresponds to a superposition of the true structure and its inverse.

Hence, the isomorphous replacement method is most valuable when a centre of symmetry is present, if not for the structure as a whole, at least for a projection of the structure. In the latter case, resolution of peaks is the important limiting factor.

It may be noted that, in theory, to fix phase angles experimentally a minimum of three isomorphous crystals,  $RX_1Y_1$ ,  $RX_1Y_2$ ,  $RX_2Y_1$  would be required, R representing the organic part of the molecule, X the site of one type and Y the site of a second type of "heavy atom". This technique of multiple isomorphous replacement has been recently used with marked success in the analysis of protein structures by Bragg and Perutz (1954) and Kendrew and co-workers (Bluhm et al. (1958)).

#### 1.4.5. Direct Methods.

It is possible using amplitude relationships between structure factors to establish some phases using certain mathematical relationships (Harker and Kasper (1948)). These relations depend on the fact that the electron density is never negative (Pepinsky and MacGillavry (1951), Karle and Hauptman (1950)). Many more analytical approaches

have subsequently been made on the phase problem (Sayre (1952), Zachariasen (1952) and others) which suggest that these methods can be of advantage for the solution of centrosymmetric structures, but that solution of moderately complex non-centric structures is less likely unless centrosymmetrical projections are available.

### 1.5. Refinement of Crystal Structures.

Once the general outline of a structure has been solved various methods can be used in order to derive accurate positional and thermal parameters. Of course, the final accuracy of any structure determination depends on the precision with which the structure amplitudes have been found experimentally.

It has been found convenient to express the overall agreement between the observed and calculated structure amplitudes in terms of the reliability index or residual

$$R = \frac{\sum ||F_o| - |F_c||}{\sum |F_o|}$$

Expressed as a percentage R is usually called the discrepancy.

Although R is a useful guide in deciding whether any particular change in parameters has produced a better agreement with the observed data, it is not entirely a satisfactory index in that, especially when a "heavy atom" is present, serious individual discrepancies may exist and yet the overall R value may seem acceptable.

While a low value of R provides some internal evidence that the crystal structure so derived is essentially correct other factors need to be examined. The deduced structure must be chemically reasonable. The bond lengths and bond angles together with the intermolecular contacts should be both reasonable and acceptable. Also the electron-density distribution should not contain regions of appreciable negative density.

Among the more important methods of refinement may be mentioned the Fo synthesis, the differential synthesis (Booth, 1946), the method of steepest descents (Booth, 1947; Vand, 1948; Qurashi, 1949), the difference synthesis which has been discussed theoretically by Booth (1948) and Cochran (1951) and the method of least squares (Hughes, 1941). The two methods of refinement used in the present studies will now be described.

#### 1.5.1. The Fo synthesis.

The Fo synthesis was the first systematic method of structure refinement. The electron-density distribution is calculated using the observed amplitudes,  $|F_o|$ , and phases calculated on the basis of the approximate trial structure. From the resulting map it should be possible to allocate improved co-ordinates to the atomic positions.

Calculation of structure factors then provides a new, better set of phase angles and the whole process is reiterated until there is no further decline in the R value.

The successive Fourier refinement of a centrosymmetrical structure has converged completely when there is no change in any of the signs as derived from the previous step. In a non-centrosymmetrical structure any change in the co-ordinates necessarily brings about a change in the phases and so the process of Fourier refinement theoretically never ends. An acceptable limit, however, may be reached more quickly by applying co-ordinate shifts which are between one and two times the indicated values, the exact factor depending on the space group. This is the "n-shift rule" introduced by Shoemaker et al. (1950). Truter (1954) has pointed out that it is only strictly applicable when no one atom predominately determines the phases.

The electron density distributions derived using  $F_0$  syntheses differ from the true electron density because the series do not include all terms of appreciable magnitude and, moreover, the Fourier coefficients are subject to at least random errors. Booth (1946) has suggested a technique - the back-shift method - for the correction of such series

termination errors. Other inherent limitations in the  $F_0$  synthesis are that some of the measured coefficients may be more in error than others and that excessive weight is ascribed to high order  $F$  values. These latter disadvantages can be overcome if the procedure outlined in the next section is followed.

### 1.5.2. The Method of Least Squares.

As was shown by E.W. Hughes (1941) the method of least squares can be used in structure refinement by minimising some function of the observed and calculated structure amplitudes with respect to the structural parameters,  $\xi_i$ . The function most commonly used is:-

$$\begin{aligned} R &= \sum \omega \{ |F_o| - |F_c| \}^2 \\ &= \sum \omega \Delta_{hkl}^2 \end{aligned} \quad \dots\dots\dots (1.11.)$$

where  $F_o$  and  $F_c$  have their usual significance, the summation being carried out over the set of crystallographically independent planes. A weighting factor,  $\omega$ , is applied to allow for the fact that the  $F_o$  values are not all measured with the same accuracy. The absolute values of the weights are unknown, these being dependent on the reliability of the  $F$  values. This being the case, relative estimations of the weights are usually made.

Each structure factor supplies one observational

equation of the type 
$$\sum_{j=1}^N \left( w \frac{\partial |F_c|}{\partial \xi_j} \right) \Delta \xi_j = w \Delta^2$$
 ..... (1.12.)

to the least squares matrix.  $\Delta \xi_j$  are the corrections to be solved for and applied to the values of  $\xi_j$  used in calculating  $|F_c|$  values. If the errors in the positional parameters are small then these parameters can be refined by the standard least squares procedure (Whittaker and Robinson (1944)) of successive solution of N simultaneous linear equations in the N unknown parameters (the normal equations).

The use of the least squares method is not restricted to the refinement of atomic co-ordinates. It may be applied to the adjustment of atomic scale and temperature factors (Hughes and Lipscomb (1946)), and refinement is continued until R and  $\sum w \Delta^2$  approach constancy. The parameter shifts - positional, vibrational and scale - indicated at this stage should only be small fractions of the corresponding standard deviations.

The relation between the Fourier and least squares methods of refinement was deduced by Cochran (1948) who showed that for resolved peaks the co-ordinates found by the least squares procedure with  $w = 1/f$  are the same as those resulting from a Fourier synthesis when back-shift corrections for finite series are applied.

CHAPTER II.

The Chemistry of Isoclovene and Related Compounds.

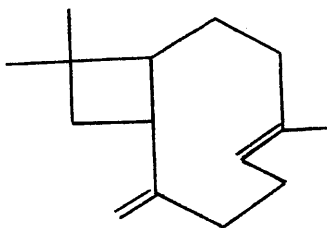
## II. THE CHEMISTRY OF ISOCLOVENE AND RELATED COMPOUNDS.

### 2.1. Introduction:

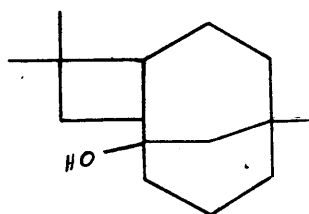
The classical approach to structural elucidation in the terpene field was by chemical degradation, whereby small fragments of the original molecule were isolated for recognition. Difficulties, however, exist in this series in that these compounds are liquids which, in some cases, have very similar physical properties. Furthermore, the chemical investigation can be complicated due to the fact that molecular transformations can and do readily occur in this series (de Mayo (1959)).

These structural investigations have been greatly aided by the recent use of physical methods. In particular, I.R. and U.V. spectroscopic work have been of invaluable assistance, but are of limited value in that only certain functional groups are detected by these methods. Increasing progress in this field has resulted from the application of X-ray crystallographic methods, which can, in favourable cases, solve structural problems directly. Of particular interest is the analysis of longifolene hydrobromide and hydrochloride by Moffett and Rogers (1953), since the structure derived by them has still to be confirmed chemically.

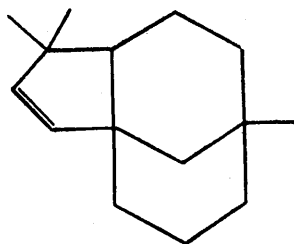




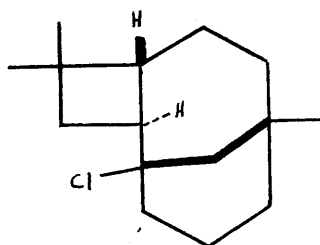
I



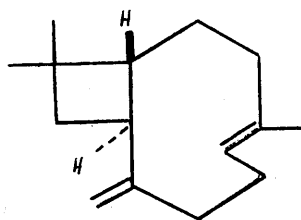
II



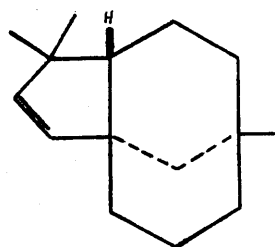
III



IV



V

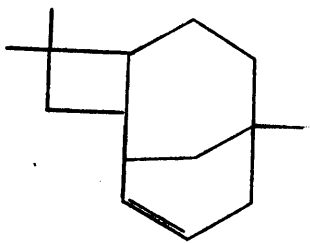


VI

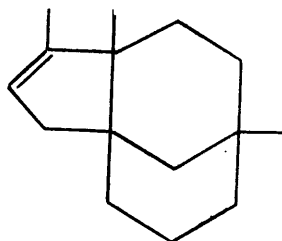
Robertson (1929) dehydrated  $\beta$ -caryophyllene alcohol using phosphorus pentoxide. This is reaction 2. They separated the hydrocarbon mixture so obtained by distillation under reduced pressure into a new isomer, isoclovene, and another hydrocarbon, (A), which they believed to be clovene because of the similarity in refractive index, boiling point and density. Lutz and Reid (1953, 1954) showed that hydrocarbon, (A), differed from clovene in specific rotation as well as in its I.R. spectrum. This new isomer, A, they called pseudoclovene.

It is only in the last decade that it has been possible to deduce the structural formulae of these compounds. Barton and Lindsey (1951) provided convincing chemical evidence that  $\beta$ -caryophyllene had constitution (I). Further chemical work by Barton, Bruun and Lindsey (1952) indicated that  $\beta$ -caryophyllene alcohol possessed structure (II) while degradative work by the same group unequivocally proved that clovene had structure (III).

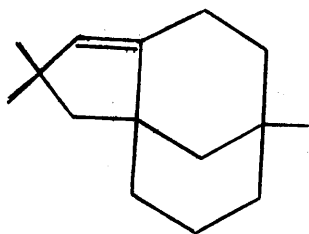
The X-ray crystallographic analysis of the isomorphous hydrohalide derivatives of  $\beta$ -caryophyllene alcohol by Robertson and Todd (1953, 1955) not only independently confirmed Barton's chemical work but also gave proof of the stereochemistry of the halide (IV).



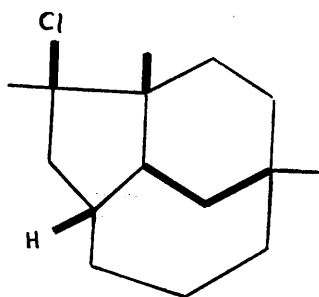
VII



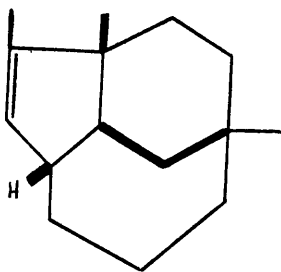
VIII



IX



X



XI

On the basis of relative electrophilicity and other considerations, Aebi, Barton and Lindsey (1953) using the result of Robertson and Todd's X-ray investigation as a basis were able to advance a rational presentation of all the stereochemical relationships:

Formula (VII) was ascribed to pseudoclovene by Lutz and Reid (1953). No investigations were made by the latter on the problem of the structure of isoclovene. Some initial work has, however, been done by Money (1957). In the short time at his disposal Money showed:

- (1) that isoclovene possessed a secondary-tertiary ethylenic linkage (peaks at  $795\text{ cm.}^{-1}(\text{s})$  and  $840\text{ cm.}^{-1}(\text{m})$  in the I.R. spectrum). It can therefore be inferred that isoclovene is tricyclic.
- (2) Kuhn-Roth oxidation indicated the presence of three methyl groups in the molecule.

Little else of any value was deduced from this limited degradative approach. Nevertheless, from logical mechanistic considerations and using the dehydration of clovene as analogy, Money tentatively proposed two possible structures, (VIII) and (IX), for isoclovene.

For the sake of comparison, the structure of isoclovene hydrochloride as established by the subsequent

X-ray investigations is correctly represented as in (X).  
The structure of isoclovene is therefore represented by (XI).

### 2.5. The X-ray Crystallographic Approach to Structure Determination.

While structures (VIII) and (IX) can be considered as perhaps useful guides for the postulation of trial structures, any X-ray investigation of a crystalline derivative of isoclovene must embody a constitutional as well as a configurational problem. With a moderately complex molecule of the sesquiterpene type it is clear that some phase determining heavy atom technique is required although it may be noted in the passing that Grant's (1957) analysis of hydroxydihydroeremophilone dispensed with any such aid.

To date, two main approaches have been employed in the analysis of terpene derivatives. After the initial determination of the heavy atom location in the crystal structure, the signs for centrosymmetric electron-density projections have been determined either by comparison of two isomorphous compounds as in the analysis of  $\alpha$ -chloro (bromo) camphor by Wiebenga and Krom (1946) and  $\beta$ -caryophyllene chloride (bromide) by Robertson and Todd (1953, 1955) or from a single heavy atom derivative as in the case of lanostenyl iodoacetate (Fridrichsons and Mathieson (1953)).

Since Money, on the basis of a mixed melting point determination, claimed that isoclovene hydrobromide and hydrochloride were isomorphous, it seemed possible to follow the same broad strategy in the present structural determination. Access to a high speed digital computer was not possible at the beginning of this research and, in consequence, an attempt was made initially to carry through an analysis using two dimensional data.

-----

### CHAPTER III.

#### The Structure of Isoclovene: the Two-dimensional Analysis.

III. THE STRUCTURE OF ISOCLOVENE:  
THE TWO-DIMENSIONAL ANALYSIS.

3.1. The preliminary X-ray crystallographic survey.

Samples of isoclovene hydrochloride and hydrobromide, crystallised from ethyl acetate by Mr. T. Money, were kindly supplied by Professor D.H.R. Barton. The colourless crystals of the former possessed a finely acicular habit, but the few, initially colourless, crystals of the latter had all but decomposed into a dark green oil. A fresh sample of the hydrobromide derivative was therefore prepared, the scheme originally adopted by Money being followed (see Appendix 1). Both derivatives were then recrystallised from acetone solutions as well formed prismatic needles which exhibited straight extinction when examined under the polarising microscope.

The unit cell dimensions were obtained from rotation photographs calibrated by copper powder lines, oscillation photographs and equatorial layer-line Weissenberg photographs. Copper  $K\alpha$  radiation ( $\lambda = 1.542 \overset{\circ}{\text{A}}$ ) was used throughout. The densities of the crystals were determined by the flotation method, the media being aqueous solutions of zinc chloride.

The relevant crystallographic data for these two hydrohalide compounds are listed in Table 1. While the systematic absences in spectra -  $(OkO)$  for  $k = 2n + 1$  -

TABLE 1.

Crystallographic data for isoclovene hydrochloride  
and isoclovene hydrobromide.

	isoclovene hydrochloride	isoclovene hydrobromide
molecular formula	$C_{15}H_{25}Cl$	$C_{15}H_{25}Br$
molecular weight	240.8	285.3
melting point	87°	74°
system	monoclinic	
a (Å)	6.35 ± 0.01	6.48 ± 0.01
b (Å)	13.91 ± 0.04	13.81 ± 0.04
c (Å)	7.89 ± 0.02	7.96 ± 0.01
$\beta$	95.3°	91.9°
unit cell volume (Å <sup>3</sup> )	694	712
molecules per cell	2	2
d (flotation) (g.cm. <sup>-3</sup> )	1.151	1.323
d (calc.) (g.cm. <sup>-3</sup> )	1.152	1.330
Absorption (cm. <sup>-1</sup> ), ( $\lambda = 1.542 \text{ \AA}$ )	22.2	38.6
Absent Spectra	(Ok0) when k = 2n + 1	
Space group	$C_2^2 - P_2,$	$C_2^2 - P_2,$
F (000)	264	300

are characteristic of two space groups,  $P_{21}$  and  $P_{21/m}$ , the latter is rejected since this space group cannot possibly accommodate two molecules possessing neither a plane nor a centre of symmetry. (Isoclovene is optically active with a specific rotation

$[\alpha]_D^{14} = -56.6^\circ$ .) The complete molecule is therefore regarded as the asymmetric unit.

### 3.2. Choice of derivative for structure determination.

The isomorphism of isoclovene hydrochloride and hydrobromide has been confirmed, but, as indicated in section 1.4.4., the isomorphous replacement method in the case of a non-centric space group such as  $P_{21}$ , where there is only a single centrosymmetric projection and that one almost 14 Å long, holds no advantage over the "heavy atom" technique. Indeed, the latter is to be preferred since less labour is involved and there are no besetting scaling factor difficulties.

Since the value of the ratio  $Z_{na}^2 / \sum z_j^2$  (section 1.4.3.) is 2.2 in the case of the bromo compound but only .5 for the chloro derivative, isoclovene hydrobromide, despite its higher linear absorption coefficient, was selected as being the more suitable derivative for the initial two dimensional analysis. Furthermore, due to the

unstable nature of this compound (life time of a few days when exposed to air and X-rays), it was preferable to collect intensity data immediately.

### 3.3. Collection of Intensity Data.

Intensity data for the (hk0), (h0l) and (0kl) zones of isoclovene hydrobromide were recorded photographically using copper K $\alpha$  radiation ( $\lambda = 1.542 \text{ \AA}$ ). The correlation of strong and weak reflections was achieved using the multiple film technique (Robertson (1943)) with a pack of 5 films (Ilford Industrial - G). A film factor of 3.3 was assumed. The integrated intensities finally obtained were the arithmetic average of three visual estimates each made with the aid of a different series of calibrated spots of known relative intensity.

TABLE 2.

Zone	number of reflections recorded	% of total possible	ratio of strongest to weakest intensity	cross-section of specimen
(0kl)	123	82	11,000 : 1	.2 x .2 mm. <sup>2</sup>
(h0l)	118	81	2,800 : 1	.2 x .3 mm. <sup>2</sup>
(hk0)	116	86	4,200 : 1	.4 x .36 mm. <sup>2</sup>

The mean intensities were converted into structure factors (listed in Table 3), after the usual Lorentz and polarisation corrections had been applied. No corrections were made for absorption or extinction.

### 3.4 Two Dimensional Structure Analysis of Isoclovene Hydrobromide.

The calculations of Fourier and Patterson syntheses described in this chapter were carried out using the Beevers-Lipson strip method with intervals of  $12^\circ (.216 \text{ \AA})$  along a,  $6^\circ (.230 \text{ \AA})$  along b, and  $6^\circ (.133 \text{ \AA})$  along c. The computation of structure factors was performed using a desk calculating machine. The Thomas-Fermi scattering factors for bromine listed in Internationale Tabellen (Zweiter Band) (1935) were used, while the atomic form factors for carbon were those compiled by Hoerni and Ibers (1954). Empirical modifying temperature factors of  $B = 4.4 \text{ \AA}^2$  for bromine and  $B = 3.5 \text{ \AA}^2$  for carbon were used, these being the values deduced by Robertson and Todd (1955) for the halogen and carbon atoms respectively in  $\beta$ -caryophyllene chloride.

### 3.5 The (100) Projection.

As the a axis is the shortest, a projection of the structure onto the (100) plane would seem to present the most open view of the molecule. Clearly, the first step was to find the location of the heavy atom within the asymmetric unit. This was achieved by computing the (100) Patterson projection using as Fourier coefficients

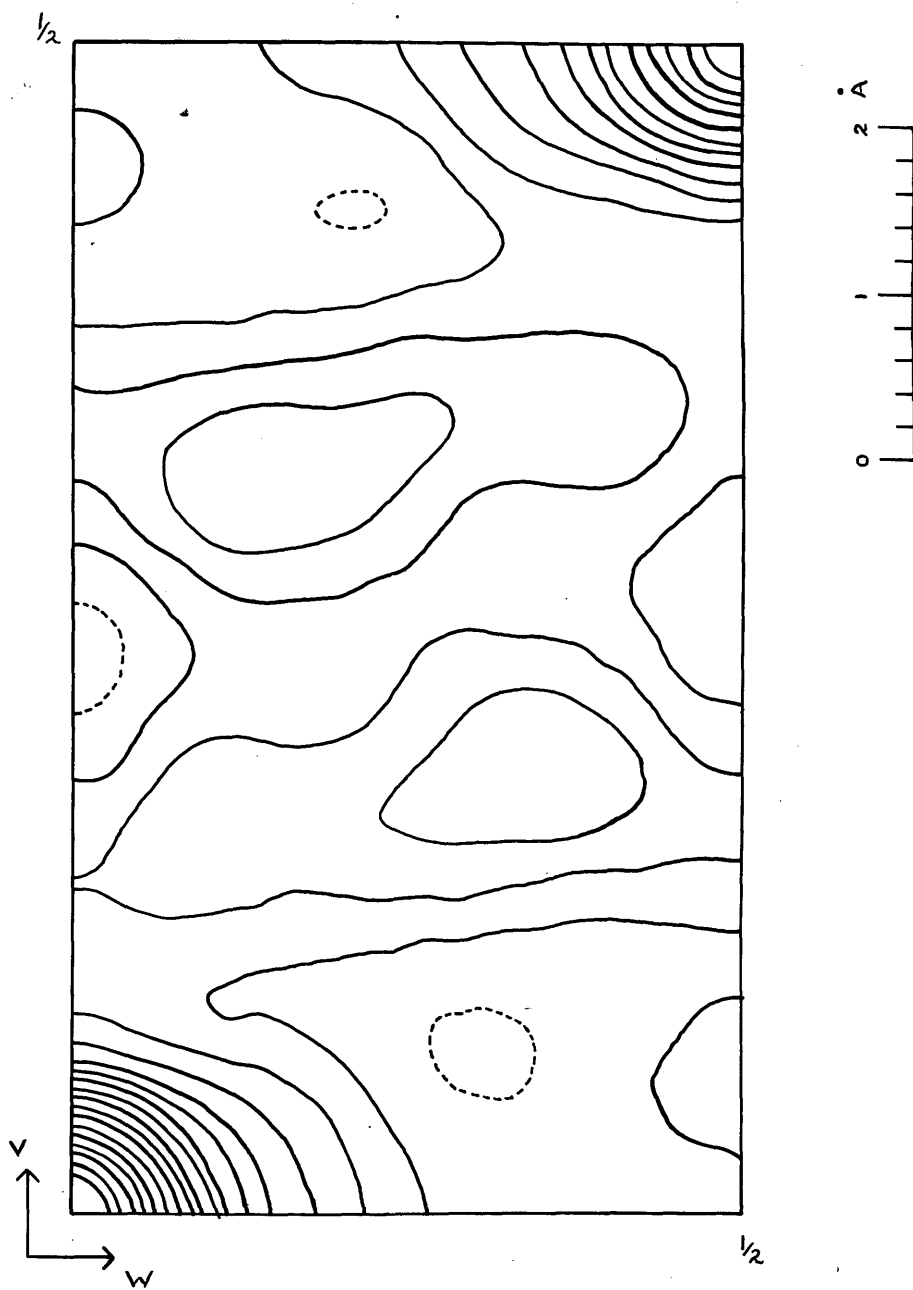


Fig.1. (100) Patterson projection for isoclovene hydrobromide.

the squares of the 123 observed structure amplitudes. The vector set space group,  $P2_1/m$ , (Buerger (1950)) has  $p$  mm. symmetry in this projection and hence the expression evaluated was:-

$$P(OVW) = \frac{1}{A} \sum \sum |F(Ok\ell)|^2 \cos 2\pi(kV + \ell W) \dots (3.1.)$$

The resulting Patterson map is depicted in Figure 1, the function having been evaluated from  $V = 0$  to  $V = \frac{1}{2}$  and from  $W = 0$  to  $W = \frac{1}{2}$ .

Since the positions of the two bromines within the real unit cell may be designated by co-ordinates  $(x, y, z)$  and  $(\bar{x}, \frac{1}{2} + y, \bar{z})$  the expected vector between these two atoms has components  $V = \frac{1}{2}$  and  $W = 2z$ . The largest peak on the map, other than the origin peak, represents the bromine - bromine vector. Unfortunately, this peak is not clearly resolved since it overlaps with the corresponding peak produced by the operation of the symmetry centre at  $V = \frac{1}{2}, W = \frac{1}{2}$ . The following co-ordinates were believed to represent a reasonable approximation for the peak maximum.

$$V = .500 \qquad W = .468$$

Hence the co-ordinates of the two bromine atoms in the unit cell were deduced as being:

$$Br_1 (y = .250, \quad z = .234) \qquad Br_2 (y = .750, \quad z = .766)$$

In the derivation of these positional parameters, it should be remembered that space group,  $P2_1$ , permits an

arbitrary choice of origin, and it is convenient for calculation purposes to choose this origin mid-way between the two bromine atoms.

In calculating structure factors for this projection the expressions evaluated were:

$$\begin{array}{ll}
 \text{for } k = 2n & A = 2 \cos 2\pi ky \cos 2\pi \ell z \\
 & B = 2 \sin 2\pi ky \cos 2\pi \ell z \\
 \\ 
 \text{for } k = 2n + 1 & A = - 2 \sin 2\pi ky \sin 2\pi \ell z \\
 & B = 2 \cos 2\pi ky \sin 2\pi \ell z \quad \dots(3.2)
 \end{array}$$

Hence, not only does the bromine atom in the asymmetric unit have zero contribution to the B part of each structure factor but also very small contributions to the class of reflections satisfying the condition  $k + \ell = 2n + 1$ . Therefore, phases (signs in this case) can only with certainty be ascribed to about half the observed structure amplitudes, the discrepancy over those terms satisfying the condition  $k + \ell = 2n$  being  $R = 36\%$ .

An electron-density projection on (100) was calculated using as Fourier coefficients those 68  $F_0$  terms deemed to be sign-determined by the bromine contributions. For a projection with plane group symmetry  $p g$  the expression to be evaluated is

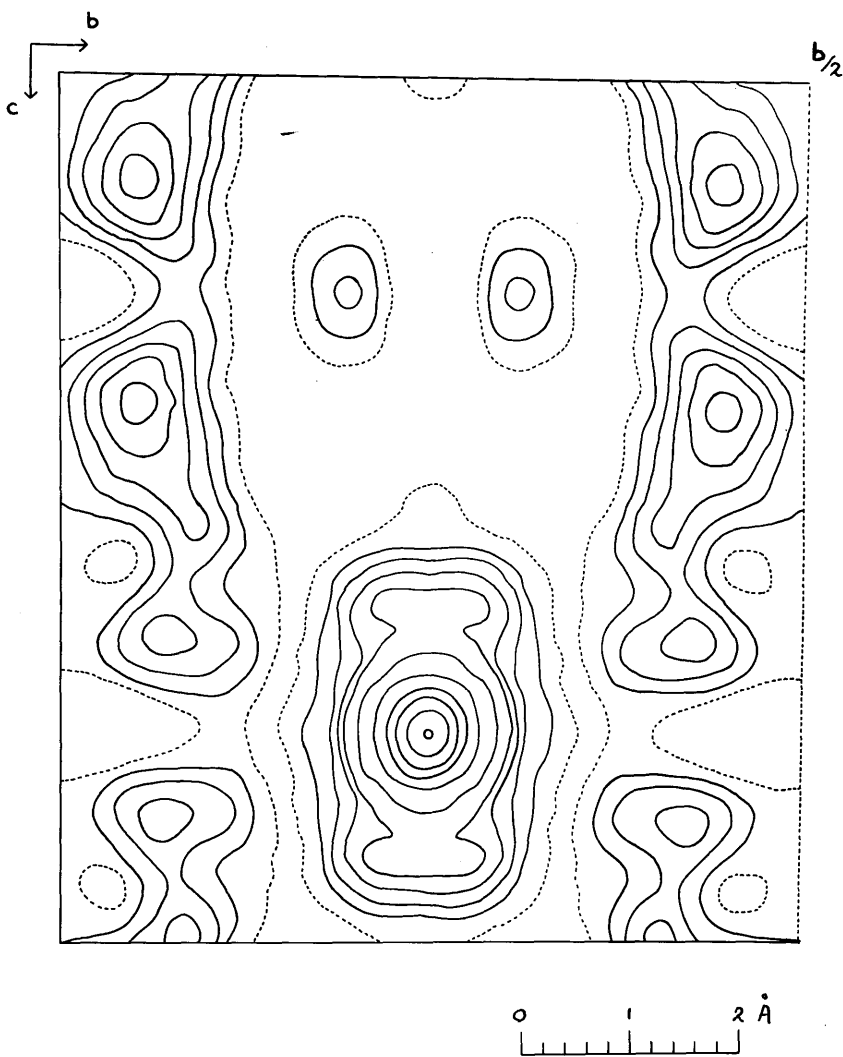
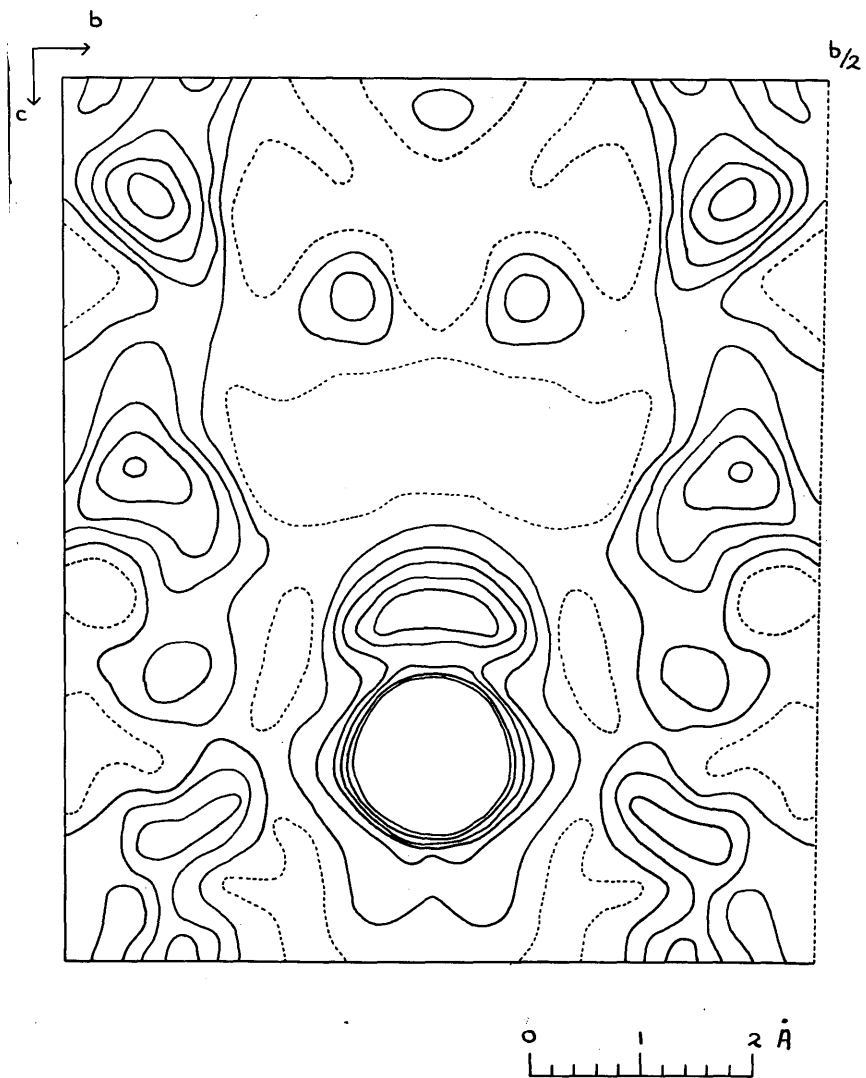


**Fig.2.** Electron density distribution projected on (100).  
 Contours at intervals of  $1 e \text{ \AA}^{-3}$ ,  
 the one-electron line being dotted.

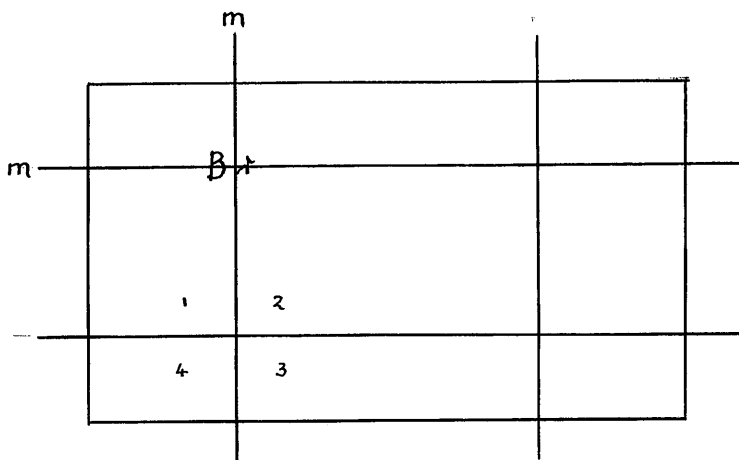
$$\rho(oyz) = \frac{1}{A_c} \left[ F(00) + 2 \left\{ \sum_k^{\infty} \left| F(ok) \right| \cos(2\pi ky - \alpha(ok)) + \sum_l^{\infty} \left| F(ol) \right| \cos 2\pi lz \right\} + 4 \left\{ \sum_k^{\infty} \sum_l^{\infty} \left| F(kl) \right| \cos 2\pi lz \cos(2\pi ky - \alpha(kl)) - \sum_k^{\infty} \sum_l^{\infty} \left| F(kl) \right| \sin 2\pi lz \sin(2\pi ky - \alpha(kl)) \right\} \right] \dots(3.3)$$

As signs and not general phase angles are used the resulting map possesses pseudo mirror planes at  $y = \frac{1}{4}$  and  $y = \frac{3}{4}$ , while as a consequence of including only those terms for which  $k + l = 2n$ , further pseudo mirror planes are generated at  $z = \frac{1}{4}$  and  $z = \frac{3}{4}$ .

Consequently the summation need only be effected for the range  $y = 0/60$  to  $15/60$  and  $z = 15/60$  to  $45/60$ . Thus, the original non-centrosymmetric projection is transformed into a centred plane group simulating c mm. symmetry. A four-fold ambiguity is thereby introduced into the electron density projection which is illustrated in figure 2. Diagram I schematically illustrates the fact that for every real atom at position 1, spurious peaks exist at positions 2, 3, 4.



**Fig. 3.** Second electron density distribution projected on (100).

Diagram I.

This added spurious symmetry precludes any resolution and it is difficult to envisage even how the molecule may be lying in this projection.

A second Fourier projection on (100) was computed with 33 additional terms included for which  $k + \ell = 2n + 1$ . This helped partially to destroy the mirror planes at  $z = \frac{1}{4}$  and  $z = \frac{3}{4}$  as is shown in figure 3, but the complexity of this electron-density map defeated all attempts at interpretation.

### 3.6 The (001) Projection.

As the basic symmetry of this projection is the same as that possessed by the a axis projection, the computational expressions are analogous to those described in section 3.5.

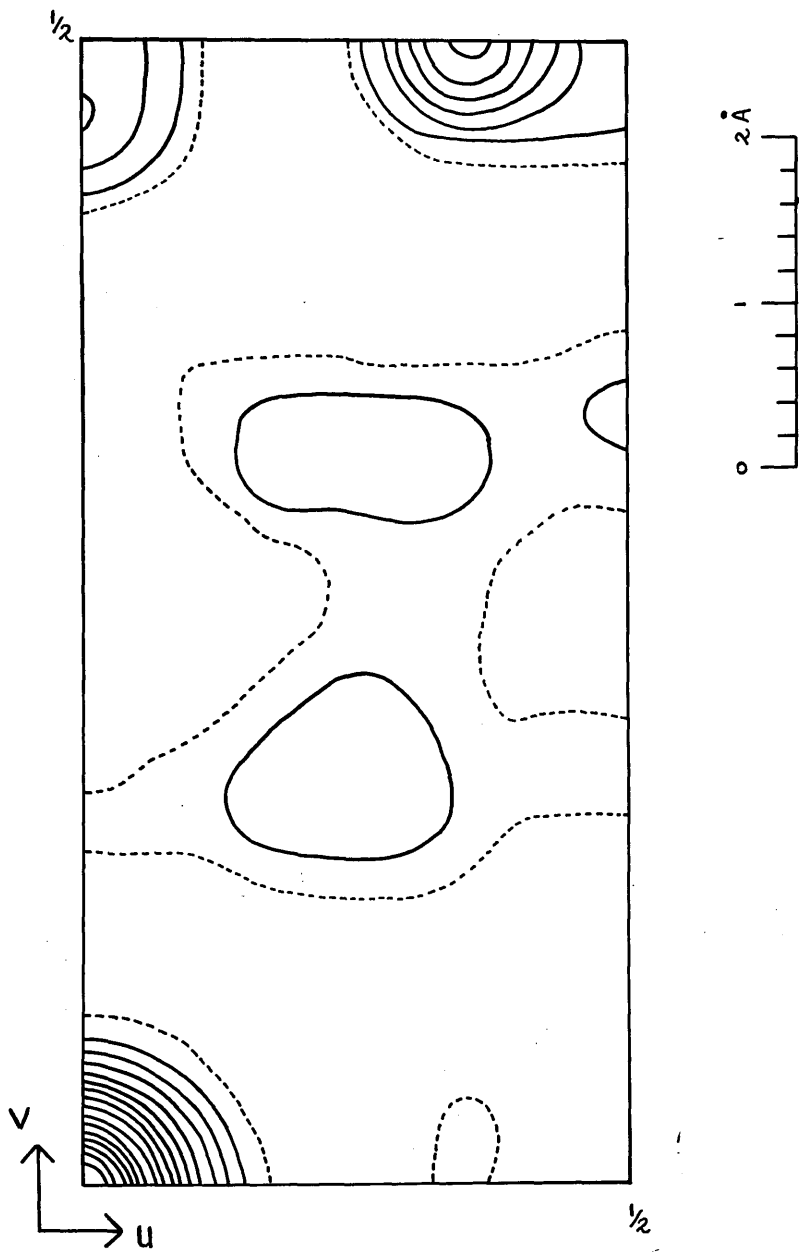


Fig.4. Projection of Patterson function on (001).

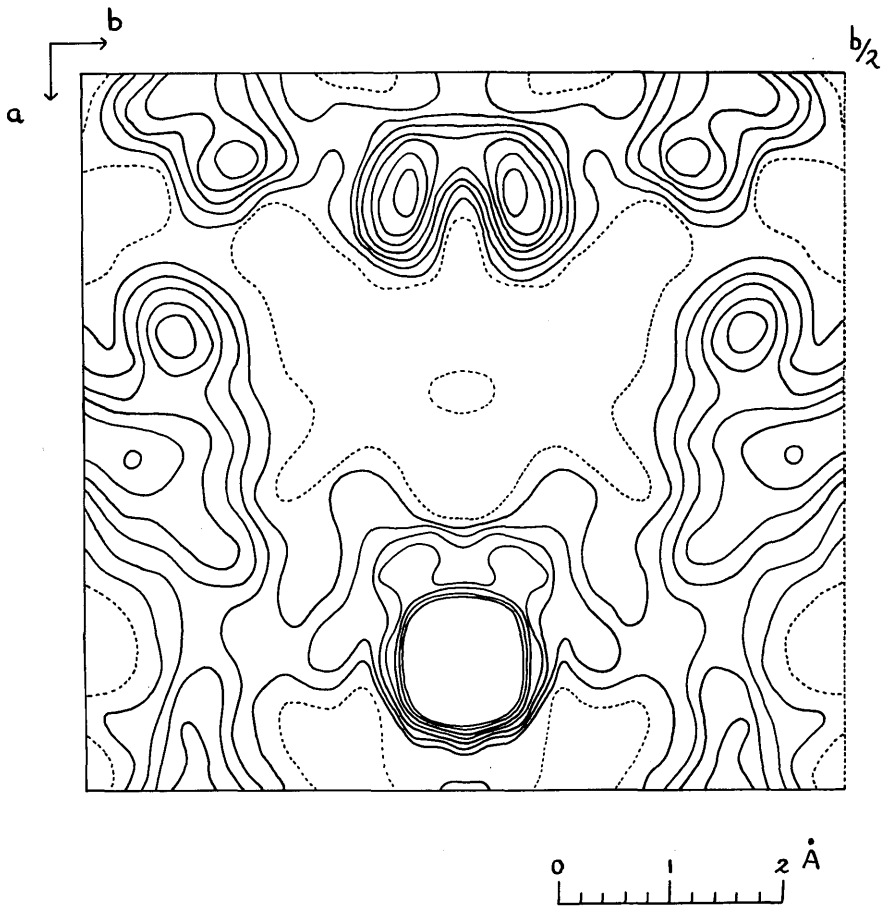


Fig.5. Projection of the electron density distribution on (001).

The Patterson projection, shown in figure 4, was first computed, whence the bromine atom co-ordinates could be deduced as being:

$$\text{Br}_1 \quad x = .175 \quad y = .250$$

$$\text{Br}_2 \quad x = .825 \quad y = .750$$

These results when combined with those deduced from the (100) projection yield the following co-ordinates for the positions of the two bromine atoms in the unit cell:

$$\text{Br}_1 \quad (.175 \quad .250 \quad .234)$$

$$\text{Br}_2 \quad (.825 \quad .750 \quad .766)$$

The bromine atom contributions to the structure factors for the (hk0) zone were calculated, giving an R factor of 34.5%. As previously, the B parts of the expressions reduce to zero but no further restrictions are imposed. Signs were allocated to 103 observed structure amplitudes which were used in the computation of the (001) electron density projection. The resulting map is illustrated in figure 5.

As with the (100) projection, pseudo mirror planes exist at  $y = \frac{1}{4}$  and  $y = \frac{3}{4}$ , with a resultant symmetry centre at  $x = \frac{1}{2}$ ,  $y = \frac{1}{2}$ . The symmetry of the projection is no longer pg but pmg, and the electron-density map may be said to contain a two-fold ambiguity, because for every real atom at (x,y) a spurious atom appears at  $(\bar{x}, \frac{1}{2} - y)$ .

In order to unravel the correct structure, judicious selection of one peak from two possibilities had to be made for every light atom in the structure. At this stage, these attempts to deduce an acceptable trial structure were not successful.

### 3.7. The (010) Projection.

From a purely crystallographic aspect, a projection of the electron-density onto the (010) plane has the advantage that no spurious symmetry will be introduced into the resulting map, because all the phases are 0 or  $\pi$ .

The bromine contributions to the structure factors were calculated (R = 49%). The electron-density projection on (010), shown in figure 6, was computed using 77 terms. Since this projection has plane group symmetry  $p_2$  the expression used was:

$$\rho(xoy) = \frac{1}{A_c} \left\{ F(00) + 2 \sum_h F(h0) \cos 2\pi hx + 2 \sum_l F(0l) \cos 2\pi lz + 2 \sum_h \sum_l \left[ F(hl) \cos 2\pi(hx + lz) + F(h\bar{l}) \cos 2\pi(hx - lz) \right] \right\} \dots\dots\dots(3.4)$$

As was not unexpected, the prohibitive length of projection did not permit any apparent resolution of the molecule to be achieved. No obvious chemical fragments could be discerned, and although trial and error methods were attempted no satisfactory interpretation of the electron density map in terms of plausible structures was obtained.

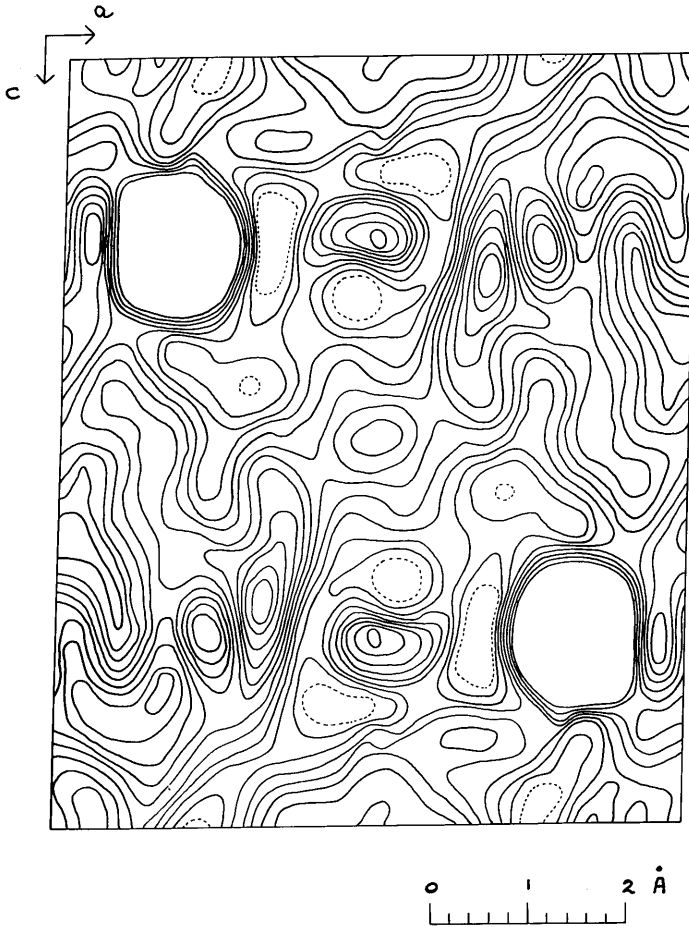


Fig.6. Projection of the electron density distribution on (010).

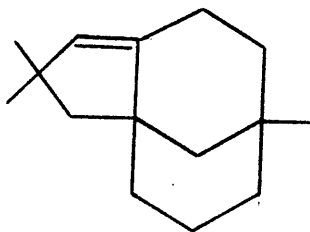
3.8. Attempted Correlation of the (hk0) and (h0 ) Projections.

It appeared, at this stage, that the best hope for trial-and-error analysis lay in studying two projections simultaneously, the unambiguous but unresolved (h0 $\ell$ ) projection and the ambiguous (hk0) projection.

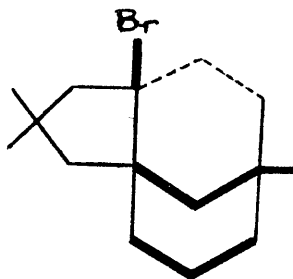
Two principal model compounds were systematically studied, structures (VIII) and (IX), section 2.2. Scale, ball and wire, models of these molecules were constructed and shadows of them were thrown by means of two parallel light beams at right angles onto the calculated electron density patterns, as in the analysis of the structure of penicillin by Crowfoot et al. (1949). When the best fit was obtained the atomic co-ordinates were recorded on a tracing paper overlay covering the (001) projection. Structure factor calculations were performed for a range of reflections in the (hk0) zone.

A wide variety of different conformations and orientations were tested, and an exhaustive trial of all possible variants was conducted.

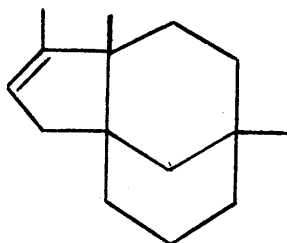
For example, in structure (IX) after normal addition of hydrogen bromide there are three asymmetric carbon atoms present in the molecule. There are, therefore, 8 possible isomers, but since enantiomers are not distinguished by X-ray methods unless under special



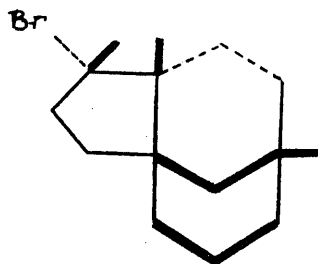
IX



XII



VIII



XIII

circumstances (Bijvoet (1949)) there are 4 distinct possibilities to be investigated. These consist of essentially 4 different ring forms. Non-Markownikoff addition of hydrogen bromide to the original double bond, while having a very small probability, was also considered. An overall agreement factor for the (hk0) zone of  $R = 29.6\%$  was obtained using structure (XII) as a basis.

For structure (VIII) again considering normal hydrogen bromide addition there are, in all, 16 stereoisomers, of which the 8 distinct (non-enantiomorphous) possibilities were investigated. A discrepancy of  $R = 26.2\%$  for the (hk0) zone of reflections was obtained with structure (XIII).

This latter figure appeared promising but the actual placement of atoms on the electron-density maps involved, in some cases, distortion of the recognised valency angles. Furthermore, care was necessary in gauging the importance to be attached to an R value in a case where the "heavy atom" was dominant and where some of the "light atoms" had almost certainly been placed on the correct sites. It was felt that the degree of approximation arrived at did not warrant the immediate application of the Fourier method of refinement.

### 3.9. Pseudo three-dimensional approach.

In an attempt to correlate the three projections at once and also to try and assist in the breakdown of the confusing spurious symmetry, a pseudo three-dimensional approach was suggested by Dr. G.A. Sim. This method was used by him, but without success, in the analysis of serine phosphate (personal communication; see also McCallum et al. (1959)) and is primarily of value in overcoming difficulties associated with the overlapping of atoms in projection. This technique entails the definition of the following function:

$$\rho\{\min(xyz)\} = \min\{\rho(xy), \rho(xz), \rho(yz)\} \dots (3.5)$$

There were no serious scaling problems involved since each zone of reflections had been scaled to the bromine atom contributions.

A three-dimensional grid was constructed, consisting of sections from  $x = 0/30$  to  $30/30$  each section covering the limits  $y = 0/60$  to  $15/60$  and  $z = 0/30$  to  $30/30$ . By considering the three projections simultaneously a figure could be allocated for the electron density at each grid point within the asymmetric unit. The resolution proved to be very poor. Nevertheless, a search was made for peaks at a distance of  $1.9 \overset{\circ}{\text{A}}$  from the bromine atom.

These were marked on separate sheets of tracing paper and a similar search was made for peaks  $1.5 \overset{\circ}{\text{Å}}$  away from and making suitable bond angles with these initially selected sites. Thereafter, the whole process was repeated using these new locations.

A survey of the resulting sections revealed that several plausible five membered rings attached to the bromine atom could be selected and, indeed, most had been considered in the trial structures already investigated. Lack of resolution prevented any other molecular features from being discovered.

### 3.10. Appraisal of the Results of the two-dimensional Analysis.

Although it did not prove possible to interpret the two-dimensional Fourier syntheses, computation of the latter did lead to a useful refinement of the bromine positions.



Also an effort was made at this juncture to circumvent these space group difficulties. In the hope that it might crystallise in a form belonging to a different space group, an attempt was made to prepare a hydroiodide derivative (Appendix 2), but it proved too unstable to be isolated as a crystalline product.

It was at this time, July, 1958, that it became known that computing facilities would be available by the end of that year, making it possible to plan a three-dimensional approach to the problem.

-----

TABLE 3.

Observed relative structure factors for the three principal zones of isoclovene hydrobromide.

h	k	l	F <sub>obs</sub>	F <sub>calc</sub>
1	0	0	1.00	1.00
2	0	0	0.95	0.95
3	0	0	0.90	0.90
4	0	0	0.85	0.85
5	0	0	0.80	0.80
6	0	0	0.75	0.75
7	0	0	0.70	0.70
8	0	0	0.65	0.65
9	0	0	0.60	0.60
10	0	0	0.55	0.55
11	0	0	0.50	0.50
12	0	0	0.45	0.45
13	0	0	0.40	0.40
14	0	0	0.35	0.35
15	0	0	0.30	0.30
16	0	0	0.25	0.25
17	0	0	0.20	0.20
18	0	0	0.15	0.15
19	0	0	0.10	0.10
20	0	0	0.05	0.05
21	0	0	0.00	0.00

TABLE 3.

Isoclovene Hydrobromide.

(Okℓ) zone.

F<sub>0</sub> on a relative scale.

hkℓ	F <sub>0</sub>	hkℓ	F <sub>0</sub>	hkℓ	F <sub>0</sub>	hkℓ	F <sub>0</sub>
020	82	031	187	071	127	0,11,1	36
040	140	032	59	072	42	0,11,2	19
060	211	033	66	073	50	0,11,3	38
080	26	034	41	074	28	0,11,4	9
0,10,0	35	035	71	075	38	0,11,5	21
0,12,0	35	036	13	076	7	0,11,7	9
0,14,0	18	037	35	077	17	0,11,8	10
0,16,0	9	038	8	079	5		
						0,12,1	9
001	56	041	44	081	24	0,12,2	22
002	117	042	107	082	51	0,12,3	10
003	43	043	12	083	32	0,12,4	24
004	84	044	54	084	56	0,12,6	9
005	8	045	12	085	10		
006	28	046	42	086	20	0,13,1	24
007	7	047	12	087	12	0,13,3	22
008	19	048	15	088	6	0,13,4	6
009	8					0,13,5	10
						0,13,6	5
011	194	051	102	091	69		
012	72	052	40	092	18	0,14,1	5
013	86	053	105	093	66	0,14,2	18
014	46	055	41	094	18	0,14,3	8
015	57	056	22	095	32	0,14,4	14
016	24	057	26	096	10		
017	27	058	6	097	11	0,15,1	16
018	8			098	7	0,15,2	8
019	8	061	51			0,15,3	15
		062	73	0,10,1	33	0,15,4	6
021	50	063	26	0,10,2	41		
022	172	064	52	0,10,3	9	0,16,1	6
023	45	065	18	0,10,4	19	0,16,2	10
024	106	066	22	0,10,6	13		
025	42	068	9	0,10,8	5	0,17,1	8
026	68	069	6				
027	17						
028	17						

TABLE 3. (Cont'd)

(hk0) zone.

hkℓ	F <sub>0</sub>						
100	74	210	43	410	72	640	29
200	66	220	167	420	29	660	39
300	109	230	86	430	48	670	21
400	55	240	77	440	15	680	23
500	24	250	89	450	66	690	12
600	58	260	52	460	37	6,10,0	13
800	4	270	72	470	40	6,11,0	4
		280	39	480	16	6,12,0	12
020	82	290	62	490	56		
040	154	2,10,0	19	4,10,0	7	710	31
060	227	2,11,0	70	4,11,0	38	720	9
080	24	2,12,0	17	4,12,0	10	730	27
0,10,0	36	2,13,0	20	4,13,0	23	750	19
0,12,0	36	2,14,0	11	4,14,0	8	760	9
0,14,0	18	2,15,0	17	4,15,0	16	770	26
0,16,0	10	2,16,0	7			780	8
		2,17,0	9	510	46	790	9
110	149			520	52		
120	136	310	50	530	50	810	9
130	111	320	139	540	33	820	10
140	44	330	12	550	37	830	11
150	108	340	112	560	23	840	12
160	74	350	7	570	31		
170	94	360	66	580	10		
180	47	370	37	590	32		
190	78	380	79	5,10,0	19		
1,10,0	23	390	15	5,11,0	16		
1,11,0	59	3,10,0	36	5,12,0	15		
1,12,0	18	3,11,0	12	5,13,0	12		
1,13,0	41	3,12,0	37				
1,14,0	15	3,13,0	8	610	16		
1,15,0	18	3,14,0	21	620	34		
1,16,0	7	3,15,0	10	630	12		
1,17,0	12	3,16,0	9				

- Cont'd -

TABLE 3. (Cont'd)

(h0l) zone.

hkℓ	F <sub>0</sub>						
100	73	201	82	306̄	28	602	23
200	73	202	146	307̄	26	603	26
300	110	203	73	308	10	604	28
400	53	204	5			605	14
500	24	205	34	401	99	606	10
600	53	206	34	402	58		
800	3	207	29	403	85	601̄	10
		208	12	404	20	602̄	32
001	54	209	15	405	22	603̄	9
002	112			406	6	604̄	39
003	44	201̄	115	407	15	606̄	15
004	86	202̄	47			607̄	4
005	10	203̄	100	401̄	78		
006	33	204̄	16	402̄	80	701	35
007	8	205̄	64	403̄	68	703	20
008	22	206̄	40	404̄	10	704	9
009	8	207̄	44	405̄	41	705	15
		208̄	18	408	14		
101	30	209̄	5			701̄	26
102	106			501	12	702̄	16
103	54	301	20	502	20	703̄	14
104	43	302	72	503	26	704̄	13
105	65	303	76	504	17	705̄	4
106	37	304	63	505	8		
107	41	305	11	506	22	802	13
109	10	306	28	507	11	803	9
		307	14				
101̄	53	308	4	501̄	67	802̄	14
102̄	55			502̄	37	803̄	8
103̄	145	301̄	100	503̄	40		
104̄	67	302̄	70	504̄	17		
105̄	44	303̄	43	505̄	23		
106̄	39	304̄	74	506̄	9		
107̄	13	305	23	507̄	8		
108	11			508	8		

CHAPTER IV.

The Three-dimensional Analysis  
of Isoclovene Hydrochloride.

IV. THE THREE-DIMENSIONAL ANALYSIS  
OF ISOCLOVENE HYDROCHLORIDE.

4.1. Introduction.

Although the value of the ratio  $z_{Cl}^2 / \sum z_j^2$  (section 3.2) suggests that the chlorine atom would not dominate the phases of a sufficient number of reflections to permit it to be used directly as a "heavy atom" for phase determination, the chlorine-chlorine vector should still be easily located in the three-dimensional Patterson function even without the prior knowledge supplied by the initial study of the bromo isomorph. The general plan evolved was to obtain some approximation to the electron-density by operating on the three-dimensional Patterson function with the Buerger minimum function.

Several reasons exist for the choice of the chloro derivative rather than the bromo compound. The former has the lower linear absorption coefficient indicating that it should be possible to obtain a more accurate intensity record. Diffraction effects due to the halogen atom would be less serious. In addition, a better refinement of the light atoms should be effected because of their greater relative contribution to each structure factor. This should also accelerate the breakdown of the inherent pseudosymmetry resulting from the placement

of the chlorine atoms on the planes  $y = \frac{1}{4}$  and  $y = \frac{3}{4}$ . Finally, and perhaps equally important, isoclovene hydrochloride is the more stable isomorph.

#### 4.2. Collection and Processing of the Experimental Data.

Photographic records of the intensities supplied by the following layer lines:  $(0k\ell)$ ...  $(5k\ell)$ ,  $(hk0)$ ...  $(hk4)$ ,  $(h0\ell)$ , were obtained using an equi-inclination Weissenberg goniometer. The intensities of the X-ray reflections were estimated visually using the multiple film technique and standard series of calibrated spots. For the film factor, a value of 3.3 was assumed, this being modified for upper layers by an obliquity factor due to Rossmann (1956), which takes into account the variation of film factor with angle of incidence. For every zone each individual intensity was estimated at least twice using a different step-wedge before the averaging process was performed. Crystal specimens cut to the following dimensions (cross-section x length) were used:

.2 x .2 x .4 mm.<sup>3</sup> for the  $(nk\ell)$  set of series,  
.25 x .3 x .2 mm.<sup>3</sup> for the  $(hkm)$  set and  
.4 x .3 x .15 mm.<sup>3</sup> for the  $(h0\ell)$  series.

In Table 4 are listed some of the data relevant to this section.

TABLE 4.

Zone	$\mu_e$ (equi- inclination angle)	No. of reflections recorded	No. of possible reflections	Film factor	Ratio of strongest to weakest intensity
0kl	0°	79	150	3.30	5,500
1kl	6° 58'	192	298	3.30	4,400
2kl	14° 3'	182	292	3.40	1,800
3kl	21° 20'	142	280	3.54	1,350
4kl	29° 3'	158	264	3.78	500
5kl	37° 18'	124	240	4.13	110
hk0	0°	113	121	3.30	8,700
hk1	5° 36'	123	242	3.30	6,900
hk2	11° 16'	94	238	3.36	700
hk3	17° 3'	113	233	3.46	570
hk4	23° 1'	70	225	3.53	50
h0l	0°	95	142	3.30	4,500

#### 4.3. Correction and Correlation of Intensities.

The averaged observed intensities were corrected for the usual Lorentz and polarisation factors as well as for the Tunell (1939) rotation factor. An " $\alpha$ -code" programme for Deuce devised by Dr. T.A.Hamor was used for this purpose. No absorption corrections were made.

There now existed sets of data from different zones of the reciprocal lattice, each set being on a different scale. Placing these reflections on the same scale was achieved by first correlating each series of the  $(nkl)$  group using the appropriate members of the  $(hkm)$  group of series thus:

A value  $F_1 = \sum_k |F(nk0)|$  for each  $n = 0 \dots 5$  was determined from the  $(nkl)$  series, and, similarly,  $F_2 = \sum_k |F(hk0)|$  for each  $h = 0 \dots 5$  from the  $(hk0)$  data.

$K(nk0) = \left\{ F_2 / F_1 \right\}_{n=h=0\dots 5}$  were determined and also  $A_0 = \sum_{n=0}^5 F_2$ ,  $B_0 = \sum_{n=0}^5 F_1$  and  $S_0 = A_0 / B_0$

Each  $K(nk0)$  was a factor suitable for placing each  $(nkl)$  series on the same scale as the  $(hk0)$  series.

In the same way, using the  $(nkl)$  series with the  $(hkl)$  zone there were determined  $K'(nkl) = \frac{\left( \sum |F(hkl)| \right)}{\left( \sum |F(nkl)| \right)}_{h=n=0\dots 5}$

$A_1$ ,  $B_1$  and  $s_1$

$K(nkl) = K'(nkl) \times S_0 / s_1$  so that the scaling is referred to the  $(hk0)$  series.

This procedure was performed with successive members of the (hkm) group. 5 Factors for each  $K_{(nkl)}$  were obtained. Ideally these should have been equal. An average scaling factor  $\bar{K} = \frac{1}{5} \sum K_{(nkl)}$  was used.

Similarly, scaling factors to place each (hkm) set of data on the same scale as the (Ok $\ell$ ) zone were derived. These factors  $\bar{K}'_{(hkm)}$  were used to derive factors  $\bar{K}_{(hkm)}$  consistent with the  $\bar{K}_{(nkl)}$  group.

The 1,485 measured reflections were thus placed on the same relative scale. Where more than one estimate of a particular  $F_0$  value was made then these values were averaged. The 976 independent reflections so obtained were set onto an approximately absolute scale by comparing the observed values for the (hk0) zone with values calculated for that zone. The latter were computed on the assumption that there was strict isomorphism with the trial structure deduced for isoclovene hydrobromide which gave an R value of 26.2% for the (hk0) zone of reflections (section 3.8).

$\sigma(F_i)$  values were evaluated for the 389 structure amplitudes observed more than once (Lipson and Cochran (1953), p.286) and the mean standard deviation was found to be an approximately constant percentage of its numerical value,  $\sigma(F_i) \approx .09 |F_i|$ .

4.4. The Three-dimensional Patterson Synthesis.

Sharpening of a Patterson function is a process whereby greater weight is ascribed to reflections in the middle and higher ranges of  $\sin \theta$ , and less weight to the low order terms. The modification function used in the present work, shown in Fig.7, was devised and has been successfully used by Dr. H.N. Shrivastava (1960) in his two-dimensional analysis of potassium p-nitrobenzoate. (To be published.)

The three-dimensional sharpened Patterson function was evaluated over the repeating volume of a  $x^{b/2} \times c/2$  at intervals of  $a/30$ ,  $b/48$  and  $c/30$ . The function  $P(xyz)$  was computed using expression (4.1) in sections perpendicular to the unique b axis.

$$P(xyz) = \frac{4}{V} \sum_{h=0}^{\infty} \sum_{k=0}^{\infty} \left\{ |F(hk\ell)|^2 \cos 2\pi(hx + \ell z) + |F(hk\bar{\ell})|^2 \cos 2\pi(hx - \ell z) \right\} \cos 2\pi ky \dots (4.1)$$

The values of the sharpened function at each point on the 25 computed sections were recorded on a tracing paper grid. Contours at specific levels were drawn by subjective interpolation. The Harker section of this function is illustrated in Fig.8. Although the peaks due to the chlorine-chlorine vectors were easily discerned they were still unresolved and a reasonable approximation

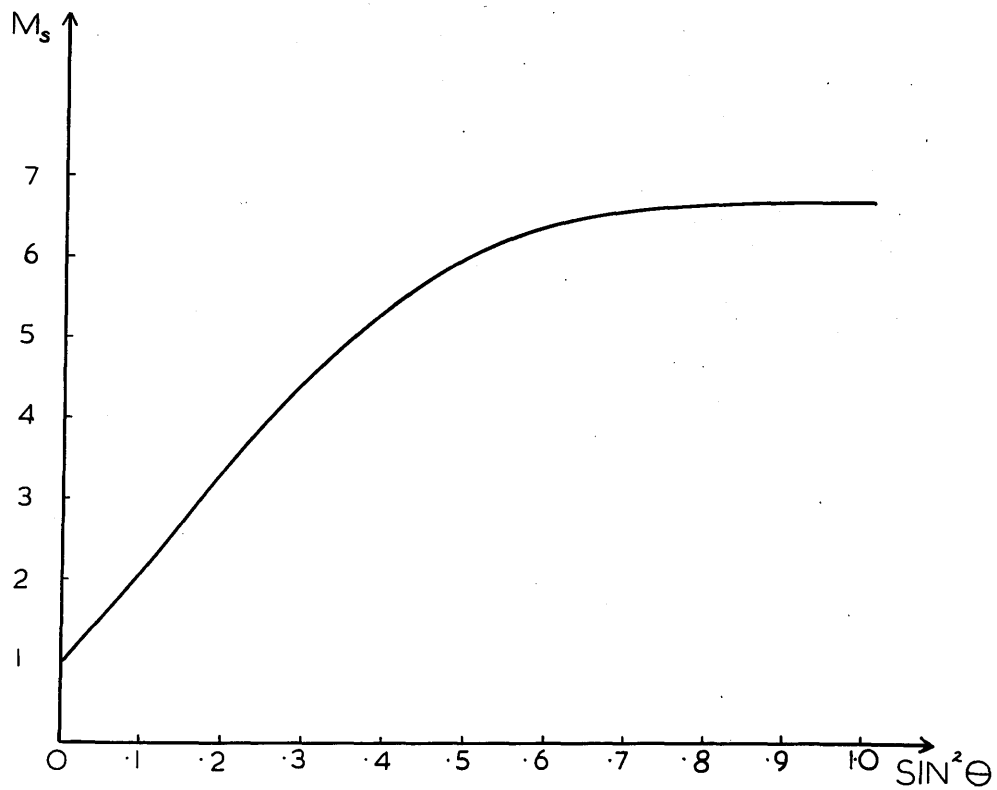
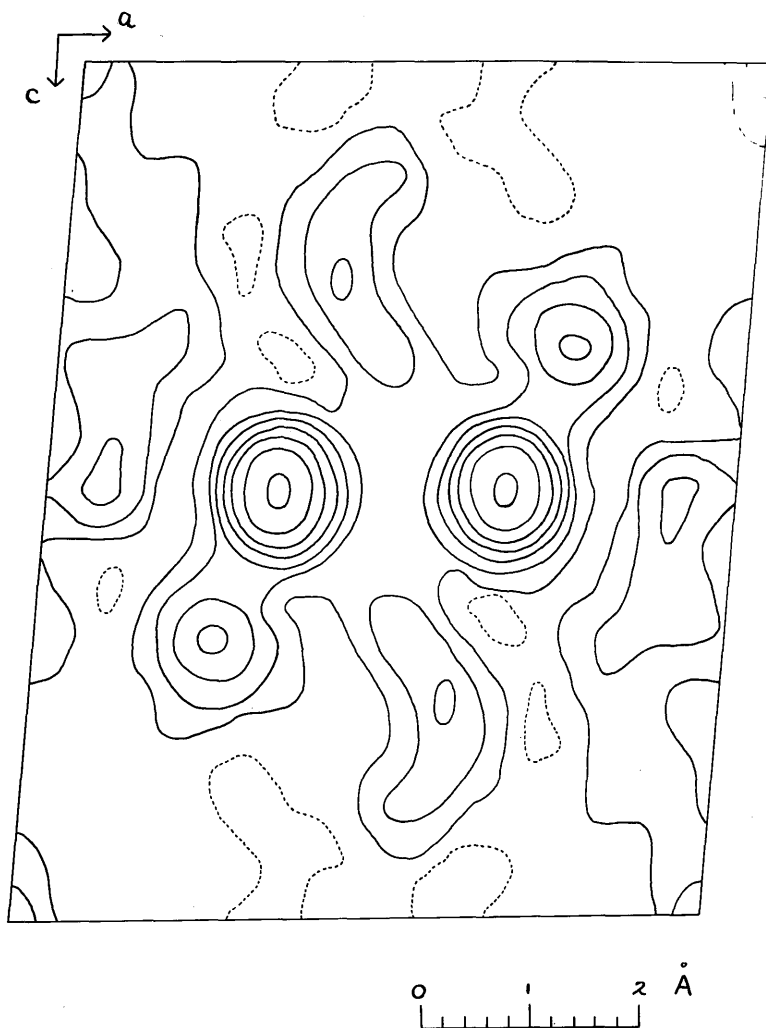


Fig.7. Modification function used in 3-dimensional Patterson synthesis.



**Fig.8.** Harker section of the three-dimensional Patterson function.

for the co-ordinates of the chlorine atom in the asymmetric unit had to be advanced.



(In this case, a different origin has been selected from that used in Chapter III.)

#### 4.5. The Buerger Minimum Function.

Patterson sections covering the area of several unit cells were traced out and duplicated using differently coloured crayon for specific levels. Since the chlorine-chlorine vector was the most pronounced peak this was used as a line image. Now, if the co-ordinates of the two chlorine atoms in the real cell are  $(x \ y \ z)$  and  $(\bar{x}, \frac{1}{2} + y, \bar{z})$  then the vector produced by them will give rise to a peak on the Patterson map at  $(2x, \frac{1}{2}, 2z)$ . Thus, when the chlorine-chlorine vector peak is superposed on the origin peak, the origin of the resulting minimum function will be placed mid-way along this displacement. Thus, when the Patterson section  $y = 0/48$ , containing the origin peak is superposed on the Patterson section  $y = 24/48$  containing the chlorine-chlorine vector peak, this gives rise to section  $y = 12/48$  in the minimum function. A contoured map of this latter function was derived by superposing, with the appropriate displacement, the two

transparent contoured Patterson sections,  $y = 0/48$  and  $y = 24/48$ . A third transparent sheet was laid on top and the drawing of contours for the minimum function was performed using the technique advocated by Buerger (1951). In an analogous manner Patterson sections  $y = 1/48$  and  $y = 23/48$  were superposed giving section,  $y = 11/48$ , of the minimum function. Thirteen sections in all were obtained,  $y = 0/48 \dots 12/48$ .

Now, the minimum function, M, so formed is based on a pair of atoms related by a symmetry operation other than a centre, and it is a consequence of vector set theory, that, if the crystal is non-centrosymmetric, then a centre of symmetry is added to the symmetry of the electron-density as approximated to by the minimum function. In other words, by using a line image of the above type a "reduced map" is obtained possessing a pseudo mirror plane at  $y = \frac{1}{4}$  (and  $y = \frac{3}{4}$ ). The overall asymmetric unit, therefore, contains an approximate representation of the molecule and its superimposed mirror image with "real" light atoms at (1)  $x y z$  (2)  $\bar{x}, \frac{1}{2} + y, \bar{z}$  accompanied by spurious atoms at (3)  $\bar{x} \bar{y} \bar{z}$  (4)  $x, \frac{1}{2} - y, z$ . Of these, atoms (1) and (4) and atoms (2) and (3) are related by the pseudo mirror planes sited at  $y = \frac{1}{4}$  and  $y = \frac{3}{4}$ , so that selection

of a y co-ordinate for any light atom in the structure is restricted to choosing between  $\frac{1}{4} + Y$  and  $\frac{1}{4} - Y$ , where  $Y = \frac{1}{4} - y$ .

#### 4.6. Interpretation of the Minimum Function.

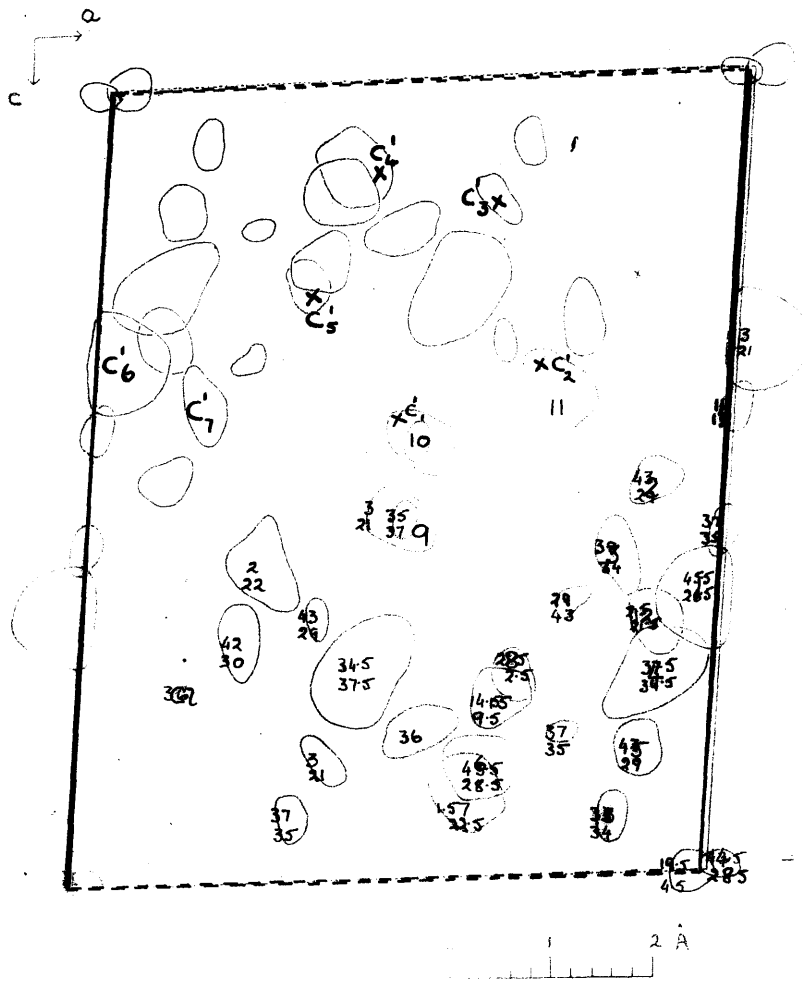
In an attempt to unravel this ambiguity a three-dimensional model was constructed. A large sheet of cardboard was taken to represent the (xOz) plane. On this were marked the x and z co-ordinates of the peaks in the minimum function unit cell. Holes were bored at these sites and through these holes were threaded lengths of string weighted at their lower extremities by pieces of lead. For each (x, z) pair of co-ordinates there were two possible y co-ordinates, represented by pieces of plasticine stuck to the string. The whole arrangement was then supported on a metal framework thereby giving a three-dimensional representation of the whole unit cell which incorporated the two screw-axis related molecules and their mirror images. Attempts were made to recognise possible ring systems and, although several plausible but unconnected carbocyclic rings could be isolated, this approach proved, on the whole, more confusing than helpful and was abandoned in favour of an alternative strategy.

A composite diagram was constructed by projecting the three-dimensional sections onto the basal, (010), plane and the two possible y co-ordinates for each peak were noted on the diagram. Several unit cell areas were drawn out and consideration of the van der Waals distances enabled the projected region occupied by two molecules (and their mirror images) to be delineated. This is shown in Figure 9.

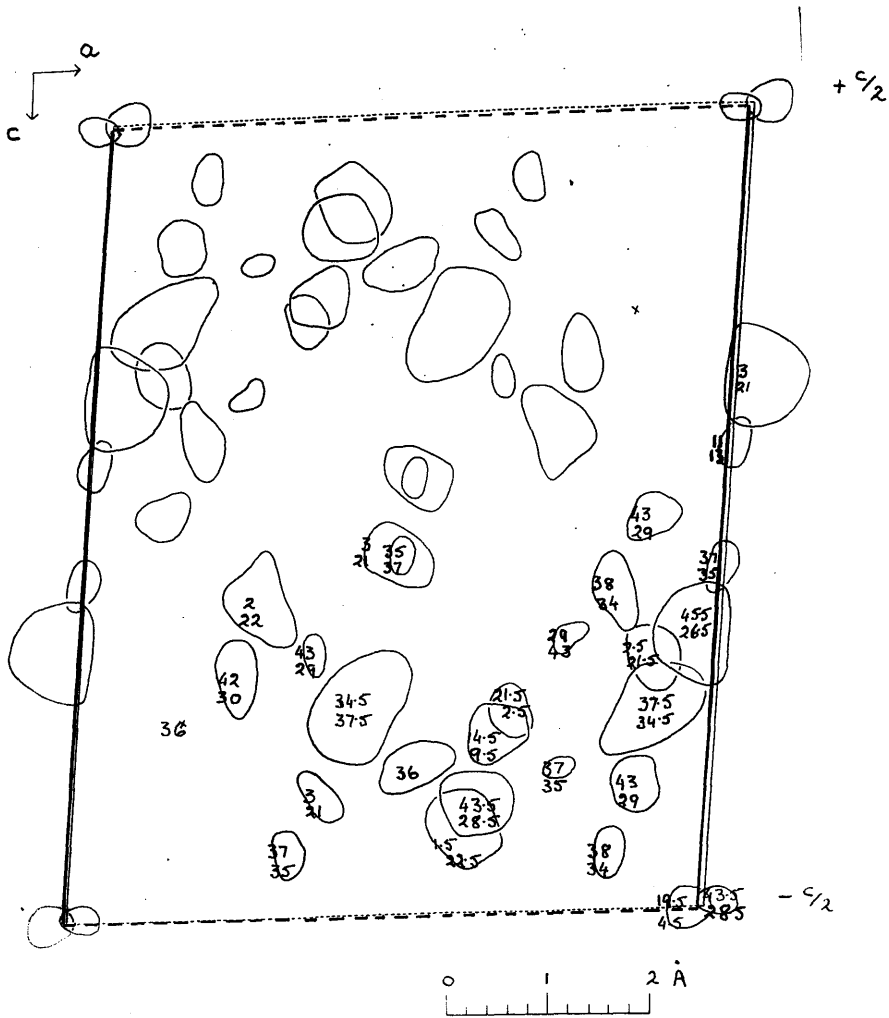
All preconceived notions regarding the possible molecular structure were ignored, and interpretation was attempted merely by recognising the restrictions imposed by adherence to proper bond lengths and angles. An obvious five membered ring ( $C_1'$ ,  $C_2'$ ,  $C_3'$ ,  $C_4'$ ,  $C_5'$  indicated in overlay to fig.9) could be picked out on fig.9.

Calculation of three dimensional structure factors (S.F.2) based on the contributions of the chlorine atom and the carbon atoms of this ring gave an R value of 38.8%. The scattering factors of James and Brindley (1932) for chlorine and Berghuis et al. (1955) for carbon were used, while isotropic temperature factors of  $4.4 \text{ \AA}^2$  for chlorine and  $3.5 \text{ \AA}^2$  for carbon were assumed.

Since the R value for the chlorine contributions alone is 47.4% (S.F.1) it was decided to calculate a triple Fourier synthesis,  $\rho_1$ , on the basis of these



Overlay to Fig.9.  
 Numbering System adopted in Sections 4.6 and 4.7.  
 Record of two possible y co-ords (in Å) for all peaks in the asymmetric unit.  
 The y co-ords of the other peaks are obtained by operation of the screw axis.



Overlay to Fig. 9.  
 Composite diagram illustrating the projection  
 Record of two possible y co-ords in 480 Å for all  
 peaks in the three-dimensional sections of the  
 minimum function onto the (010) plane.  
 The y co-ords of the other peaks are obtained by  
 operation of the screw axis.

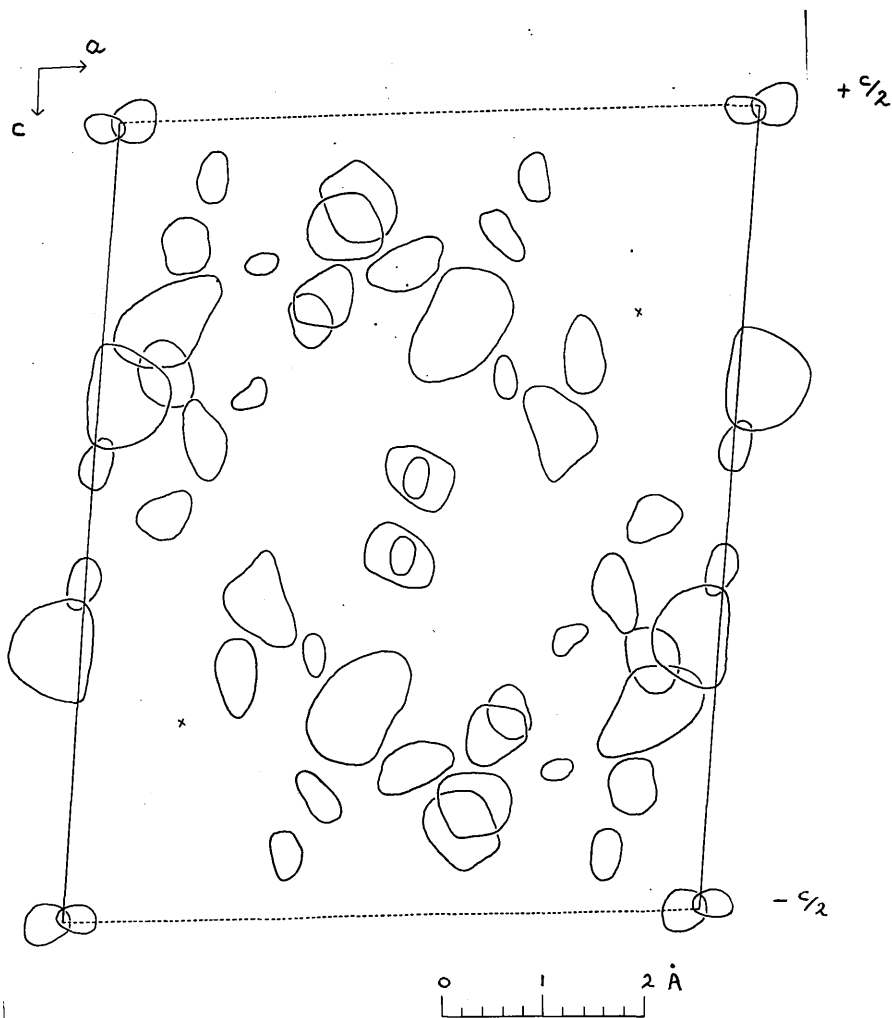


Fig.9. Composite diagram illustrating the projection of the three-dimensional sections of the minimum function onto the (010) plane.

phases calculated in (S.F.2) in sections perpendicular to the b axis at intervals of  $1/48$  from  $y = 0$  to  $y = 1/2$ , with intervals of subdivision of  $1/30$  along the entire lengths of a and c. The map of  $\rho 1$ , like all subsequent maps, was drawn out on tracing paper sheets by subjective interpolation in the calculated electron-density figure field. A survey of the 25 sections revealed that all the peaks other than those used for the phasing calculations were accompanied by their mirror image peaks. Further, only C'<sub>3</sub> of those atoms inserted did not possess a spherical shape. All 5 carbon atoms rose to peak heights of about 5 electrons/ $\text{\AA}^3$ . Two additional atoms, C'<sub>6</sub> and C'<sub>7</sub>, were included in a structure factor calculation, (S.F.3), prior to the computation of a further three-dimensional electron density map,  $\rho 2$ . In this map there were no further sites indicating the position of "real" carbon atoms, each unincluded peak being accompanied by a mirror-image peak of equal height. C'<sub>3</sub> still had an unacceptable shape.

Since there was no further breakdown in the pseudo-symmetry, an ab initio approach was preferred to the possibility of phasing other Fourier syntheses on the basis of an alternative five membered and six membered ring. Retrospective examination indicated that these rings did, in fact, constitute parts of the true molecular structure.

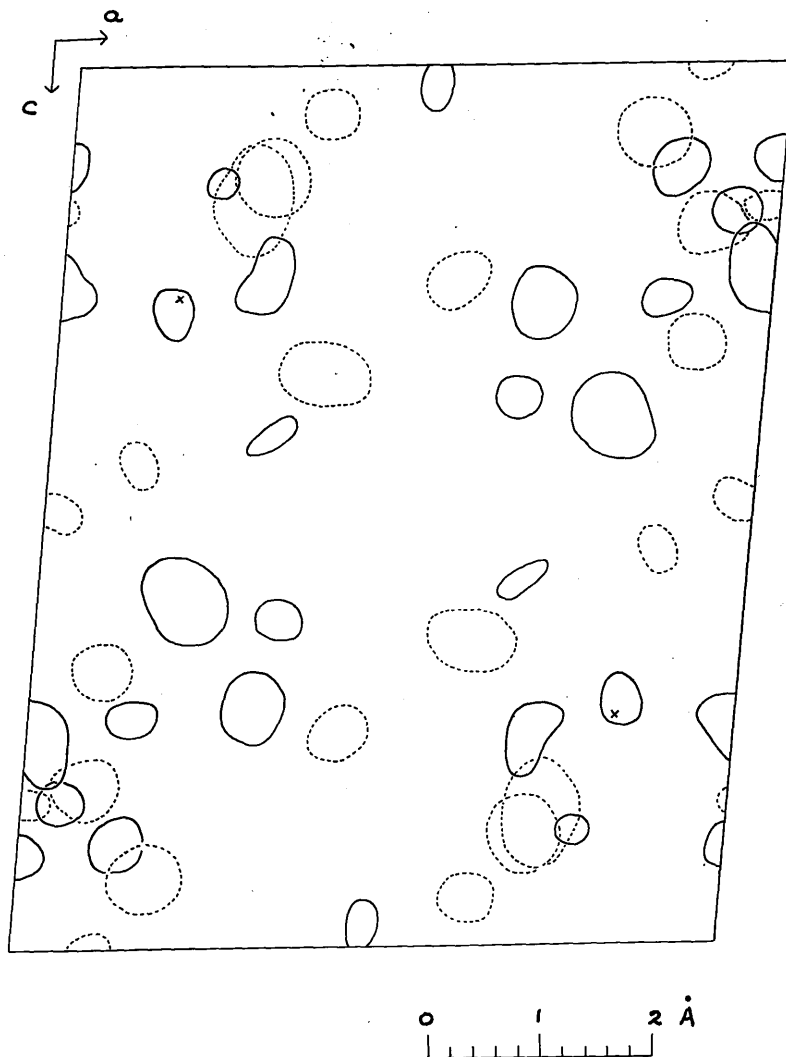


Fig.10. Composite diagram of triple Fourier series computed on heavy atom phases. X marks position of the chlorine atom. Dotted contours indicate peaks with heights  $>1e\text{\AA}^{-3}$  but  $<2e\text{\AA}^{-3}$ . Full contours indicate peaks with heights  $>2e\text{\AA}^{-3}$ .

#### 4.7. Objective Approach to Structure Elucidation.

This entailed computation of the three dimensional Fo synthesis, F1, using 885 terms based solely on the chlorine atom phases. The result, shown in Fig.10 as a composite diagram, is essentially analogous to the minimum function "reduced map" only the weighting system may be said to differ and the maxima, as expected, were less well resolved and more spurious peaks existed. As an aid in rejecting suspected spurious peaks the centrosymmetric (hOl) projection was computed on the basis of the chlorine signs (Fig.11). As a result of comparing the (010) projection and F1 several peaks in the latter could be labelled as dubious.

The composite diagrams of F1 and the "reduced map" of the minimum function, M, were then carefully scrutinised and the correspondences were recorded on a separate sheet of tracing paper. The criteria of greatest peak height and best approach to spherical shape were then used in selecting the most prominent corresponding peaks as representing the most likely atomic sites. Of course, for each peak there still existed two possible y co-ordinates. From the spatial distribution of the selected peaks it appeared that the molecule did not straddle the pseudo mirror planes, a feature which aided in the ultimate solution of the problem.

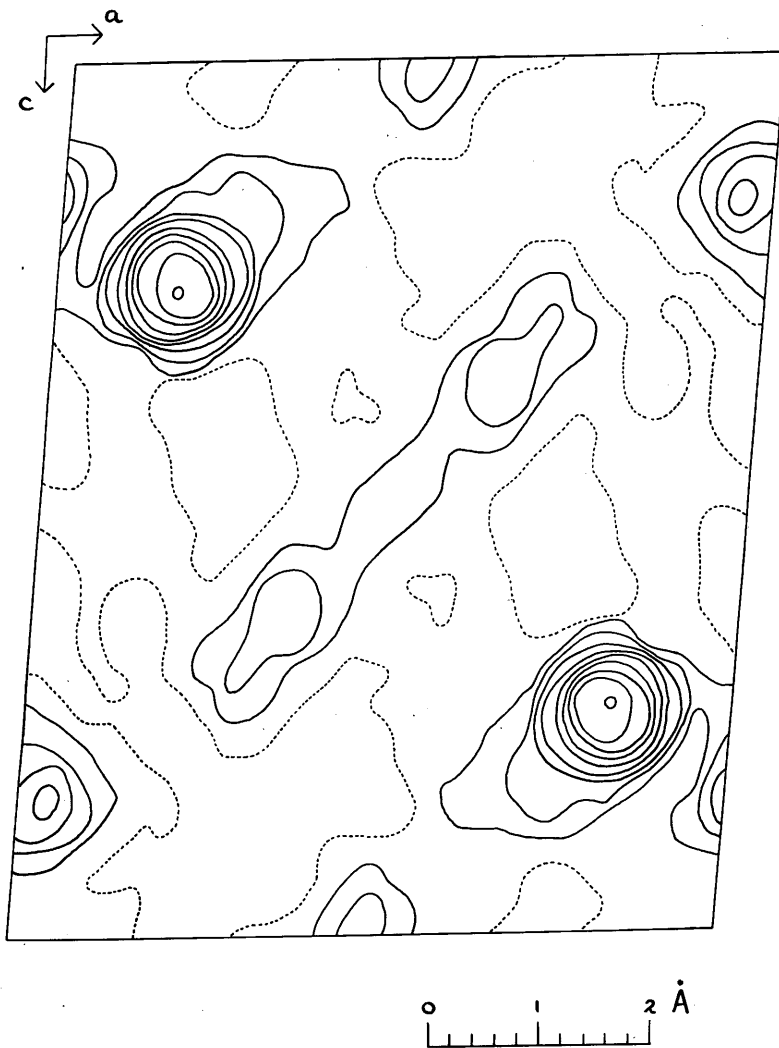


Fig.11. Electron density projection on (010).

Two lines of approach were then instituted.

1) Attempts were made to discover how, all peaks considered, these plausible sites could be linked together while paying proper attention to bond length and bond angle restrictions. It was possible in this way to deduce a partial structure incorporating the following atoms:

Cl      C<sub>1</sub> C<sub>2</sub> C<sub>3</sub> C<sub>4</sub> C<sub>5</sub> C<sub>6</sub> C<sub>7</sub> C<sub>8</sub> C<sub>12</sub> C<sub>13</sub> C<sub>15</sub>

(Fig.9 and Fig.12)

Calculation of structure factors for the 976 observed terms gave an R factor of 38.8%, a value equal to that obtained with the originally considered five membered ring and chlorine. Since this previous work had shown that the incorporation of recognisable chemical features into the phasing calculations tended to retard rather than accelerate progress it was considered preferable to adopt the most objective approach available.

2) The 5 most prominent peaks on both M and Fl, viz. C<sub>4</sub>, C<sub>1</sub>, C<sub>6</sub>, C<sub>15</sub>, C<sub>9</sub> (Fig.9 and Fig.12) were selected as being the most likely locations for carbon atoms. From a consideration of the dimensions of possible molecular models and from the disposition of these peaks it seemed evident that they were sited entirely on the same side of the mirror plane at  $y = \frac{1}{4}$ . It was also possible to

select two further atoms, C<sub>8</sub> and C<sub>12</sub>, which though slightly less prominent could possibly be bonded to members of the originally selected set.

These 7 carbon atoms plus the chlorine atom were the basis for the phasing calculations used for triple Fourier synthesis, F2. Examination of this map revealed that the inserted carbon atoms had peak heights of between 5 and 6 electrons/Å<sup>3</sup> and were all of acceptable shape. There was virtually no trace of their mirror image peaks. The next highest group of peaks, having peak heights of between 1 and 2 electrons/Å<sup>3</sup> and accompanied by their mirror images, was then examined in the light of this shape-height criterion.

For the next cycle of structure factor calculations, four additional carbon atoms seemed worthy of inclusion. The value taken for the y co-ordinate depended on the slight difference in peak height between the "real" and the "spurious" peak, e.g. the atoms chosen had the following peak heights (mirror image peak height in brackets):

C <sub>3</sub>	1.7 electrons/Å <sup>3</sup>	(unspecified due to proximity to mirror plane)
C <sub>2</sub>	1.5 electrons/Å <sup>3</sup>	(1.1 electrons/Å <sup>3</sup> )
C <sub>7</sub>	1.2	" " (1.0 " " )
C <sub>13</sub>	1.3	" " (1.0 " " )

Atom C<sub>9</sub> was excluded from this cycle because there was a corresponding mirror image peak 1.1 electrons/Å<sup>3</sup> in height. There was also another reason for omitting this peak (vide seq.).

A survey of the results at this stage seemed to indicate that the presence of a six and a five membered ring was well-nigh certain. Speculation regarding the nature of the third ring was now restricted to the belief that ring closure must be effected beyond the line  $z = 0$  (Fig.9). If the remaining ring were six membered then possible bond lengths would be of the order of 1.8 Å, a value much greater than that expected, viz. 1.54 Å; a seven membered ring seemed distinctly possible if an atom were located at the mirror image position to C<sub>9</sub>. To test this latter hypothesis, C<sub>9</sub> was omitted from the next cycle.

Hence 10 carbon atoms were involved in the phasing calculations preceding the evaluation of F3. A survey of the resulting map showed that the following atoms should be included in the next cycle.

C <sub>5</sub>	1.1 electrons/Å <sup>3</sup>	(.9 electrons/Å <sup>3</sup> )	
C <sub>9</sub>	1.7	" "	(1.9 " " ≡ C <sub>10</sub> )
C <sub>10</sub>	1.9	" "	(1.7 " " ≡ C <sub>9</sub> )

In F2 and F3 it was observed that a spurious cylinder of electron density rising to two electrons/ $\text{\AA}^3$  existed on section  $y = 12/48$ . The main axis of this cylinder was along the line  $z = \frac{1}{4}$  and ran for the entire length of  $x$ . A similar effect has been observed by Pitt (1952) in his refinement of the penicillin structure, and is probably a diffraction effect. Another interesting feature in F3 is that  $C_{14}$  (which was not included in the next cycle) had a mirror image peak  $1.2 \text{ e}/\text{\AA}^3$  in height while the true peak only rose to  $1.0 \text{ e}/\text{\AA}^3$ . Rossmann and Lipscomb (1958) have reported a similar observation.

The results at this stage seemed to indicate that a seven membered ring was present but the positions of the methyl groups were still uncertain.

Two further Fourier syntheses F4 and F5 sufficed to indicate the complete molecular structure. The course of the structure determination is illustrated in Table 5.

From F5 accurate co-ordinates for all the carbon atoms and the chlorine atom were obtained by Booth's (1942) method of interpolating in a figure field. A further triple Fourier series, F6, was computed using the phases calculated from these new parameters.

Figure 12.

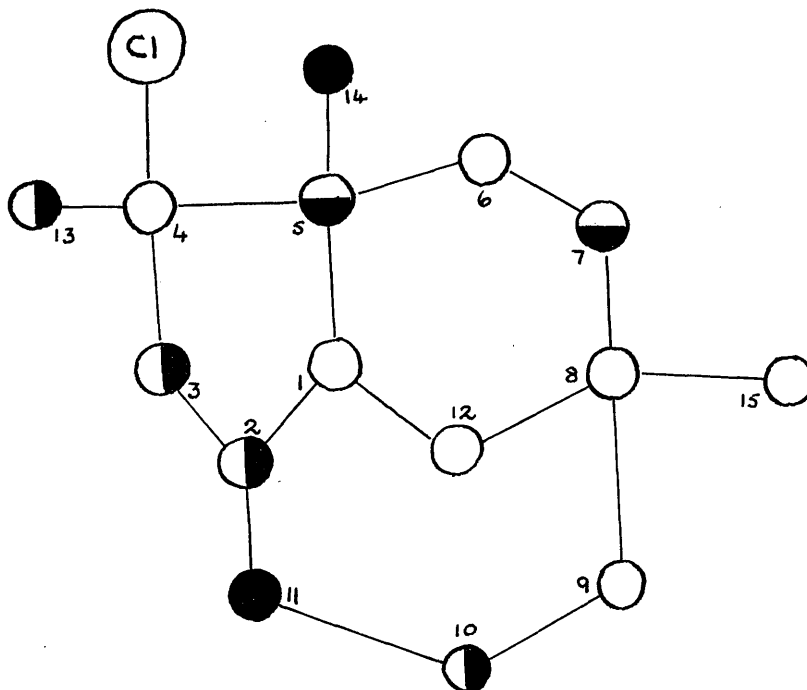


Fig.12. Numbering of the atoms in the molecule of isoclovene hydrochloride.

The drawing illustrates the process of selection of the atomic positions. Atoms shaded according to the stages at which they were accepted into the structure factor calculations (see Table 5.).

TABLE 5.

No. of atoms included in S. F. calculations	Symbol (fig. 12)	R	No. of terms used in Fourier Synthesis.	Fourier Synthesis
C1	C1	47.4%	885	F1
(C1) + 7C	○	40.2%	614	F2
(C1 + 7C - C <sub>9</sub> ) + 4C	◐	38.7%	776	F3
(C1 + 10C + C <sub>9</sub> ) + 2C	◑	33.8%	788	F4
(C1 + 13C) + 2C	●	27.9%	882	F5
Full complement		23.4%	976	F6
Full complement		20.4%	976	F7

In the resulting map there were no other significant peaks save the spurious cylinder of height 1.7 electrons/ $\text{\AA}^3$ . There were no large negative regions in the electron density.

To the new co-ordinates calculated from F6, the "n shift" rule of Shoemaker et al. (1950) with  $n = 1.6$  was applied. A structure factor calculation showed that R had dropped to 23.4%

#### 4.8. Refinement of the Structure.

##### 4.8.1. Fo synthesis.

The refinement of the crystal structure of isoclovene hydrochloride was conducted by performing a further structure factor calculation - three dimensional Fo synthesis cycle. The mean shift in carbon atom co-ordinates at this stage, F7, was  $.03 \overset{\circ}{\text{\AA}}$ ; maximum shift =  $.08 \overset{\circ}{\text{\AA}}$ .

Calculation of bond lengths gave a mean carbon-carbon distance of  $1.55 \overset{\circ}{\text{\AA}}$  (maximum  $1.63 \overset{\circ}{\text{\AA}}$ , minimum  $1.40 \overset{\circ}{\text{\AA}}$ ) and a carbon-chlorine distance of  $1.84 \overset{\circ}{\text{\AA}}$ .

The contoured sections of F7 were redrawn on perspex sheets which were stacked above each other with perspex spacers inserted between them so as to maintain the proper interval between the sections. Examination

of this electron-density distribution showed that the packing of the two molecules in the unit cell was acceptable.

The atomic co-ordinates derived from F7 are listed in Table 6.

#### 4.8.2. Least Squares Refinement.

Further refinement of the structure was accomplished by the iterative least squares procedure, using the programme devised for Deuce by Dr. J.S. Rollett. This programme, which neglects the off-diagonal terms in the matrix of normal equations, refines both the individual atomic positional parameters and anisotropic temperature factors as well as the scale factor.

The atomic parameters listed in Table 6 were used as input data for the first cycle. The weighting system employed was as follows:

$$\begin{aligned} \text{If } |F_o| \leq |F^*| , \quad \sqrt{w_i} &= 1 \\ \text{If } |F_o| > |F^*| , \quad \sqrt{w_i} &= |F^*| / |F_o| \\ \text{where } |F^*| &= 8 |F_{\min}| \end{aligned}$$

The atomic form factors used were those of Berghuis et al. (1955) for carbon and James and Brindley (1932) for chlorine.

For the initial 4 cycles of refinement only the atomic

TABLE 6.

Fractional Atomic Co-ordinates derived from F7.

	$x/a$	$y/b$	$z/c$
C <sub>1</sub>	- .04751	- .05405	.16430
C <sub>2</sub>	- .13716	- .11055	.00345
C <sub>3</sub>	- .20159	- .20990	.06859
C <sub>4</sub>	- .11476	- .21069	.25588
C <sub>5</sub>	- .11470	- .09577	.31960
C <sub>6</sub>	- .34904	- .07884	.37042
C <sub>7</sub>	- .38980	.02765	.37621
C <sub>8</sub>	- .33446	.08702	.21147
C <sub>9</sub>	- .49373	.06977	.05149
C <sub>10</sub>	.49885	- .03170	- .03590
C <sub>11</sub>	- .30046	- .06432	- .12593
C <sub>12</sub>	- .13163	.05190	.18714
C <sub>13</sub>	- .20675	- .29082	.36760
C <sub>14</sub>	.03479	- .09363	.49313
C <sub>15</sub>	- .32686	.19653	.26026
Cl	.16188	- .25000	.24886

positional parameters were refined, the empirical isotropic temperature factors of  $B = 4.4 \text{ \AA}^2$  for chlorine and  $B = 3.5 \text{ \AA}^2$  for carbon and the scale factor being kept constant. Throughout the least squares refinement process, the course of which is shown in Table 7, only  $\frac{1}{2}$  shifts were applied to the calculated corrections at each stage.

Over the next 4 cycles the full data available were used and the calculated anisotropic temperature factors and the scale factor were allowed to vary. In the succeeding 2 cycles the hydrogen atom contributions to the structure factors were included, the hydrogen scattering curve of McWeeny (1952) being used. The hydrogen atom parameters were not refined.

The hydrogen atom positional parameters were roughly determined by casting shadows of a scale model onto the basal ( $h0l$ ) plane, assuming a carbon-hydrogen bond length of  $1.05 \text{ \AA}$ . Of the 25 hydrogen atoms in the molecule, 16 are fixed in space by the geometry of the molecular skeleton; the 9 others belonging to the 3 methyl groups were placed in their favoured conformations - staggered with respect to the substituents on the adjacent carbon atoms. Thus two co-ordinates,  $x$  and  $z$ ,

TABLE 7.

Course of Least Squares Refinement.

L. S. cycle	Data used	Remarks	R	$\sum w\Delta^2$	
1	60% of available observed data	$x_i, y_i, z_i$ variable empirical $B_e$ constant (3.5 for carbon 4.4 for chlorine)	18.9%		
2			16.4%		
3			15.3%		
4			16.7%		
	80% of available observed data				
5	Full data	$x_i, y_i, z_i, B_{ij}$ variable	15.6%	259	
6			14.6%	221	
7			13.7%	209	
8			13.3%	194	
9			H atom contri- butions included in S.F.'s but not varied	13.0%	191
10				12.9%	185
11				12.6%	179
12				12.5%	179

$\sum w\Delta^2$  is the quantity minimised in the least squares process where  $w$  = a weight and  $\Delta = \left| k |F_o| - |F_c| \right|$ .

TABLE 8.

Table of zonal scaling factors.

	Scaling factor (k)	$\sum \Delta$	$\sum  F_c $	$k \sum  F_o $
0kℓ	.8978	136.88	1033.99	1033.99
1kℓ	.9542	214.90	2002.47	2002.39
2kℓ	<b>.9481</b>	180.81	1595.59	1595.65
3kℓ	.9443	157.99	1232.91	1232.88
4kℓ	.9220	117.00	1019.80	1019.82
5kℓ	.8908	107.23	633.63	633.63
6kℓ	.9829	48.90	186.06	186.06
7kℓ	.8327	16.58	71.28	71.28
Overall scaling factor which had been used =				.9365

for each hydrogen atom were obtained. The third co-ordinate was deduced by calculation.

No allowance was made for unobserved reflections in any of the cycles undertaken. Over the initial 10 cycles the discrepancy, R, fell from 20.4% to 12.9%. Although the overall scaling factor appeared to be satisfactory, individual zonal discrepancies between  $\sum k |F_o|$  and  $\sum |F_c|$  existed (see Table 8). After correction of these scaling errors two further least squares cycles were undertaken. The almost constant value of R and  $\sum w \Delta^2$  in the final 2 cycles indicated that the refinement process within the scope of the present data and following the present mode of refinement was now complete. Further, examination of the co-ordinate shifts, ( $\Delta \xi_i = .002 \text{ \AA}$ ), of the last cycle and the corresponding standard deviations of these co-ordinates, ( $\sigma \xi_i = .03 \text{ \AA}$ ), revealed that the former were not significant.

A final three-dimensional  $F_o$  synthesis, F8, has been evaluated using the phases obtained from the 12th cycle of least squares. Fig.13 represents a composite diagram of the molecule, obtained by selecting that section of the three-dimensional map nearest to each atomic centre and projecting the contours onto the

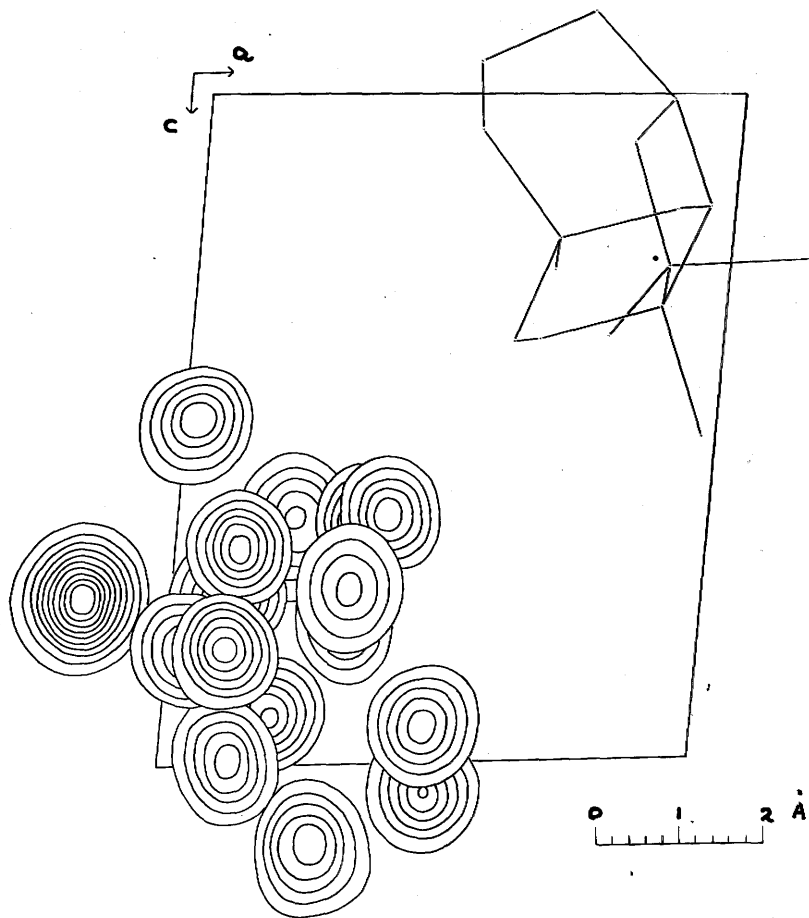


Fig.13. Part of the electron density distribution,  $F_8$ , represented by superimposed contours showing the molecule in the asymmetric unit.

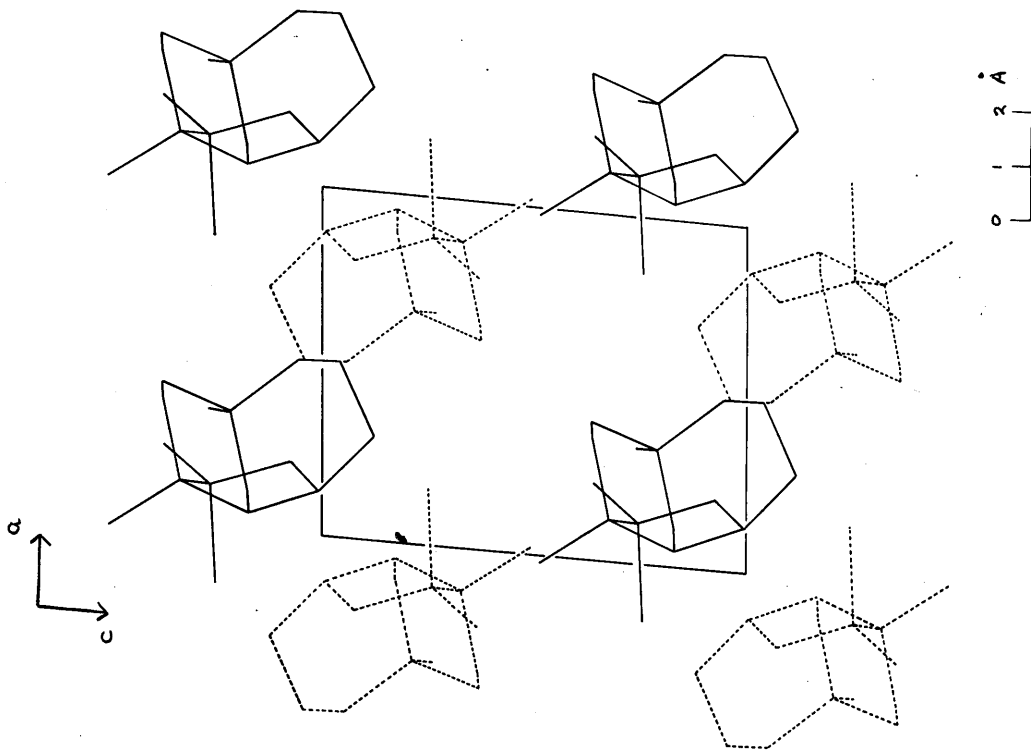


Fig.14. Arrangement of the atoms in (010) projection.

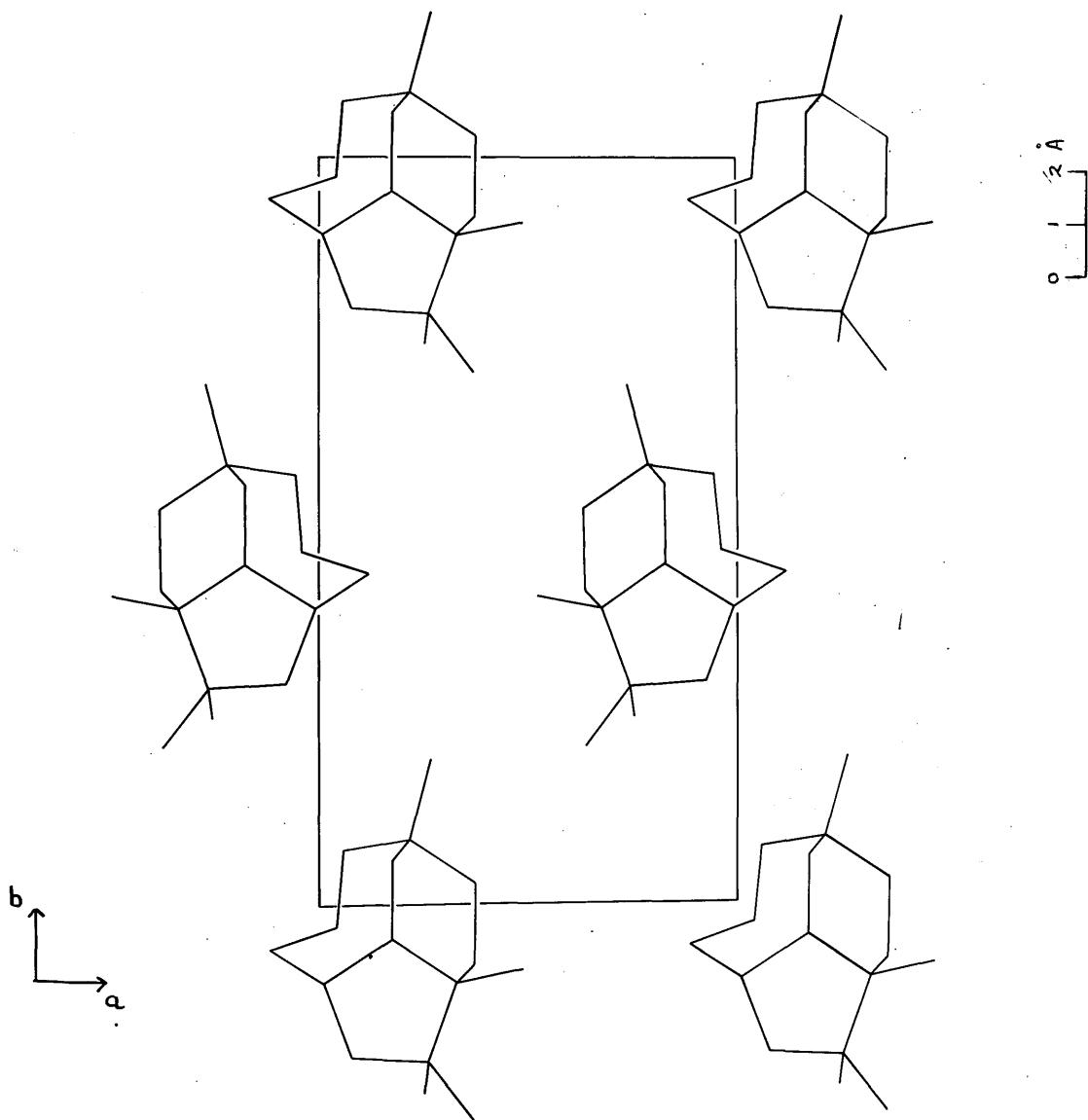


Fig.15. Arrangement of the atoms in (001) projection.

basal (010) plane. The spurious cylinder of electron density on section  $y = 1^2/48$  still existed but barely rose above 1 electron/ $\text{\AA}^3$  in height.

Fig.14 illustrates the structure projected onto the (010) plane, while fig. 15 shows the arrangement of the atoms in the (001) projection. In Appendix 3 are listed values for observed and calculated structure factors.

#### 4.9. Co-ordinates and Molecular Dimensions.

The fractional atomic co-ordinates and the anisotropic thermal parameters resulting from the 12th least squares cycle are listed in Tables 9 and 10 respectively. Table 11 gives the final average parameter shifts.

The standard deviations in the positional co-ordinates, listed in Table 12, were calculated directly from the least squares output using a standard procedure, viz.

$$\sigma(x/a) = \left\{ \frac{\sum w \Delta^2}{(m - s) \sum w \left( \frac{\partial \Delta}{\partial x/a} \right)^2} \right\}^{\frac{1}{2}} \quad \dots (4.2)$$

where  $\underline{m}$  is the number of observational equations, and  $\underline{s}$  is the number of independent parameters to be determined. The overall positional standard deviation is

$$\sigma(r) = \left\{ \frac{1}{3} \left( \sigma^2(x) + \sigma^2(y) + \sigma^2(z) \right) \right\}^{\frac{1}{2}}$$

TABLE 9.Final fractional atomic co-ordinates.

Atom	$x/a$	$y/b$	$z/c$
C <sub>1</sub>	- .04395	- .04699	.17230
C <sub>2</sub>	- .12750	- .10549	.00741
C <sub>3</sub>	- .20270	- .20452	.07624
C <sub>4</sub>	- .11367	- .21104	.25955
C <sub>5</sub>	- .11790	- .10477	.32671
C <sub>6</sub>	- .35160	- .08061	.36708
C <sub>7</sub>	- .39717	.02740	.37046
C <sub>8</sub>	- .33162	.08694	.21312
C <sub>9</sub>	- .49471	.07338	.05531
C <sub>10</sub>	.49607	- .02741	- .04019
C <sub>11</sub>	- .29800	- .05780	- .11928
C <sub>12</sub>	- .10692	.06067	.17435
C <sub>13</sub>	- .22076	- .28933	.36594
C <sub>14</sub>	.02283	- .08780	.48870
C <sub>15</sub>	- .33449	.19599	.26328
Cl	.16498	- .25120	.24992

Hydrogen Atom Co-ordinates.

Atom No.	$x/a$	$y/b$	$z/c$
16	-.348	-.228	-.018
17	-.252	-.154	-.130
18	+.362	-.077	-.073
19	-.438	-.049	+.001
20	-.140	-.001	+.269
21	-.030	-.069	-.058
22	.391	.100	-.025
23	.536	.087	-.099
24	-.352	.067	-.244
25	-.153	.049	.109
26	.116	.164	-.013
27	.022	.226	.105
28	-.448	.295	-.133
29	-.530	.441	.058
30	-.288	.449	.067
31	-.345	.492	-.113
32	.665	.150	.241
33	.526	.333	.218
34	.800	.345	.208
35	.636	.347	.752
36	.841	.350	.639
37	.838	.497	.724
38	.881	.560	.926
39	.970	.586	.862
40	.132	.492	.945

TABLE 10.

Final anisotropic temperature factors.

Atom	$\beta_{11}$	$\beta_{22}$	$\beta_{33}$	$\beta_{23}$	$\beta_{31}$	$\beta_{12}$
C <sub>1</sub>	.03260	.00692	.02221	- .00429	.01739	- .00534
C <sub>2</sub>	.04236	.00970	.02613	.00020	.03058	.00634
C <sub>3</sub>	.03936	.00641	.02788	- .00104	- .00105	.00085
C <sub>4</sub>	.04056	.00624	.02548	- .00092	- .00067	.00022
C <sub>5</sub>	.03037	.00749	.02209	.00033	.00936	.01026
C <sub>6</sub>	.01995	.01070	.02540	.00821	.00312	- .00364
C <sub>7</sub>	.04065	.00881	.02472	.00067	.00932	.00714
C <sub>8</sub>	.04161	.00687	.02891	- .00068	.01984	- .00206
C <sub>9</sub>	.03329	.00920	.03094	.00474	.00181	- .00725
C <sub>10</sub>	.03871	.00846	.02246	- .00481	- .00496	.00020
C <sub>11</sub>	.04376	.00988	.02185	.00403	- .00539	- .00313
C <sub>12</sub>	.03310	.00674	.02549	- .00108	.00986	- .00250
C <sub>13</sub>	.05135	.00857	.03294	.00952	- .01010	- .00358
C <sub>14</sub>	.03419	.01016	.02672	.00063	- .01193	- .00166
C <sub>15</sub>	.06149	.00839	.03842	- .00267	.00599	- .00189
Cl	.03413	.00869	.03468	- .00427	.00488	.00761

Thermal parameters of the carbon and chlorine atoms as determined from the anisotropic diagonal least squares analysis, cycle 12.

$$T = 2^{-\left(\beta_{11}h^2 + \beta_{22}k^2 + \beta_{33}l^2 + \beta_{12}hk + \beta_{23}kl + \beta_{31}lh\right)}$$

$$= \exp \left( -\left(B_{11}h^2 + \dots\right) \right)$$

Hence  $\beta_{11} = 1.4427 B_{11}$  etc.

TABLE 11.

Parameter Shifts indicated by  
anisotropic diagonal least squares analysis.

	Average shift Cycle 1	Final average shift Cycle 12
$\Delta x$ ( $\text{\AA}$ ) <sup>o</sup>	.0718	.0027
$\Delta y$ ( $\text{\AA}$ )	.0396	.0019
$\Delta z$ ( $\text{\AA}$ )	.0474	.0024

TABLE 12.Standard Deviations in the positional co-ordinates.

Atom	$\sigma(x)$ Å	$\sigma(y)$ Å	$\sigma(z)$ Å	$\sigma(r)$ Å*
C <sub>1</sub>	.0116	.0116	.0118	.0234
C <sub>2</sub>	.0123	.0129	.0147	.0266
C <sub>3</sub>	.0131	.0140	.0127	.0266
C <sub>4</sub>	.0131	.0129	.0133	.0262
C <sub>5</sub>	.0111	.0117	.0123	.0234
C <sub>6</sub>	.0102	.0126	.0154	.0258
C <sub>7</sub>	.0133	.0131	.0143	.0272
C <sub>8</sub>	.0121	.0129	.0130	.0254
C <sub>9</sub>	.0126	.0136	.0146	.0272
C <sub>10</sub>	.0133	.0120	.0139	.0262
C <sub>11</sub>	.0140	.0133	.0152	.0284
C <sub>12</sub>	.0115	.0125	.0130	.0248
C <sub>13</sub>	.0148	.0157	.0149	.0302
C <sub>14</sub>	.0132	.0154	.0153	.0294
C <sub>15</sub>	.0161	.0166	.0163	.0326
Cl	.0029	.0037	.0048	.0078

\*Factor of 2 included to allow for non-centrosymmetry.

TABLE 13.

Molecular dimensions: the bond lengths within a molecule of isoclovene hydrochloride together with the corresponding standard deviations.

Bond	Bond length ( $\text{\AA}$ )
C <sub>1</sub> - C <sub>2</sub>	1.600 $\pm$ .036
C <sub>1</sub> - C <sub>5</sub>	1.547 $\pm$ .033
C <sub>1</sub> - C <sub>12</sub>	1.550 $\pm$ .034
C <sub>2</sub> - C <sub>3</sub>	1.563 $\pm$ .038
C <sub>2</sub> - C <sub>11</sub>	1.583 $\pm$ .039
C <sub>3</sub> - C <sub>4</sub>	1.527 $\pm$ .037
C <sub>4</sub> - C <sub>5</sub>	1.570 $\pm$ .035
C <sub>4</sub> - C <sub>13</sub>	1.550 $\pm$ .040
C <sub>5</sub> - C <sub>6</sub>	1.568 $\pm$ .035
C <sub>5</sub> - C <sub>14</sub>	1.540 $\pm$ .038
C <sub>6</sub> - C <sub>7</sub>	1.531 $\pm$ .038
C <sub>7</sub> - C <sub>8</sub>	1.561 $\pm$ .037
C <sub>8</sub> - C <sub>9</sub>	1.590 $\pm$ .037
C <sub>8</sub> - C <sub>12</sub>	1.518 $\pm$ .036
C <sub>8</sub> - C <sub>15</sub>	1.568 $\pm$ .041
C <sub>9</sub> - C <sub>10</sub>	1.590 $\pm$ .038
C <sub>10</sub> - C <sub>11</sub>	1.533 $\pm$ .039
C <sub>4</sub> - Cl	1.860 $\pm$ .027

TABLE 14.

Molecular dimensions: the valence angles within the molecule of isoclovene hydrochloride together with the corresponding standard deviations.

C <sub>2</sub> - C <sub>1</sub> - C <sub>5</sub>	105.7° ± 1.9°
C <sub>2</sub> - C <sub>1</sub> - C <sub>12</sub>	113.9° ± 1.9°
C <sub>5</sub> - C <sub>1</sub> - C <sub>12</sub>	115.1° ± 1.9°
C <sub>1</sub> - C <sub>2</sub> - C <sub>3</sub>	105.2° ± 2.0°
C <sub>1</sub> - C <sub>2</sub> - C <sub>11</sub>	119.2° ± 2.1°
C <sub>3</sub> - C <sub>2</sub> - C <sub>11</sub>	112.1° ± 2.1°
C <sub>2</sub> - C <sub>3</sub> - C <sub>4</sub>	105.9° ± 2.1°
C <sub>3</sub> - C <sub>4</sub> - C <sub>5</sub>	104.5° ± 2.0°
C <sub>3</sub> - C <sub>4</sub> - C <sub>13</sub>	113.5° ± 2.2°
C <sub>3</sub> - C <sub>4</sub> - C <sub>1</sub>	106.9° ± 1.8°
C <sub>5</sub> - C <sub>4</sub> - C <sub>1</sub>	109.2° ± 1.6°
C <sub>5</sub> - C <sub>4</sub> - C <sub>13</sub>	117.7° ± 2.2°
C <sub>13</sub> - C <sub>4</sub> - C <sub>1</sub>	104.7° ± 1.8°
C <sub>1</sub> - C <sub>5</sub> - C <sub>4</sub>	102.4° ± 1.9°
C <sub>1</sub> - C <sub>5</sub> - C <sub>6</sub>	111.8° ± 1.9°
C <sub>1</sub> - C <sub>5</sub> - C <sub>7</sub>	112.6° ± 2.0°
C <sub>4</sub> - C <sub>5</sub> - C <sub>14</sub>	113.8° ± 2.0°
C <sub>6</sub> - C <sub>5</sub> - C <sub>14</sub>	108.5° ± 2.0°
C <sub>5</sub> - C <sub>6</sub> - C <sub>7</sub>	113.3° ± 2.1°
C <sub>6</sub> - C <sub>7</sub> - C <sub>8</sub>	116.7° ± 2.2°

- Cont'd -

TABLE 14. (Cont'd)

C <sub>7</sub> - C <sub>8</sub> - C <sub>12</sub>	108.6° ± 2.1°
C <sub>7</sub> - C <sub>8</sub> - C <sub>15</sub>	107.9° ± 2.2°
C <sub>9</sub> - C <sub>8</sub> - C <sub>12</sub>	113.5° ± 2.1°
C <sub>9</sub> - C <sub>8</sub> - C <sub>15</sub>	107.2° ± 2.1°
C <sub>15</sub> - C <sub>8</sub> - C <sub>12</sub>	107.8° ± 2.2°
C <sub>8</sub> - C <sub>9</sub> - C <sub>10</sub>	118.8° ± 2.1°
C <sub>9</sub> - C <sub>10</sub> - C <sub>11</sub>	114.9° ± 2.2°
C <sub>2</sub> - C <sub>11</sub> - C <sub>10</sub>	115.6° ± 2.2°
C <sub>1</sub> - C <sub>12</sub> - C <sub>8</sub>	118.7° ± 2.1°

These calculated values have been increased by a factor of 2 to allow for non-centrosymmetry (Cruickshank (1950)).

The bond lengths and bond angles within one molecule are shown in Tables 13 and 14 respectively, these dimensions having been computed from the atomic co-ordinates listed in Table 9. The standard deviations in these values are also included in these Tables. The standard deviation,  $\sigma(l)$ , of the distance between two atoms whose positions have been determined independently with standard deviations in position of  $\sigma(A)$  and  $\sigma(B)$  is given by :

$$\sigma(l) = \left\{ \sigma^2(A) + \sigma^2(B) \right\}^{\frac{1}{2}} \quad \dots\dots (4.3)$$

The standard deviation,  $\sigma(\theta)$  of the interbond angle between three atoms was computed by the equation given by Cruickshank and Robertson (1953).

The mean standard deviation of a carbon atom's position is .027 Å. This gives a value for the mean standard deviation of a carbon-carbon bond of .037 Å and a mean standard deviation of 2.2° in the interbond angle.

The intermolecular distances less than 4 Å in this crystal were also determined and are listed in Table 15. There are no contacts less than the expected van der Waals distances.

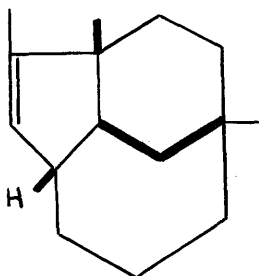
TABLE 15.

Intermolecular Distances: atoms in the reference molecule are unprimed whereas those in other molecules are designated by one, two or three primes respectively.

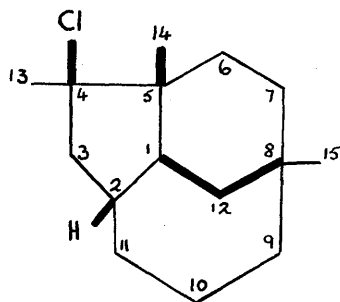
Intermolecular distance	Length (Å)
$C_1 - C_9^I$	$3.856 \pm .036$
$C_1 - C_{10}^I$	$3.495 \pm .035$
$C_1 - C_6^I$	$3.922 \pm .027$
$C_1 - C_{13}^I$	$3.959 \pm .031$
$C_{14} - C_{11}^{II}$	$3.880 \pm .041$
$C_{15} - C_1^{III}$	$3.960 \pm .034$
$C_9 - C_3^{IV}$	$3.734 \pm .038$

Reference molecule	$x \quad y \quad z$
Molecule I	$1 + x, y, z$
Molecule II	$x, y, 1 + z$
Molecule III	$1 - x, \frac{1}{2} + y, \bar{z}$
Molecule IV	$\bar{x}, \frac{1}{2} + y, \bar{z}$

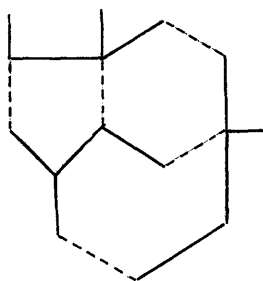
4.10. Discussion of the Structure.



(I)



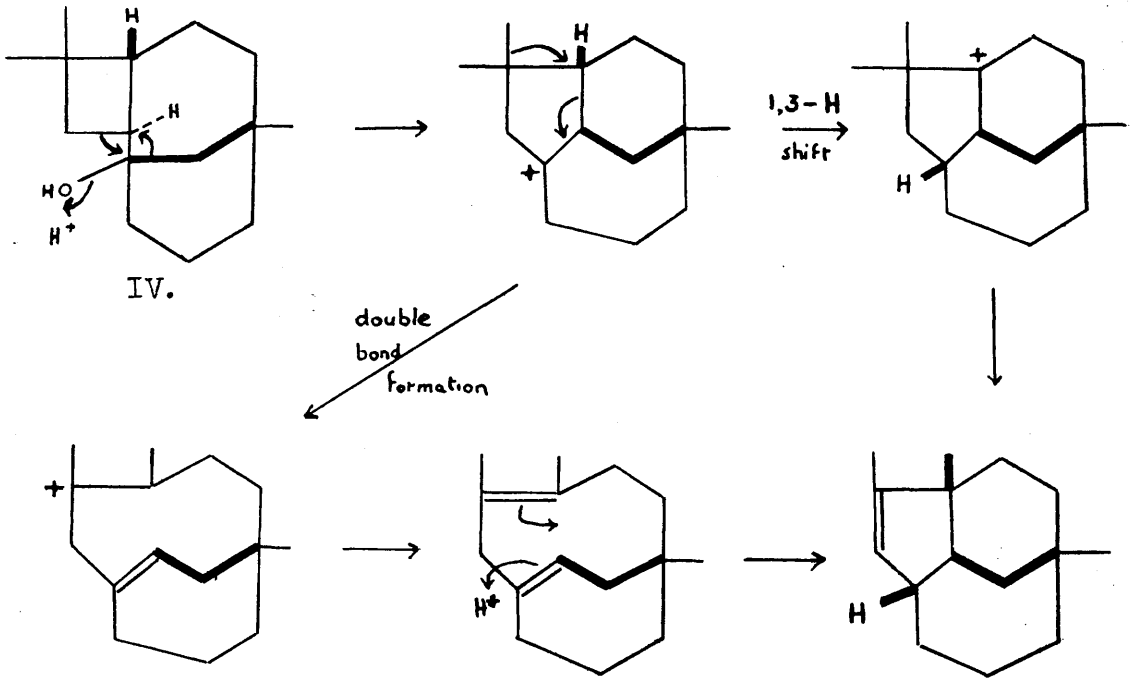
(II)



(III)

The structure (I) as deduced from the X-ray analysis of isoclovene hydrochloride (II) agrees with the known chemical evidence, in that it contains three methyl groups and possesses a secondary-tertiary double bond. In addition, the structure of isoclovene can be shown to obey the isoprene rule (III).

Professor D.H.R. Barton, in reconciling the final structure with that of its known precursor,  $\beta$ -caryophyllene alcohol (IV) has considered the possible mechanism of formation. In the preliminary communication on this work (Clunie and Robertson (1960)) Professor Barton stated that the conversion of  $\beta$ -caryophyllene alcohol



into isoclovene represented "an unusual problem in carbonium ion mechanism". While two schemes could be proposed as shown opposite both routes involved intermediates which would have to be excluded if Bredt's Rule were strictly applied. It is known, however, that the rule breaks down in the reactions of  $\beta$ -caryophyllene alcohol and the rearrangements involved here are considered by Professor Barton to be of a similar degree of unexpectedness.

To describe pictorially the overall shape of molecule II is not easy but the three rings can be considered to form a basket-like arrangement. Perhaps the best view of the structure is presented in the (001) projection, (see Fig.15). All three rings are present in their preferred conformations. The five-membered ring is hinge-shaped; the six-membered ring has the chair conformation; the seven-membered ring is also in the chair form, but in this case the chair is obviously distorted for all the angles are consistently greater than the tetrahedral value. This ring can be said to have become somewhat flattened, a situation probably due to steric repulsion. For example, in an ideal structure  $C_6$  and  $C_{10}$  would be about  $2.6 \overset{O}{\text{Å}}$  apart thereby bringing the two hydrogen atoms attached to these atoms to within

about 1 Å of each other. In the actual molecule C<sub>6</sub> and C<sub>10</sub> are 3.38 Å apart.

The five and six-membered rings are cis fused as are the five and the seven-membered rings. The six and seven-membered rings are linked via a methylene bridge in the cis position relative to C<sub>14</sub> and chlorine.

The bond lengths and bond angles together with their standard deviations are not sufficiently precise to permit detailed discussion but it may be noted that the carbon-chlorine distance of 1.86 Å can be perhaps considered as being significantly longer than the expected value of 1.78 Å obtained from a mere consideration of atomic radii. A value as high as 1.82 Å for an equatorial carbon-chlorine bond has been quoted for gammexane (van Vloten et al. (1950)), whilst Pasternak (1951) has reported values of 1.85 Å and 1.84 Å for similar distances in pentachlorocyclohexene. For an axial carbon-chlorine bond in 1:2:3:4 tetrachloro-1:2:3:4-tetrahydronaphthalene (Lasheen, 1952) a value of 1.81 Å is cited. For β-caryophyllene chloride the corresponding bond length was 1.79 Å. The bond lengthening found in the present case may be simply a steric effect due to the proximity of two methyl and one methylene group.

The average carbon-carbon distance is 1.55 Å with a maximum spread of .05 Å which is very slightly greater

than the average standard deviation of  $.04 \text{ \AA}$ . These variations are within the limits reported in the analysis of hydroxydihydroeremophilone by Grant (1958) and of  $\beta$ -caryophyllene chloride (loc.cit.), both analyses being restricted to two-dimensional methods and less highly refined. Nevertheless, the values of the standard deviations are of the order of magnitude generally found in the analysis of a non-centric structure of similar complexity with a heavy atom present, e.g. ibogaine hydrobromide (Arai et al.(1960)) and iresin (Rossmann and Lipscomb (1958)).

As for the disposition of substituent groups in isoclovene hydrochloride  $C_{15}$  is equatorial,  $C_{14}$  is axial,  $C_{13}$  quasi-equatorial and chlorine quasi-axial.

Equivalent isotropic temperature factors have been deduced by the method due to Hirshfeld et al.(1959). The  $\beta_{ij}$ 's were averaged and converted into  $B_{ij}$  values whence resulting isotropic temperature factors,  $B_{\theta}$ , of  $4.4 \text{ \AA}^2$  for the average carbon atom and  $4.45 \text{ \AA}^2$  for the chlorine atom were obtained.

The reliability of the structure analysis is confirmed by the value for R of 12.5% which is low enough to provide some internal evidence that the solution of this crystal structure is essentially correct. The agreement could

perhaps be improved slightly if a more recent scattering factor curve for chlorine, e.g. that of Viervoll and Ögrim (1949) or Berghuis et al. (1955) had been used.

-----

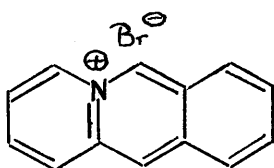
CHAPTER V.

Attempts to Solve the Crystal Structure  
of Photo-irradiated Acridizinium Bromide.

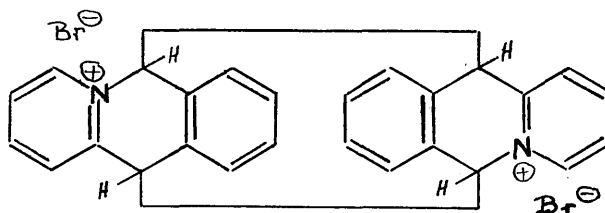
V. ATTEMPTS TO SOLVE THE CRYSTAL STRUCTURE OF PHOTO-IRRADIATED ACRIDIZINIUM BROMIDE.

5.1. Introduction:

Bradsher and Beavers (1955) have recently synthesised a new heterocyclic aromatic compound (i) closely related in structure to anthracene but differing only in having a quaternary nitrogen at one of the bridgehead positions. Like anthracene, when crystals of acridizinium bromide are exposed to irradiation by sunlight or from a sun lamp they are converted into a higher melting, less soluble compound (ii) lacking the yellow colour and fluorescence characteristic of the starting material. The U.V. absorption spectrum of the new compound indicates that irradiation has destroyed the conjugation of the acridizinium system. Bradsher, Beavers and Jones (1957) claim that photodimerization has occurred and from the U.V. absorption spectrum it appears to them that, like anthracene, connection is through the meso position. The possibility that photo-oxidation has taken place is eliminated by the observation that there is no change in weight during irradiation.



(i)



(ii)

A preliminary investigation has been carried out on (i) (Clunie,(1957)). The unit cell dimensions were reported. The crystals were found to belong to the triclinic system and to be twinned along a diagonal axis.

Little attention had been directed, at this stage, to the photo-irradiated dimer because the material supplied by Professor Bradsher was in the form of white, opaque, micaceous crystals which gave X-ray rotation photographs indicating a large degree of disorder. Recrystallisation from various common solvents did not furnish markedly better formed crystals.

## 5.2. Preparation of Crystals.

Further attempts at recrystallisation from mixed solvents using the technique of slow evaporation at room temperature have since been undertaken. Well shaped, almost colourless, crystals were obtained from a 50:50 mixture of methanol/dioxan. Examination under the polarising microscope indicated that some surface deposition of secondary material had occurred. This effect could be rendered more apparent by washing the crystals with methanol whence complete surface decomposition seemed to occur and the crystals became

opaque. By varying the proportions of the two solvents two different types of crystals could be grown.

(1) The initial material was dissolved in cold methanol, dioxan was added dropwise till a slight precipitate was produced. Heat was supplied until a clear solution was obtained. (Heating to boiling point gave rise to a red solution.) After several days tabular crystals of modification (A) were deposited. They were usually white and opaque.

(2) To a solution of the material in cold methanol, several drops of dioxan were added. The crystallising vessel was lightly corked to ensure slower evaporation. Translucent, platey, crystals of modification (B) were deposited after a few days.

The fact that dimorphs occurred was confirmed by the subsequent determination of unit cell parameters. A plausible explanation can perhaps be given by considering the appearance of the crystals of modification (A). These were produced by more rapid crystallisation and the quicker the crystallisation the more evidence there was of a secondary deposition on the surface of the crystals as shown by microscopic examination. Moreover, these crystals gave extremely poor X-ray photographs, unsuitable for the collection

of intensity data both due to the poor, drawn-out, shape of the reflections and to the paucity in their number. For example, on a Weissenberg photograph exposed for 25 hrs. to unfiltered copper radiation for a fairly large crystal rotated about its needle axis ( $7.9 \overset{\circ}{\text{Å}}$  in length) only 30 reflections were recorded. A similar type of Weissenberg photograph resulted when a second crystal was rotated about an alternative axis,  $11.0 \overset{\circ}{\text{Å}}$  long.

Further work was confined to modification (B) which, fortunately, gave photographs suitable for measuring intensity data.

### 5.3. Unit Cell Dimensions.

The unit cell parameters have been determined by means of rotation, oscillation and Weissenberg photographs, using copper  $K\alpha$  radiation, and the values obtained are listed in Table 16.

### 5.4. Measurement of Intensities.

Detailed exploration of the  $(0kl)$ ,  $(h0l)$  and  $(hk0)$  zones has been made by moving film exposures of the equatorial layer lines for crystals rotated about the a, b and c axes respectively.

TABLE 16.Unit Cell Parameters of  
photo-irradiated acridizinium bromide.

Molecular formula	$C_{26}N_2H_{20}Br_2$
Molecular weight	519.8
Melting point	240°C.
System	monoclinic
a (Å)	7.75 ± .01
b (Å)	17.08 ± .04
c (Å)	9.88 ± .02
$\beta$	99° 18'
Unit cell volume (Å <sup>3</sup> )	1,308
Molecules per unit cell	2
d (flotation) (g.cm. <sup>-3</sup> )	1.529
d (calc.) (g.cm. <sup>-3</sup> )	1.480
Absorption coefficient ( $\lambda = 1.542 \text{ \AA}$ )	41.7 cm. <sup>-1</sup>
Absent Spectra	0k0 for k = 2n + 1
Space Group	$P_2, (C_2^2)$ or $P_2/m (C_{2h}^2)$

TABLE 17.

Zone	Cross-section of crystal	Intensity range	Number of reflections recorded	Maximum number of possible reflections
Okℓ	.23 x .16 mm <sup>2</sup>	3,500:1	146	225
hk0	.16 x .30 mm <sup>2</sup>	3,000:1	132	176
h0ℓ	.16 x .10 mm <sup>2</sup>	4,000:1	124	185

The main record of intensities was taken by the multiple film technique, all the intensities of the X-ray reflections having been estimated visually by comparison with a standard series of spots of known exposure. Each zone was estimated twice, using a different arithmetic step-wedge. To these averaged intensities corrections for the usual Lorentz and polarisation factors were applied and relative structure factors were evaluated. No corrections for extinction or absorption were applied. The relative structure factors are listed in Appendix 4.

#### 5.5. N(Z) Distribution.

In order to ascertain the correct space group the N(Z) test for centrosymmetry was performed on the (hk0) and (Okℓ) zones of intensities.

Howells, Phillips and Rogers (1950) have shown that the fraction,  $N(Z)$ , of all the reflections (other than those systematically absent) of which the intensities are less than or equal to  $Z$  times the average intensity  $\langle I \rangle$  is for the non-centrosymmetric case

$$N(Z) = 1 - \exp(-Z) \quad \dots\dots\dots (5.1)$$

and for the centrosymmetrical case

$$N(Z) = 2^{-\frac{1}{2}} \int_0^{(Z/2)^{\frac{1}{2}}} \exp(-x^2) dx = \text{erf}(Z/2)^{\frac{1}{2}} \dots (5.2)$$

These functions have been tabulated and show that there is a higher proportion of weak reflections for the centrosymmetrical case.

The intensities of the two zones considered were divided into 3 ranges as shown in Table 13 and the results are shown in Fig.16.

Since the heavy atoms present in the molecule possess a considerable fraction of the total scattering power ( $Z_{\text{H.A.}}^2 / \sum Z_j^2 = 1.95$ ) reservations must be entertained concerning the validity to be attached to the conclusion that the space group is more likely to be  $P_{21/m}$  in which case the molecule should possess a centre or a plane of symmetry.

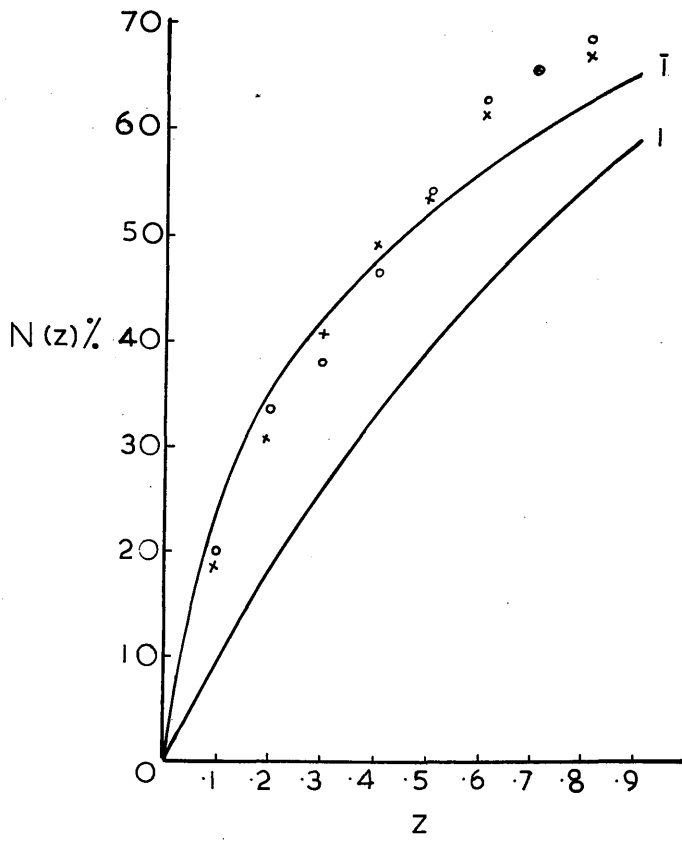


Fig.16. Results of N(Z) test performed on (hk0) and (Okℓ) data are denoted by X and O respectively.

TABLE 18.

Zone		Range I	Range II	Range III
hk0	$2 \sin \theta$	.4 → .9	.9 → 1.25	1.25 → 1.60
	number of reflections included	30	32	34
Okℓ	$2 \sin \theta$	.4 → .9	.9 → 1.20	1.20 → 1.50
	number of reflections included	33	33	35

5.6. Attempted Structure Determination using Two-dimensional methods.

5.6.1. The (100) Patterson Projection.

With the squares of the structure amplitudes of the (Okℓ) zone as coefficients, a Patterson synthesis was performed, giving a projection of the interatomic vectors onto the (100) plane. Both monoclinic space groups  $P_{21}$  and  $P_{21/m}$  have vector set space group  $P_{2/m}$ . Consequently, the symmetry of the considered projection is pmm and expression (5.3) was evaluated using Beever-Lipson strips for y from  $0/60$  to  $30/60$  and for z from  $0/60$  to  $30/60$ .

$$P_{(0yz)} = \frac{1}{A} \sum \sum |F(Ok\ell)|^2 \cos 2\pi(ky + \ell z) \dots (5.3.)$$

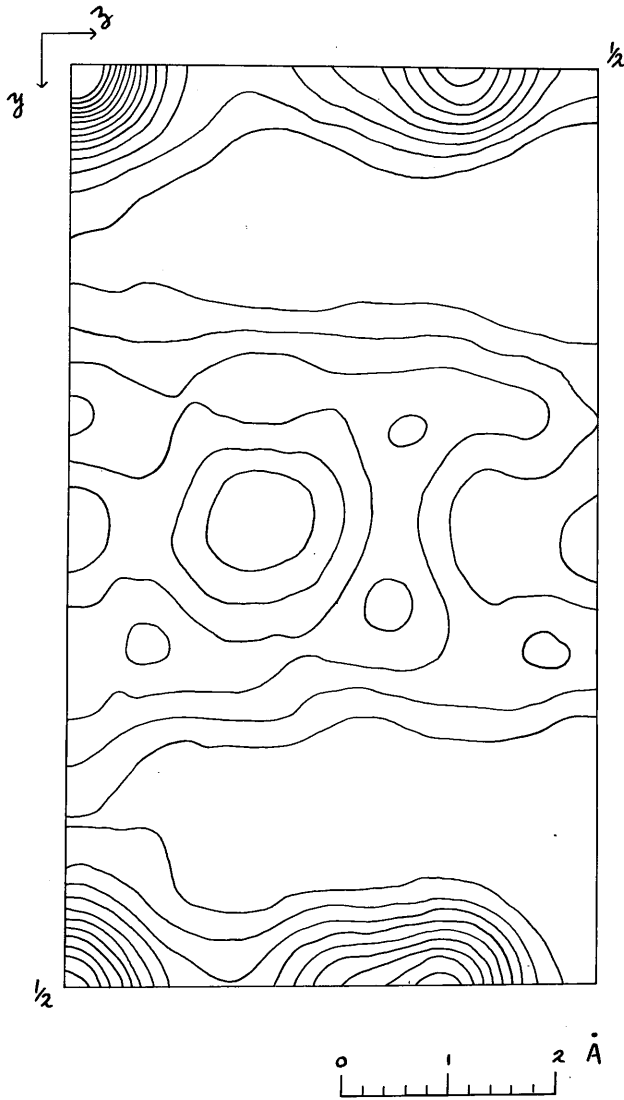


Fig.17. Projection of Patterson function on (100).

A contour map on an arbitrary scale showing this projection of the Patterson function was constructed. (Fig.17.)

The concentration of high peaks (assumed to be bromine-bromine vectors) along the lines  $y = 0$  and  $y = \frac{1}{2}$  seemed to verify the choice of  $P_{2/m}$  as the true space group.

If the four bromine ions in the unit cell have the following co-ordinates:

$$\begin{array}{ll} (1) & y_1, z_1 \\ (2) & \frac{1}{2} + y_1, \bar{z}_1 \\ (3) & y_2, z_2 \\ (4) & \frac{1}{2} + y_2, \bar{z}_2 \end{array}$$

then the expected vectors are:

$$\begin{array}{ll} (A) & \frac{1}{2}, 2z_1 \\ (B) & \frac{1}{2}, 2z_2 \\ (C) & (y_1 - y_2), (z_1 - z_2) \\ (D) & (\frac{1}{2} - y_2 + y_1), (z_1 + z_2) \end{array}$$

(A) and (B) are single peaks; (C) and (D) are double peaks.

Since no large peaks are observed in the interior of the map, other than along the line  $y = \frac{1}{2}$ , it may be deduced that  $y_1 - y_2 = 0$  or  $\frac{1}{2}$ . Also, since there are two molecules in a unit cell whose symmetry demands four asymmetric units, half a molecule must be the asymmetric unit. At first attempts were made to place the centre of the organic part of the molecule on a centre of symmetry and the bromine ions on the mirror planes. That is, it was assumed that  $y_1 - y_2 = \frac{1}{2}$ .

Difficulties arise from this interpretation in that the peak at  $(\frac{1}{2}, 0)$  in this Patterson projection would be expected to be elliptical on the basis of the solutions attempted but, in fact, this peak is almost spherical. This would seem to indicate that  $z_1 = z_2$ . But incongruities existed in this case too. This interpretation did not explain the elliptically shaped peak at  $y = \frac{1}{2}$ ,  $z = \frac{21}{60}$ .

The best solution obtained at this stage appeared to be:  $z_1 = \frac{8.5}{60}$ ,  $y_1 = .250$ ;  $z_2 = \frac{29.5}{60}$ ,  $y_2 = .750$ , but evaluation of structure factors and the calculation of a bromine phased Fourier synthesis were deferred until the other Patterson projections were computed.

#### 5.6.2. The (001) Patterson Projection.

The symmetry of this projection is pmm so that the expression evaluated was exactly analogous to that used for the (100) projection. The series was computed using Beavers-Lipson strips for the intervals  $x = \frac{0}{60}$  to  $\frac{30}{60}$  and  $y = \frac{0}{60}$  to  $\frac{30}{60}$ . The projection of the Patterson function on (001) is illustrated in Fig.18.

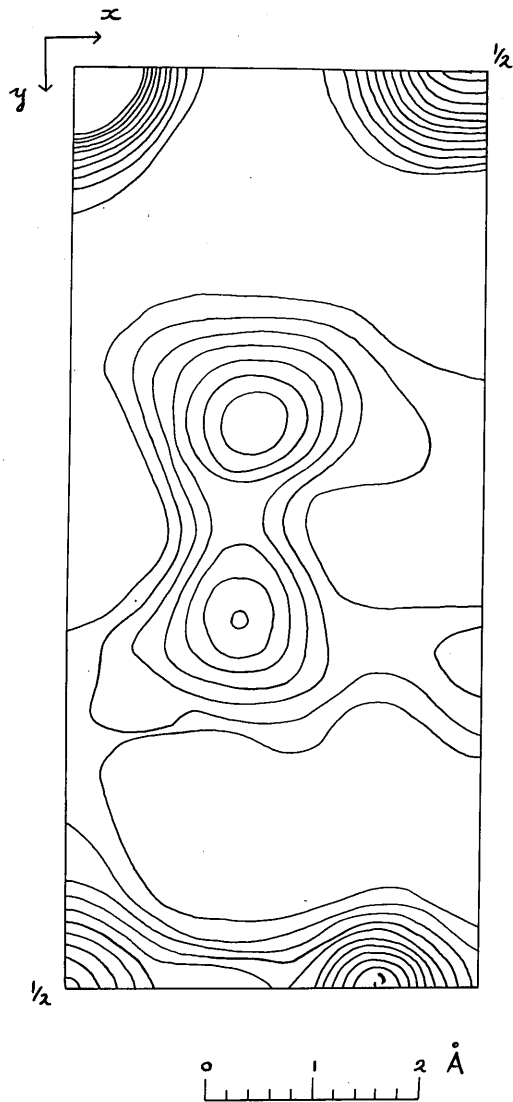


Fig.18. Projection of Patterson function on (001).

If the co-ordinates of the bromine ions are:

$$(1) \ x_1 \ y_1 \quad (2) \ \bar{x}_1, \ \frac{1}{2} + y_1$$

$$(3) \ x_2 \ y_2 \quad (4) \ \bar{x}_2, \ \frac{1}{2} + y_2$$

then the expected vectors between the bromine ions are:

$$(A) \ 2x_1 \ \frac{1}{2} \quad (B) \ 2x_2 \ \frac{1}{2}$$

$$(C) \ (x_1 - x_2)(y_1 - y_2) \quad (D) \ (x_1 + x_2) \left(\frac{1}{2} + y_1 - y_2\right)$$

(A) and (B) are single peaks; (C) and (D) are double peaks.

The map revealed the presence of three prominent peaks along the line  $y = \frac{1}{2}$ . Further, since the large peaks at  $x = \frac{25.5}{60}$ ,  $y = 0$  and  $x = \frac{22.7}{60}$ ,  $y = \frac{1}{2}$  would be expected to have the same x value if  $y_1 = y_2 = 0$ , this would seem to lend support to the view that  $y_1 - y_2 = \frac{1}{2}$ . A tentative, but not entirely satisfactory solution of the bromine vector set, was advanced, viz.

$$x_1 = \frac{1}{60} \quad y_1 = \frac{1}{4}$$

$$x_2 = \frac{24.5}{60} \quad y_2 = \frac{3}{4}$$

### 5.6.3. The Patterson Projection on (010).

This summation was carried out using Robertson's Universal Fourier Synthesiser, "RUFUS" (Robertson 1954, 1955) with intervals of x from  $0/30$  to  $30/30$  and z from  $0/60$  to  $30/60$ . The map of this projection is shown in Fig.19 and since there is more than one

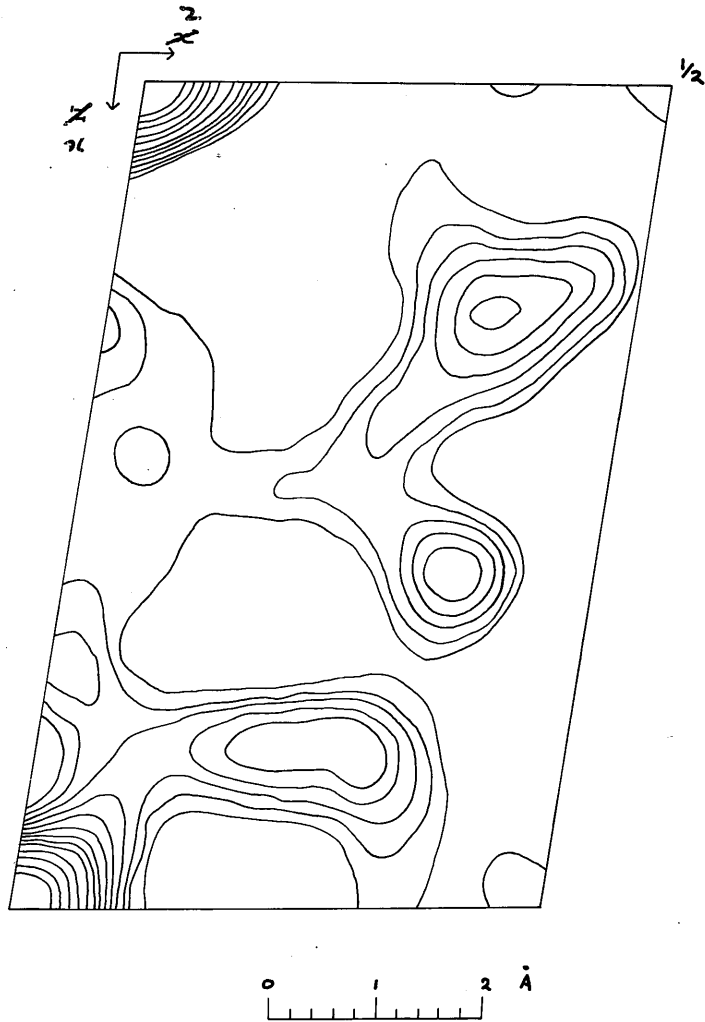


Fig.19. Projection of Patterson function on (010).

prominent peak in the interior of this map this would seem to support the interpretation that  $y_1 - y_2 = \frac{1}{2}$ . An accurate solution of the vector set of the bromine ions was not possible in this projection.

#### 5.6.4. Analysis of (100) projection.

The first step entailed the calculation of bromine ion contributions to the structure factors for this zone on the basis of the following co-ordinates

Br<sub>1</sub>     (.025, .250, .492)

Br<sub>2</sub>     (.408, .750, .142)

An R factor of 47% was obtained. 83 terms were then incorporated into a Fourier series which was computed on "RUFUS". A representation of the entire electron-density projected onto the (100) plane was drawn out on tracing paper. It appeared that the requisite number of carbon atom peaks was present together with several peaks close to the bromine positions at  $y = \frac{1}{4}$  and  $y = \frac{3}{4}$ . These were suspected to belong to solvent molecules, an indication of their possible presence having been given by the discrepancy between observed and calculated densities (Table 16). These latter peaks were ignored for the present, attention being concentrated on the maxima due to the carbon skeleton.

Atomic co-ordinates were allocated to the 14 light atoms in the asymmetric unit. Structure factors were

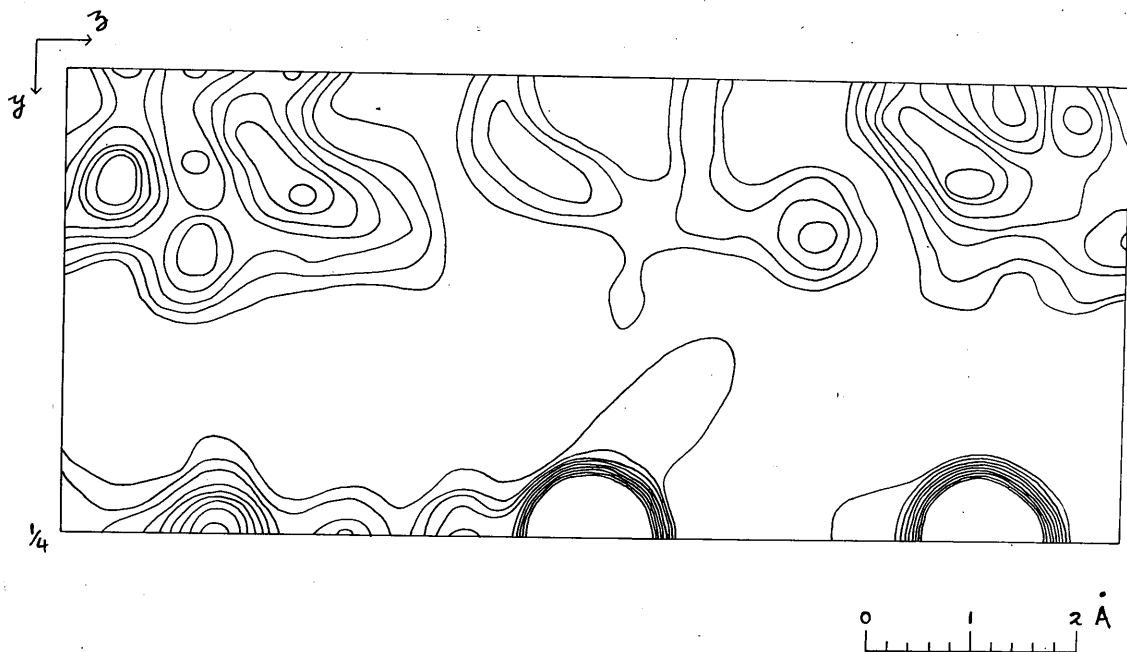


Fig. 20. Projection of electron density on (100).

recalculated giving an R factor of 32% but the agreement for several reflections was poor, particularly so for the (020) reflection where  $|F_C| = 79$  and  $|F_O| = 15$ . Nevertheless, a second Fourier synthesis was computed using 102 terms. The resulting electron-density projection, shown in Fig.20, revealed little significant improvement. A second calculation of structure factors gave an R factor of 30.6%, solvation again being neglected. On including the solvent molecules' contributions into the structure factor calculations there was no noticeable difference. A disquieting feature is that if the solvent molecule is assumed to be methanol then the oxygen atom of this molecule occupies a position on  $y = \frac{1}{4}$  with a z co-ordinate of  $(1 - z_1)$  if  $z_1$  is the co-ordinate of the bromine ion sited on this mirror plane. Furthermore, the (0k4) set of reflections all calculated too low, principally due to the very small bromine ion contributions but still the (0k4) festoon was observed as being weak on the Weissenberg film.

No really satisfactory structure emerged from the various other interpretations of this projection based on the supposition that the bromine ions were sited on the mirror planes.

A sharpened Patterson projection on (100) has since been computed on 'Deuce'. This is shown in Fig.21 and

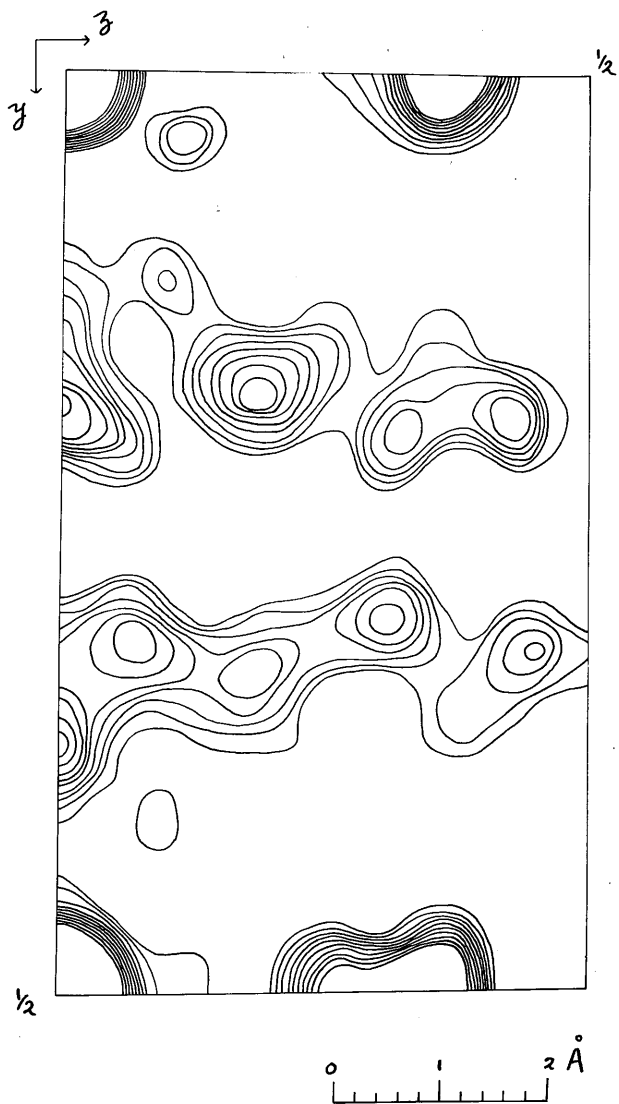


Fig.21. Projection of Sharpened Patterson on (100).

contains interesting detail. This projection would seem to indicate that the organic part of the molecule is sited on the mirror plane and that the bromine ions lie on the line  $y = 0$ . This being so, the bromine ions do not contribute to reflections for which  $k = 2n + 1$  and the organic part of the molecule does not contribute sufficiently to reflections (032), (052), (055), (092) in order to give good agreement between calculated and observed values.

A further possibility as yet not fully investigated is the existence of a disordered structure. Trotter (1958) claims that evidence of weak intermediate layer lines (which do exist in the  $b$  axis rotation photograph) indicates an ordered arrangement of two different orientations. Substitution of bromine ion co-ordinates into the three dimensional structure factor expression also shows that this effect could result from the placement of the bromine ions at  $y = 0$  but not, on first sight at any rate, at  $y = \frac{1}{4}$ .

Axial reflections have been calculated with the following co-ordinates for  $\text{Br}_1$  :  $y = 0$ ,  $z = .179$  and with postulated carbon atom co-ordinates. The agreement between calculated and observed values was not particularly promising.

A further but less likely possibility is that the space group may, in reality, be  $P_2$ , and that the bromine ions, but not the rest of the structure, occupy positions equivalent to  $P_{2/m}$ . Spurious symmetry would then be present in Fig. 20.

In view of these aforementioned circumstances it is considered that the best approach to structure determination will result from the application of three-dimensional methods.

-----

REFERENCES.

- Aebi, A., Barton, D.H.R. and Lindsey, A.S. (1953).  
J.Chem.Soc. p.3124.
- Arai, G., Coppola, J. and Jeffrey, G.A. (1960).  
Acta Cryst. 13, 553.
- Barton, D.H.R., Bruun, T. and Lindsey, A.S. (1952).  
J.Chem.Soc. p.2210.
- Barton, D.H.R. and Lindsey, A.S. (1951). J.Chem.Soc.p.2988.
- Beevers, C.A. and Robertson, J.H. (1950). Acta Cryst. 3, 164.
- Berghuis, J., Haanappel, I.J.M., Potters, M., Loopstra, B.O.,  
MacGillavry, C.H. and Veenendaal, A.L. (1955).  
Acta Cryst. 8, 478.
- Bijvoet, J.M. (1949). Koninkl.Nederland.Akad.Wetenschap.  
52, 313.
- Bluhm, M.M., Bodo, G., Dintzis, H.M. and Kendrew, J.C. (1958).  
Proc.Roy.Soc. A 246, 369.
- Bokhoven, C., Schoone, J.C. and Bijvoet, J.M. (1951).  
Acta Cryst. 4, 275.
- Booth, A.D. (1946). Proc.Roy.Soc. A 188, 77.
- Booth, A.D. (1946). Trans.Far.Soc. 42, 444.
- Booth, A.D. (1947). Nature, 160, 196.
- Booth, A.D. (1948). Nature, 161, 765.
- Booth, A.D. (1948). Fourier Technique in X-ray  
Organic Structure Analysis.  
Cambridge: University Press.
- Bradsher, C.K. and Beavers, L.E. (1955).  
J.Amer.Chem.Soc. 77, 4812.
- Bradsher, C.K., Beavers, L.E. and Jones, J.H. (1957).  
J.Org.Chem. 22, 1740.

- Bragg, W.H. (1915). Trans.Roy.Soc. A 215, 253.
- Bragg, W.L. (1929). Proc.Roy.Soc. A 123, 537.
- Bragg, W.L. and Perutz, M.F. (1954). Proc.Roy.Soc. A225, 315
- Buerger, M.J. (1950). Acta Cryst. 3, 87.
- Buerger, M.J. (1951). Acta Cryst. 4, 531.
- Carlisle, C.H. and Crowfoot, D. (1945).  
Proc.Roy.Soc. A 184, 64.
- Church, A.H. (1875). J.Chem.Soc. 28, 113.
- Clastre, J. and Gay, R. (1950). C.R.Acad.Sci.(Paris) 230, 1976.
- Clunie, J.S. (1957). B.Sc. Thesis (Glasgow).
- Clunie, J.S. and Robertson, J.M. (1960).  
Proc.Chem.Soc. p.82.
- Cochran, W. (1948). Acta Cryst. 1, 138.
- Cochran, W. (1951). Acta Cryst. 4, 408.
- Cochran, W. (1952). Acta Cryst. 5, 65.
- Crowfoot, D., Bunn, C.W., Rogers-Low, B.W. and  
Turner-Jones, A. (1949).  
The Structure of Penicillin. Oxford: University Press.
- Cruickshank, D.J.W. (1950). Acta Cryst. 3, 10.
- Cruickshank, D.J.W. and Robertson, A.P. Acta Cryst. 6, 698.
- Ettling, C. (1834). Annalen 9, 68.
- Fridrichsons, J. and Mathieson, A.McL. (1953)  
J.Chem.Soc. p.2159.
- Garrido, J. (1950). C.R.Acad.Sci.(Paris). 230, 1878.
- Grant, D.F. (1957). Acta Cryst. 10, 498.
- Harker, D. (1936). J.Chem.Phys. 4, 381.
- Harker, D. and Kasper, J.S. (1948). Acta Cryst. 1, 70.

Henderson, G.G., McCrone, R.O.O. and Robertson, J.M. (1929).  
J.Chem.Soc. p.1368.

Hirshfeld, F.L., Jacobsen, R.A., Lipscomb, W.N. and  
Rossmann, M.G. (1959). Acta Cryst. 12, 530.

Hodgkin, D.C., Kamper, J., Lindsey, J., MacKay, M., Pickwork, J.,  
Robertson, J.H., Shoemaker, C.B., White, J.G.,  
Prosen, R.J. and Trueblood, K.N. (1957).  
Proc. Roy. Soc. A 242, 228.

Hoerni, J.A. and Ibers, J.A. (1954). Acta Cryst. 7, 774.

Howells, E.R., Phillips, D.C. and Rogers, D. (1950).  
Acta Cryst. 3, 210.

Hughes, E.W. (1941). J.Amer.Chem.Soc. 63, 1737.

Hughes, E.W. and Lipscomb, W.N. (1946).  
J.Amer.Chem.Soc. 68, 1970.

Internationale Tabellen zur Bestimmung von Kristallstrukturen.  
Berlin : Bornträger.

James, R.W. and Brindley, G.W. (1932). Phil.Mag. 12, 81.

Karle, J. and Hauptman, H. (1950). Acta Cryst. 3, 181.

Lasheen, M.A. (1952). Acta Cryst. 5, 593.

Lipson, H. and Cochran, W. (1953).  
The Determination of Crystal Structures.  
London : G.Bell and Sons, Ltd.

Lutz, A.W. and Reid, E.B. (1953). Chem. and Ind. p.749.

Lutz, A.W. and Reid, E.B. (1954). J.Chem.Soc. p.2265.

de Mayo, P. (1959). The Chemistry of Natural Products, Vol. II:  
Mono- and Sesquiterpenes. (Editor: K.W.Bentley):  
Interscience.

McCallum, G.H., Robertson, J.M. and Sim, G.A. (1959).  
Nature 184, 1863.

McLachlan, D. (1951). Proc.Nat.Acad.Sci. 37, 115.

- McWeeny, R. (1952). Acta Cryst. 5, 463.
- Moffett, R.H. and Rogers, D. (1953). Chem. and Ind. p.916.
- Money, T. (1957). B.Sc. Thesis (Glasgow).
- Pasternak, R.A. (1951). Acta Cryst. 4, 316.
- Patterson, A.L. (1934). Phys.Rev. 46, 372.
- Patterson, A.L. (1935). Z.Krist. 90, 517.
- Pepinsky, R. and MacGillavry, C.H. (1951). Acta Cryst. 4, 284.
- Pitt, G.J. (1952). Acta Cryst. 5, 770.
- Qurashi, M.M. (1949). Acta Cryst. 2, 404.
- Robertson, J.M. (1935). J.Chem.Soc. p.615.
- Robertson, J.M. (1936). J.Chem.Soc. p.1195.
- Robertson, J.M. (1943). J.Sci.Instr. 20, 175.
- Robertson, J.M. (1951). J.Chem.Soc. p.1222.
- Robertson, J.M. (1954). Acta Cryst. 7, 817.
- Robertson, J.M. (1955). Acta Cryst. 8, 286.
- Robertson, J.M. and Woodward, I. (1937). J.Chem.Soc. p.219.
- Robertson, J.M. and Todd, G. (1953). Chem. and Ind. p.437.
- Robertson, J.M. and Todd, G. (1955). J.Chem.Soc. p.1254.
- Rossmann, M.G. (1956). Acta Cryst. 9, 819.
- Rossmann, M.G. and Lipscomb, W.N. (1958). Tetrahedron 4, 275.
- Sayre, D. (1952). Acta Cryst. 5, 60.
- Shoemaker, D.P., Donohue, J., Schomaker, V. and  
Corey, R.B. (1950). J.Amer.Chem.Soc. 72, 2328.
- Shrivastava, H.N. (1960). Ph.D. Thesis (Glasgow).

- Sim, G.A. Personal communication.
- Trotter, J. (1958). Acta Cryst. 11, 355.
- Truter, M.R. (1954). Acta Cryst. 7, 73.
- Tunell, G. (1939). Am. Min. 24, 448.
- Vand, V. (1948). Nature, 161, 600.
- van Vloten, G.W., Kruissink, Ch.A., Strijk, B. and  
Bijvoet, J.M. (1950). Acta Cryst. 3, 139.
- Viervoll, H. and Ögrim, O. (1949). Acta Cryst. 2, 277.
- Wallach, O. and Walker, W. (1892). Annalen 271, 288.
- Whittaker, E.T. and Robinson, G. (1944).  
The Calculus of Observations. Glasgow : Blackie.
- Wiebenga, E.H. and Krom, C.J. (1946). Rec.trav.chim. 65, 663.
- Zachariasen, W.H. (1952). Acta Cryst. 5, 68.
- Yü, S.H. (1942). Nature 149, 638.

-----

APPENDIX 1.

Preparation of Isoclovene Hydrobromide.

1. Preparation of  $\beta$ -caryophyllene alcohol.

The method employed by Lutz and Reid (1954) was adopted. Concentrated sulphuric acid (10.5 g.) was added dropwise to anhydrous ether (20 ml.) in a 500 ml. round-bottomed flask at 0°C. 36 g. of commercial caryophyllene (previously extracted with dilute aqueous caustic soda) were added dropwise at such a rate that the temperature remained below 10°C.

The dark red mixture which resulted was kept overnight at 0°C. and then neutralised with 20% caustic soda solution followed by careful addition of solid sodium hydroxide (7.5 g.). This mixture was exhaustively distilled in steam for about 10 hours. A yield of 12.25 g. of crude  $\beta$ -caryophyllene alcohol was obtained. This was recrystallised from acetone solution, m.p.t. 91°.

2. Dehydration of  $\beta$ -caryophyllene alcohol.

The method of Henderson, McCrone and Robertson (1929) was repeated. Phosphorus pentoxide (10 g.) was added dropwise to a melt of  $\beta$ -caryophyllene alcohol (7.5 g.) and the dark red resinous material which resulted was neutralised with sodium carbonate solution. The resultant mixture separated into an aqueous layer with a thin layer of a pale yellow oil on the surface.

Steam distillation provided a pale yellow oil which was extracted with ether, the ethereal solution being dried over anhydrous sodium sulphate. The yellow oil, isoclovene, was not isolated.

### 3. Preparation of Isoclovene Hydrobromide.

Dry hydrogen bromide gas was passed through the ethereal solution of isoclovene at 0°C. until there was a very slight red tinge in the solution. The mixture was then kept at 0°C. for three days, during which time it changed to a deep red colour. The hydrogen bromide was removed by water, the ethereal solution dried, the ether removed under reduced pressure and on freezing an ethyl acetate solution at -60°C. a small deposit of yellow crystals was obtained. Some of these crystals were recrystallised from an acetone solution. The rest of the material was dissolved in an acetone-ether solution. With exposure to the air, the latter rapidly turned dark green and visible globules of a dark green oil still remained after a period of two weeks at -17°C.

- - - - -

APPENDIX 2.

Attempted Preparation of Isoclovene Hydroiodide.

Attempted Preparation of Isoclovene Hydroiodide.

Isoclovene hydrochloride (50 mg.) and sodium iodide (33 mg.) were dissolved in anhydrous acetone (10 ml.) to give a colourless solution which was heated on a steam bath for about 5 minutes. A violet residue resulted when the solution was very carefully evaporated to dryness. Extraction by common solvents such as petroleum ether (60-80° fraction) and acetone merely produced dark tars. The residue after extraction gave a slight test for ionic chlorine. It would thus appear that reaction had occurred but that the hydroiodide is even more unstable than the hydrobromide.

The entire experiment was repeated using an electric mantle as the heating agent. The solution was very gently refluxed for an hour but, again, no crystalline organic material could be recovered.

-----

APPENDIX 3.

Isoclovene hydrochloride: observed  
and calculated structure amplitudes  
together with calculated phase angles,  $\alpha(hkl)$ .  
Unobserved terms are not included.







4	0	4	3.2	7.4	180	0
4	1	4	8.2	7.7	173	96
4	2	4	9.4	9.4	248	12
4	3	4	5.1	3.9	12	12
4	4	4	5.5	6.3	207	67
4	5	4	6.3	7.5	259	50
4	6	4	3.5	3.5	50	50
4	7	4	6.6	6.3	284	0
4	8	4	4.9	3.5	90	0
4	9	4	4.9	4.7	278	67
4	10	4	2.6	5.6	67	0
4	11	4	1.9	2.1	278	0
4	12	4	1.8	2.2	296	0
4	0	-4	3.0	2.1	0	0
4	1	-4	3.0	2.9	96	0
4	2	-4	12.8	13.5	3	4
4	3	-4	20.4	21.7	0	0
4	4	-4	3.0	2.9	129	0
4	5	-4	3.0	3.8	207	0
4	6	-4	3.1	3.1	200	0
4	7	-4	3.6	4.2	18	0
4	8	-4	5.2	5.9	172	0
4	9	-4	6.0	5.8	175	0
4	10	-4	2.4	1.7	248	0
4	11	-4	2.2	2.1	297	0
4	12	-4	6.4	6.2	297	0
4	1	-5	5.6	6.0	210	0
4	2	-5	1.9	2.2	192	0
4	3	-5	6.6	5.2	208	0
4	4	-5	4.0	1	204	0
4	5	-5	1.8	1.8	198	0
4	10	-5	1.4	0.7	186	0
4	0	-5	0.8	0.2	180	0
4	1	-5	6.4	6.0	201	0
4	2	-5	4.8	4.8	202	0
4	3	-5	2.3	1.8	183	0
4	4	-5	4.1	4.0	181	0
4	5	-5	7.8	8.5	21	0
4	6	-5	6.3	6.6	200	0
4	7	-5	6.6	6.2	80	0
4	8	-5	2.6	2	202	0
4	9	-5	2.5	3.1	207	0
4	10	-5	2.1	1.8	20	0
4	11	-5	4.0	3.8	207	0
4	12	-5	2.9	2.3	180	0
4	1	-6	2.7	3.6	20	0
4	2	-6	1.7	7.9	184	0
4	3	-6	1.7	2.9	189	0
4	4	-6	7.1	7.0	202	1
4	5	-6	4.1	2.4	1	0
4	6	-6	2.9	2.8	200	0
4	7	-6	4.1	4.5	187	0
4	8	-6	2.4	2.4	121	0
4	9	-6	2.4	2.4	121	0
4	10	-6	2.0	2.6	121	0
4	0	-7	2.8	2.2	180	0
4	1	-7	3.0	2.8	179	0
4	2	-7	3.1	2.7	180	0
4	3	-7	3.5	3.2	179	0
4	4	-7	3.4	4.7	202	0
4	5	-7	3.4	4.7	202	0
4	6	-7	3.1	2.8	180	0
4	7	-7	3.1	2.8	180	0

4	0	-8	5.6	4.6	180	0
4	1	-8	3.7	3.2	159	0
4	2	-8	1.1	1.1	89	0
4	3	-8	1.4	1.6	180	0
4	4	-8	3.6	3.3	180	0
4	5	-8	7.5	8.4	184	0
4	6	-8	8.1	11.3	156	0
4	7	-8	3.7	6.3	202	0
4	8	-8	7.7	6.9	206	0
4	9	-8	1.0	1.8	214	0
4	10	-8	3.4	4.9	204	0
4	11	-8	3.0	4.8	204	0
4	12	-8	3.0	4.8	210	0
4	1	-9	4.7	4.5	20	0
4	2	-9	1.7	3.7	81	0
4	3	-9	0.8	1.8	178	0
4	4	-9	0.8	1.1	187	0
4	5	-9	6.8	5.4	180	0
4	6	-9	7.0	6.3	183	0
4	7	-9	13.4	13.9	183	0
4	8	-9	1.7	3.4	182	0
4	9	-9	4.7	5.5	20	0
4	10	-9	1.8	1.8	202	0
4	11	-9	1.8	1.8	202	0
4	12	-9	2.1	2.1	181	0
4	1	-10	2.6	2.6	180	0
4	2	-10	1.2	1.2	180	0
4	3	-10	1.2	1.2	180	0
4	4	-10	4.2	4.6	180	0
4	5	-10	4.2	4.6	180	0
4	6	-10	4.2	4.6	180	0
4	7	-10	4.2	4.6	180	0
4	8	-10	4.2	4.6	180	0
4	9	-10	4.2	4.6	180	0
4	10	-10	4.2	4.6	180	0
4	11	-10	4.2	4.6	180	0
4	12	-10	4.2	4.6	180	0
4	1	-11	5.6	5.2	180	0
4	2	-11	5.6	5.2	180	0
4	3	-11	5.6	5.2	180	0
4	4	-11	5.6	5.2	180	0
4	5	-11	5.6	5.2	180	0
4	6	-11	5.6	5.2	180	0
4	7	-11	5.6	5.2	180	0
4	8	-11	5.6	5.2	180	0
4	9	-11	5.6	5.2	180	0
4	10	-11	5.6	5.2	180	0
4	11	-11	5.6	5.2	180	0
4	12	-11	5.6	5.2	180	0
4	1	-12	4.0	4.0	0	0
4	2	-12	4.0	4.0	0	0
4	3	-12	4.0	4.0	0	0
4	4	-12	4.0	4.0	0	0
4	5	-12	4.0	4.0	0	0
4	6	-12	4.0	4.0	0	0
4	7	-12	4.0	4.0	0	0
4	8	-12	4.0	4.0	0	0
4	9	-12	4.0	4.0	0	0
4	10	-12	4.0	4.0	0	0
4	11	-12	4.0	4.0	0	0
4	12	-12	4.0	4.0	0	0

5	5	-2	4.5	3.2	204	0
5	7	-2	3.8	3.7	24	0
5	8	-2	2.3	2.8	178	0
5	9	-2	3.9	4.8	180	0
5	10	-2	3.0	2.8	180	0
5	11	-2	3.0	2.8	179	0
5	12	-2	2.8	2.7	179	0
5	10	-3	2.1	4.9	10	0
5	0	-3	3.1	2.6	180	0
5	1	-3	3.8	6.2	66	0
5	2	-3	2.9	7.8	67	0
5	3	-3	3.6	3.9	180	0
5	4	-3	3.6	3.9	180	0
5	5	-3	3.2	2.9	184	0
5	6	-3	3.2	2.9	184	0
5	7	-3	3.2	2.9	184	0
5	8	-3	3.2	2.9	184	0
5	9	-3	3.2	2.9	184	0
5	10	-3	3.2	2.9	184	0
5	11	-3	3.2	2.9	184	0
5	12	-3	3.2	2.9	184	0
5	0	-3	4.0	4.4	0	0
5	1	-3	4.0	4.4	0	0
5	2	-3	4.0	4.4	0	0
5	3	-3	4.0	4.4	0	0
5	4	-3	4.0	4.4	0	0
5	5	-3	4.0	4.4	0	0
5	6	-3	4.0	4.4	0	0
5	7	-3	4.0	4.4	0	0
5	8	-3	4.0	4.4	0	0
5	9	-3	4.0	4.4	0	0
5	10	-3	4.0	4.4	0	0
5	11	-3	4.0	4.4	0	0
5	12	-3	4.0	4.4	0	0
5	1	-4	4.6	4.7	167	0
5	2	-4	7.2	5.1	299	0
5	3	-4	6.0	6.3	299	0
5	4	-4	4.0	4.4	299	0
5	5	-4	4.0	4.4	299	0
5	6	-4	4.0	4.4	299	0
5	7	-4	4.0	4.4	299	0
5	8	-4	4.0	4.4	299	0
5	9	-4	4.0	4.4	299	0
5	10	-4	4.0	4.4	299	0
5	11	-4	4.0	4.4	299	0
5	12	-4	4.0	4.4	299	0
5	1	-4	4.6	4.7	167	0
5	2	-4	7.2	5.1	299	0
5	3	-4	6.0	6.3	299	0
5	4	-4	4.0	4.4	299	0
5	5	-4	4.0	4.4	299	0
5	6	-4	4.0	4.4	299	0
5	7	-4	4.0	4.4	299	0
5	8	-4	4.0	4.4	299	0
5	9	-4	4.0	4.4	299	0
5	10	-4	4.0	4.4	299	0
5	11	-4	4.0	4.4	299	0
5	12	-4	4.0	4.4	299	0
5	1	-5	4.6	4.5	180	0
5	2	-5	2.9	3.5	155	0
5	3	-5	2.8	3.4	14	0
5	4	-5	3.5	1.1	120	0
5	5	-5	3.5	1.1	120	0
5	6	-5	3.5	1.1	120	0
5	7	-5	3.5	1.1	120	0
5	8	-5	3.5	1.1	120	0
5	9	-5	3.5	1.1	120	0
5	10	-5	3.5	1.1	120	0
5	11	-5	3.5	1.1	120	0
5	12	-5	3.5	1.1	120	0
5	1	-6	4.5	4.5	180	0
5	2	-6	4.5	4.5	180	0
5	3	-6	4.5	4.5	180	0
5	4	-6	4.5	4.5	180	0
5	5	-6	4.5	4.5	180	0
5	6	-6	4.5	4.5	180	0
5	7	-6	4.5	4.5	180	0
5	8	-6	4.5	4.5	180	0
5	9	-6	4.5	4.5	180	0
5	10	-6	4.5	4.5	180	0
5	11	-6	4.5	4.5	180	0
5	12	-6	4.5	4.5	180	0

5	1	-6	5.9	5.4	17	0
5	2	-6	2.8	2.8	26	0
5	3	-6	2.9	2.9	26	0
5	4	-6	4.0	4.6	184	0
5	5	-6	4.0	4.6	184	0
5	6	-6	4.0	4.6	184	0
5	7	-6	4.0	4.6	184	0
5	8	-6	4.0	4.6	184	0
5	9	-6	4.0	4.6	184	0
5	10	-6	4.0	4.6	184	0
5	11	-6	4.0	4.6	184	0
5	12	-6	4.0	4.6	184	0
5	2	-7	4.0	5.4	142	0
5	3	-7	1.1	1.5	180	0
5	4	-7	2.5	1.5	199	0
5	5	-7	2.0	3.0	128	0
5	6	-7	0	0	0	0
5	7	-7	0	0	0	0
5	8	-7	0	0	0	0
5	9	-7	0	0	0	0
5	10	-7	0	0	0	0
5	11	-7	0	0	0	0
5	12	-7	0	0	0	0
5	1	-8	0.9	0.6	180	0
5	2	-8	6.0	5.2	15	0

APPENDIX 4.

Observed structure factors for  
the three principal zones of  
photo-irradiated acridizinium bromide.

(Okℓ) Zone.

hkℓ	F <sub>0</sub>								
020	11.4	023	63.3	058	4.5	091	11.9	0,13,1	5.9
040	114.5	024	23.9	059	9.4	092	34.8	0,13,2	10.4
060	130.0	025	50.8	0,5,10	6.8	094	12.0	0,13,4	20.2
080	31.6	026	31.2			095	5.0	0,13,5	11.2
0,10,0	65.8	028	37.4	061	25.1	097	8.4	0,13,6	7.9
0,12,0	45.0	0,2,10	10.4	062	18.1	099	5.4	0,13,7	4.7
0,14,0	26.8			063	43.2	0,9,10	6.5	0,13,8	12.4
0,16,0	18.4	031	23.0	064	8.7	0,9,11	2.2		
0,18,0	11.4	032	46.0	065	46.3			0,14,2	6.6
0,20,0	7.0	033	3.5	066	31.5	0,10,1	7.8	0,14,3	21.4
		034	13.9	067	10.0	0,10,2	15.6	0,14,4	11.0
001	57.6	035	8.7	068	23.3	0,10,3	37.4	0,14,5	12.1
002	36.7	036	10.1	0,6,10	3.5	0,10,4	18.9	0,14,6	8.8
003	97.3	037	9.8			0,10,5	18.9		
004	22.3	0,3,10	9.6	071	3.9	0,10,6	12.6	0,15,1	3.2
005	27.9			072	20.3	0,10,7	3.9	0,15,2	10.7
006	25.5	041	5.8	074	14.6	0,10,8	8.7	0,15,4	10.8
007	17.4	042	22.3	075	7.7	0,10,9	5.2	0,15,5	13.0
008	15.4	043	71.1	076	7.3			0,15,6	9.4
009	20.7	044	26.9	077	6.9	0,11,1	7.5		
0,0,11	14.2	045	15.6	078	3.9	0,11,2	14.4	0,16,2	8.9
		046	19.7	079	4.8	0,11,3	14.0	0,16,3	10.7
011	11.2	047	10.1	0,7,11	6.9	0,11,4	14.5	0,16,4	9.1
012	33.8	048	16.9			0,11,5	26.5	0,16,5	10.0
013	18.1	049	11.4	081	7.2	0,11,6	15.0	0,16,7	7.9
015	14.9	0,4,11	7.0	082	9.8	0,11,7	11.3		
016	17.9			083	46.0			0,17,2	8.6
017	17.5	051	6.6	084	13.5	0,12,1	3.5	0,17,7	6.7
018	8.7	052	40.6	085	24.6	0,12,2	8.1		
0,1,10	6.8	053	11.5	086	16.2	0,12,3	17.3	0,18,4	6.3
		055	30.9	087	4.5	0,12,5	14.7	0,20,4	6.5
021	44.5	056	18.6	088	21.0	0,12,6	3.9		
022	40.7	057	15.8			0,12,8	8.9		

- Cont'd -

(hk0) Zone.

hkℓ	F <sub>0</sub>	hkℓ	F <sub>0</sub>	hkℓ	F <sub>0</sub>	hkℓ	F <sub>0</sub>	hkℓ	F <sub>0</sub>
020	10.5	620	16.6	760	7.5	1,11,0	21.0	5,15,0	4.1
040	110.0	720	9.0			2,11,0	19.9	7,15,0	4.7
060	123.0	920	4.9	170	36.0	3,11,0	10.2		
080	33.5			270	44.4	4,11,0	26.8	1,16,0	5.4
0,10,0	68.1	130	13.5	370	11.4	6,11,0	6.4	2,16,0	9.7
0,12,0	45.2	230	72.2	470	27.2	7,11,0	8.4	3,16,0	5.8
0,14,0	31.6	330	5.6	670	6.1			4,16,0	6.7
0,16,0	20.5	430	46.3	770	10.7	1,12,0	5.4	5,16,0	8.4
0,18,0	13.7	530	10.6			2,12,0	28.6		
0,20,0	7.1	630	3.6	180	10.2	3,12,0	17.1	1,17,0	7.9
		730	9.7	280	49.0	4,12,0	7.4	2,17,0	15.5
100	45.1	930	4.3	380	35.3	5,12,0	13.3	3,17,0	5.5
200	10.8			480	9.5	6,12,0	9.1		
300	21.8	140	4.9	580	23.6	7,12,0	5.4	1,18,0	4.3
400	44.6	240	43.3	680	17.4			2,18,0	8.1
500	46.9	340	20.4	780	9.3	1,13,0	4.4		
600	8.1	440	10.7			2,13,0	24.4	1,19,0	7.6
700	12.6	540	45.6	190	19.6	3,13,0	6.0	2,19,0	4.9
900	3.4	640	8.6	290	41.3	5,13,0	5.3	3,19,0	5.6
		740	8.1	390	9.1	6,13,0	6.2	5,19,0	2.6
110	13.6			490	20.1	7,13,0	3.3		
210	50.5	150	8.0	590	3.8				
310	13.5	250	49.7	690	6.1	1,14,0	5.9		
410	31.6	350	21.4	790	7.5	2,14,0	9.6		
610	6.6	450	38.1			3,14,0	7.2		
710	19.8	750	17.2	1,10,0	9.9	5,14,0	8.9		
910	6.7	950	6.7	2,10,0	19.9	6,14,0	4.1		
				3,10,0	8.0	7,14,0	4.5		
120	30.9	160	29.2	4,10,0	13.3				
220	103.9	260	36.0	5,10,0	22.6	1,15,0	10.1		
320	77.3	360	26.5	6,10,0	3.8	2,15,0	7.4		
420	14.6	460	21.8	7,10,0	3.4	3,15,0	3.8		
520	25.0	560	17.1			4,15,0	17.3		

- Cont'd -

